5-9-2016

Functions of Extracellular Pyruvate Kinase M2 in Tissue Repair and Regeneration

Yinwei Zhang

Recommended Citation
Zhang, Yinwei, "Functions of Extracellular Pyruvate Kinase M2 in Tissue Repair and Regeneration." Dissertation, Georgia State University, 2016.
doi: https://doi.org/10.57709/8513687

FUNCTIONS OF EXTRACELLULAR PYTUVATE KINASE M2 IN TISSUE REPAIR AND REGENERATION

by

YINWEI ZHANG

Under the Direction of Zhi-Ren Liu, PhD

ABSTRACT

Pyruvate kinase M2 (PKM2) is a glycolytic enzyme expressed in highly proliferating cells. Studies of PKM2 have been focused on its function of promoting cell proliferation in cancer cells. Our laboratory previously discovered that extracellular PKM2 released from cancer cells promoted angiogenesis by activating endothelial cell proliferation and migration. PKM2 activated endothelial cells through integrin αvβ3. Angiogenesis and myofibroblast differentiation are key processes during wound healing. In this dissertation, I demonstrate that extracellular PKM2 released from activated neutrophils promotes angiogenesis and myofibroblast differentiation during wound healing. PKM2 activates dermal fibroblasts through integrin αvβ3 and PI3K signaling pathway. I also claim that extracellular PKM2 plays a role during liver fibrosis. PKM2 protects hepatic stellate cells from apoptosis by activating the survival signaling pathway.

INDEX WORDS: Pyruvate kinase M2, Wound healing, Angiogenesis, Myofibroblast differentiation, Liver fibrosis, Apoptosis

FUNCTIONS OF EXTRACELLULAR PYRUVATE KINASE M2 IN TISSUE REPAIR AND REGENERATION

by

YINWEI ZHANG

A Dissertation Submitted in Partial Fulfillment of the Requirements for the Degree of

Doctor of Philosophy

in the College of Arts and Sciences

Georgia State University

2016

FUNCTIONS OF EXTRACELLULAR PYRUVATE KINASE M2 IN TISSUE REPAIR AND REGENERATION

by

YINWEI ZHANG

Committee Chair: Zhi-Ren Liu

Committee: Yuan Liu

Susanna Greer

Electronic Version Approved:

Office of Graduate Studies

College of Arts and Sciences

Georgia State University

May 2016

DEDICATION

I dedicate my dissertation to my father, Suming Zhang, and my mother, Yuan Yuan. Thanks for your unconditional support in my life. I love you.

I also dedicate my dissertation to my grandma, my uncle and other family members, for the continued support and encouragement.

At last, I dedicate this work to my dear cousin Mujia Erica Yuan. I will always miss you.

ACKNOWLEDGEMENTS

I would like to thank my advisor Dr. Zhi-Ren Liu for having me in his lab. He always supports my research work and encourages me to generate novel ideas. I would like express my gratitude to my committee members Dr. Yuan Liu and Dr. Susanna Greer, for the great suggestions and supports on this research project, and also my presentation. I would like to thank Dr. Jenny Yang for letting me use the equipment in her lab and also giving me lots of good ideas. I would like to thank Dr. Siming Wang and Dr. Cheng Ma for the assistance in mass spectrometry experiment. I thank all my previous and current lab members for the help in the lab, especially Dr. Liangwei Li. I thank the biology core facility for the technical support and LaTesha Warren for the help during my PhD years. I would also like to give my appreciation to everyone in the joint group meeting.

TABLE OF CONTENTS

LIST OF FIGURES

CHAPTER 1 GENERAL BACKGROUND

1.1 Glycolysis and Pyruvate Kinase

Glycolysis is a process that consumes glucose to provide energy for cells. It is a sequential process with ten metabolic enzyme reactions. One unit of glucose generates two units of pyruvate as final product and two units of ATP and NADH as energy resources of glycolysis. Glycolysis is regulated by several enzymes which form a complex in the cytosol.

Glycolysis is divided into two phases, one is preparatory phase and another one is pay-off phase. In the preparatory phase, glucose is first converted to glucose-6-phosphate, then to fructose-6-phosphate, fructose 1, 6-bisphosphate (FBP), and finally to two units of glyceraldehyde 3-phosphate (GADP). ATP is used in the first and the third step as energy investment. In the pay-off phase, final product GADP from previous phase is converted into 1, 3-bisphosphoglycerate, then 3-phosphoglycerate, 2-phosphoglycerate, phosphoenolpyruvate and pyruvate as the final product of glycolysis. NADH is generated from the first step and ATP is generated from the second and the last step. Glycolysis is regulated by three enzymes during the reaction process, hexokinase, phosphofructokinase, and pyruvate kinase.

Hexokinase is an enzyme functions at the first step of glycolysis. It uses ATP as resource to phosphorylate glucose and forms glucose-6-phosphate (G6P). When glucose level increases, hexokinase senses the signal and starts to convert glucose to G6P (Bustamante & Pedersen, 1977). Glucokinase (human hexokinase IV) is one isoform of hexokinases. Due to its unique ability that its activity is not affected by the production amount, glucokinase can sustainably produce G6P as the storage of energy if enough glucose is provided (Robey & Hay, 2006). Phosphofructokinase is an enzyme that catalyzes the irreversible conversion from F6P to FBP. It

is regulated by ATP concentration, pH level, PEP level, and also AMP level (Wegener & Krause, 2002).

Pyruvate kinase is an enzyme functions at the last step of glycolysis. It converts phosphoenolpyruvate (PEP) to pyruvate by transferring one phosphate group from PEP to ADP and generates ATP. Pyruvate kinase is regulated by ATP and alanine as allosteric inhibitors (Schulz et al., 1975). FBP acts as an activator for pyruvate kinase that it binds to the pocket on pyruvate kinase and alternates its conformation to promote the substrate binding (Ashizawa et al., 1991). Pyruvate kinase deficiency shows slow glycolysis and abnormal metabolism. Severe metabolism defect is lethal due to extreme low level of ATP (Bowman & Procopio, 1963).

Pyruvate kinase family contains four isoenzymes with tissue dependent expression, pyruvate kinase L (in liver), pyruvate kinase R (in red blood cells), pyruvate kinase M1 (in muscle and brain), and pyruvate kinase M2 (in fetal tissue and cancer cells). PKL and PKR are products of the same gene PKLR locating on chromosome 1 band q21. PKL is a specific isoform of pyruvate kinase existing in liver. It is also found in kidney, small intestine and pancreas. PKL is regulated by epinephrine and glucagon through protein kinase A. Upon addition of epinephrine and glucagon, activated PKA inhibits the pyruvate kinase activity of PKL by adding phosphorylation (Exton & Park, 1969). PKR is another specific isoform of pyruvate kinase in erythrocytes. Since erythrocytes are important in oxygen delivering, PKR mutation leads to a severe disease called chronic nonspherocytic hemolytic anemia (Valentine et al., 1961).

PKM1 and PKM2 are products of PKM gene locating on chromosome 15 on band q22 with different mRNA splicing (Popescu & Cheng, 1990). PKM1 and PKM2 are transcribed from the same mRNA with alternatively splicing on exon 9 or exon 10 (Noguchi et al., 1986). They have a forty-five amino acids difference between 389 and 433. Compared with PKM1 expressed

in normal tissues, PKM2 is mainly expressed in highly proliferative tissues such as cancer cells, fetal tissues, and immune cells. A study found that c-Myc in cancer cells upregulates the transcription of heterogeneous nuclear ribonuleoprotein (hnRNP) and polypyrimidine tract binding protein 1 (PTBP1) to promote inclusion of exon 10 during pre-mRNA splicing in order to favors cancer cell metabolism (David et al., 2010). The expression of PKM2 is first occurred during embryonic development, and then it switches to PKM1, PKL, or PKR after fetal development. During cancer progression, expression of PKM2 is switched back (M. Chen et al., 2010). The level of PKM2 expression is correlated with cancer progression and metastasis. The pyruvate kinase activity of PKM2 is lower than PKM1 even with the association of FBP, which is the allosteric activator of pyruvate kinase.

1.2 Pyruvate Kinase M2

1.2.1 Pyruvate kinase M2 structure and regulation

PKM1 and PKM2 share more than 95% identity in the amino acid sequences because of the one exon splicing difference. PKM1 forms a tetramer in its native structure. Each monomer consists of A, B, C, and N four domains. On the other hand, PKM2 is found to have two native forms. One is the same as PKM1 as a tetramer and another one is a dimer (Dombrauckas et al., 2005). The tetrameric conformation of pyruvate kinase has higher binding affinity to phosphoenolpyruvate (PEP), compared with the dimeric form. Therefore, the pyruvate kinase activity of PKM1 is higher than that of tetrameric PKM2, giving the high affinity of PKM1 to substrate PEP. In the native structure of PKM2, different amino acid residues locate at the interface of dimer-dimer PKM2.

As a key kinase in glycolysis, PKM2 is regulated by several factors. FBP, one of the key activators PKM2, is the intermediate in glycolysis pathway. It is reported that FBP activates the

association of PKM2 monomer to form tetramer in vitro. After binding to FBP, the active site of PKM2 is partially closed as a result of the conformational change induced by FBP binding. PKM2 is also regulated by different phosphorylations. A report found that proviral insertion in murine lymphomas 2 (PIM2) induces the expression of PKM2 by direct phosphorylation on Thr 454. This threonine residue of PKM2 is critical in cancer cells. Mutation of this residue leads to glycolysis defect and proliferation reduction (Yu et al., 2013). A study revealed that epidermal growth factor receptor (EGFR)-activated extracellular signal-regulated kinase 2 (ERK2) interacts with Ile 429 and Leu 431 of PKM2 and phosphorylates Ser 37 to promote nuclear translocation of PKM2, which consequently stimulates c-Myc expression. The expression of c-Myc positively feedback facilitates the PTB-dependent PKM2 expression (W. Yang, Zheng, et al., 2012). Another study claims that in order to promote Warburg effect and tumor growth, fibroblast growth factor receptor type 1 (FGFR1), a receptor tyrosine kinase, phosphorylates PKM2 at Tyr 105 to inhibit its tetramer formation through disrupting FBP binding (Hitosugi et al., 2009). PKM2 is also found to bind phosphotyrosine peptide to promote cancer cell proliferation. The binding of phosphotyrosine peptides to PKM2 causes the dissociation of FBP which leads to inhibition of PKM2 activity (Christofk, Vander Heiden, Wu, et al., 2008). In addition, PKM2 mutations have been detected in many disease situations. As an example, PKM2 mutations (H391Y and K422R) are found in Bloom Syndrome (BS) condition. Co-expression of mutants H391Y and K422R in cancer cells significantly increased aggressive cancer metabolism, and tumorigenic potential (Akhtar et al., 2009; Gupta et al., 2010).

1.2.2 Location of pyruvate kinase M2

As a glycolytic enzyme, PKM2 is first discovered in glycolytic enzyme complex. To help the conversion from PEP to pyruvate and ATP generation, PKM2 locates in the cytosol and

catalyze the last step of glycolysis. After that, pyruvate is transported to mitochondria for the following catalysis.

PKM2 is also found in cell nucleus in numbers of studies. A study showed that interleukin-3 stimulates the nuclear translocation of PKM2 by Jak2 activation, and then promotes cell proliferation (Hoshino et al., 2007). JMJD5 is induced by hypoxia to stimulate cell proliferation. Under hypoxia, upregulated JMJD5 binds to PKM2 at the dimer-dimer interface and inhibits its pyruvate kinase activity. The binding at PKM2 dimer-dimer interface disrupts the nuclear translocation of PKM2 and promotes hypoxia-inducible factor 1-α (HIF-1-α) mediated transactivation (Wang et al., 2014). Yang et al. reported that PKM2 presents in cell nucleus to phosphorylate histone H3 at Thr 11 after EGF receptor activation (W. Yang, Xia, Hawke, et al., 2012). Our laboratory previously showed that dimeric PKM2 can translocate into cell nucleus. Nuclear PKM2 activates the transcription activity of MEK5 via phosphorylating stat3 at Tyr 105 (Gao et al., 2012). Compared with activation of proliferation, PKM2 can also translocate into cell nucleus to induce program cell death (Stetak et al., 2007).

PKM2 has been found extracellularly in several pathological conditions. PKM2 is used as a serum diagnostic marker in colorectal cancer, lung cancer, gastric cancer, and kidney cancer (Peng et al., 2011). PKM2 also exists in the stool sample of various cancer patients (Kopylov et al., 2014). One study claimed that PKM2 is secreted from colon cancer cells and is able to promote colon cancer cell migration (P. Yang et al., 2014). Our lab found that PKM2 is released from cancer cells, and extracellular PKM2 can activate endothelial cell migration and attachment. The level of extracellular PKM2 is also correlated with the progression of severe immune diseases. PKM2 is used as serum marker for inflammatory bowel disease (IBD) (Jeffery et al., 2009). Faecal PKM2 is reported to be used as noninvasive marker for ileal pouch

inflammation (Johnson et al., 2009). Recently, a study discovered that PKM2 level is increased after retinal rupture laser injury (Paulus et al., 2015).

1.3 Functions of PKM2

PKM2 is expressed during embryonic development. The function of PKM2 in fetal tissue is still not clear. PKM2 interacts with Oct-4, a key transcription factor in embryonic stem cells, to promote the transcription activity of Oct-4. The binding of Oct-4 to its target requires PKM2, possibly C terminal domain of PKM2 (Lee et al., 2008). PKM2 is also expressed in hematopoietic stem cells. Depletion of PKM2 disadvantages disease development of myeloid leukemia in mouse model (Zhu et al., 2014).

After fetal development, PKM2 is replaced by other three isozymes, PKM1, PKR, or PKL. Expression of PKM2 occurs during cancer progression. PKM2 is expressed in all cancer cells and also some highly proliferating cells, such as immune cells. All pyruvate kinase isoenzymes form similar tetramer. The pyruvate kinase activity of PKM2 is lower compared with other isoenzymes because of the low PEP binding affinity of dimer, which can be enhanced by FBP interaction.

PKM2 functions in several physiological and pathological conditions in addition to its pyruvate kinase activity in glycolysis. One well-known role of PKM2 in cancer cells is promoting Warburg effect, which is one of the common features among highly proliferative cells. As an example, cancer cells prefer to use glycolysis to produce energy but not oxidative phosphorylation even under the aerobic environment. One explanation of Warburg effect is that the pyruvate kinase activity of PKM2 is reduced by the conversion from tetramer to dimer. As a result, the glycolysis process becomes slower at the step of converting PEP to pyruvate due to the low pyruvate kinase activity of dimeric PKM2. Consequently, the upstream glycolytic

intermediates are accumulated and converted to the products which are needed for cell proliferation, such as phospholipids, amino acids and nucleic acids. Therefore, the highly proliferative cells under Warburg effect condition tend to reduce their aerobic respiration and focus on the proliferation task (Christofk, Vander Heiden, Harris, et al., 2008; Ferguson & Rathmell, 2008; W. Yang & Lu, 2013).

PKM2 is also found to act as a sensor to detect insufficiency of glucose. To accomplish the goal, PKM2 shifts glycolysis to glutaminolysis for ATP production by inactivating itself, which rescues the cells from glucose starvation induced cell apoptosis. PKM2 involves in the Raf kinase pathway that α-Raf can activate PKM2 to promote cell proliferation (Le Mellay et al., 2002; Mazurek et al., 2007). PKM2 also plays a role in the immunological response through interacting with suppressor of cytokine signaling 3 (SOCS3) and upregulating ATP production (Z. Zhang et al., 2010). Recently, a group reported that PKM2 translocates into cell nucleus and regulates gene transcription through interacting with specific gene transcription regulators such as hypoxia-inducible factors (HIF1) and signal transducer and activator of transcription 3 (STAT3) (W. Yang, Xia, Cao, et al., 2012).

Another characteristic of PKM2 is that it can be secreted by cancer cells. There are high levels of PKM2 circulating in the blood stream of cancer patients. Serum PKM2 and stool PKM2 are used as cancer markers to prognose various types of cancers. In our laboratory, we demonstrated that PKM2 was released from cancer cells and human embryonic kidney (HEK) 293 cells. PKM2 in blood circulation promoted tumor growth through stimulation of angiogenesis. We found that in xenograft tumor mouse model neutralization of PKM2 using polyclonal antibody against full length PKM2 inhibited the tumor growth compared with the pre-immune IgG as the control. We also found that addition of PKM2 to blood circulation can

promote tumor growth through stimulating angiogenesis. In vitro tube formation assay showed that the PKM2 treated human umbilical vein endothelial cells (HUVECs) had elevated tube density and increased tube sprouts number compared with the control cells, suggesting the role of PKM2 in stimulating angiogenesis. In addition, migration and attachment assays indicated that extracellular PKM2 promoted endothelial cell migration and attachment. We also found that integrin αvβ3 was the cell surface target of endothelial cells for PKM2 activated migration, attachment, and tube formation (L. Li et al., 2014).

1.4 Wound Healing

1.4.1 Wound healing process

Wound healing is a complicated process that organs and tissues repair themselves after injury. This process consists of numbers of phases in sequence. Wound healing process is mainly divided into four stages: hemostasis, inflammation, proliferation, and maturation. Hemostasis happens right after wound induction. Since blood vessel is broken caused by the injury, platelets move to the broken vessels and aggregate. The main function of platelets at wound site is to clot blood vessel in order to stop bleeding. To induce aggregation, platelets express glycoproteins on the plasma membrane to enhance cell-cell attachment. Platelets secrete large amounts of extracellular matrix, for example fibrin and fibronectin which cross-link together to seal the broken blood vessels. In addition, platelets also secrete several cytokines and grow factors, which recruit different types of immune cells to the wound site (Versteeg et al., 2013).

Hemostasis is active for several minutes at the beginning of wound healing. The second stage is called inflammation that different kinds of immune cells infiltrate into the wound site. Among them, the first one is polymorphonuclear neutrophil. Neutrophils are recruited by fibronectin and other growth factors right after hemostasis. In human, neutrophils start to

accumulate hours after wound induction, and reach the peak of population at about two days. Neutrophils kill bacteria by generating free radicals and extracellular traps, and secrete proteases to clean dead cell debris (Segal, 2005). Neutrophils also release multiple growth factors and cytokines functioning to trigger the next proliferation stage (Kolaczkowska & Kubes, 2013). The population of neutrophils declines two or three days after wound induction (Kim et al., 2008). Apoptotic neutrophils are phagocytized by macrophages, the second population of immune cells coming to the wound sites after neutrophils. Macrophages cleanse the wound site by phagocytizing other immune cells, bacteria, and cell debris (Newton et al., 2004). Another function of macrophage is to facilitate wound healing. After arriving at the wound site and being activated, macrophages secrete several cytokines and growth factors to stimulate angiogenesis and granulation tissue growth (Majno, 1998). Macrophages also play a role of anti-angiogenesis and anti-fibrosis at the late stage of wound repair (Leibovich & Wiseman, 1988).

Towards the end of inflammatory stage, proliferation stage begins that endothelial cells and fibroblasts are attracted to the wound site under the effect of chemokines and cytokines secreted by immune cells. Proliferation phase can be divided into two parallel sub phases: angiogenesis and granulation tissue formation. Angiogenesis is the process that new blood vessels grow from the pre-existing vessels. It occurs first in order to provide nutrition supply for proliferation stage. Endothelial cells are attracted by chemoattractant and sprouts out to form tube structures (Tonnesen et al., 2000). Hypoxia is a factor to stimulate endothelial cell migration and proliferation that the activated endothelial cells tend to migrate towards the area lack of oxygen. Endothelial cells also release proteases to digest extracellular matrix in order to migrate to destination. Granulation tissue formation happens simultaneously along with angiogenesis. The main source of granulation tissue is fibroblast. Quiescent fibroblasts from adjacent tissue are

activated by growth factors released from immune cells. They migrate to the wound site and proliferate rapidly to form the granulation tissue to seal the wound area (Bainbridge, 2013). While fibroblasts and capillary vessels filling the wound site, fibroblasts also differentiate to myofibroblasts to help the wound repair. Myofibroblasts secrete large amounts of collagen to help building up and strengthening granulation tissue. Myofibroblasts also facilitate the contraction of wound by increase contractile ability of granulation tissue (Grinnell, 1994). Epithelialization happens throughout inflammation and proliferation stage. Keratinocytes, with the help of granulation tissue, migrate towards wound center to cover the outside wound area (Pastar et al., 2014).

The last phase of wound healing is maturation. After wound site is filled up by granulation tissue, the secretion of collagen is slowed and type III collagen is gradually replaced by type I collagen, the original collagen in skin. The disordered collagen matrix is rearranged and cross-linked to form network. Granulation tissue in wound site is converted to the original skin tissue. Maturation stage is the longest stage in wound healing, which may take several months depending on the wound size (Teller & White, 2009).

1.4.2 Neutrophil infiltration

Neutrophils are differentiated from myeloid progenitor cells in bone marrow. Inactivated neutrophils can circulate in the blood flow for several days (Witko-Sarsat et al., 2000). After activation, neutrophils adhere to blood vessel and infiltrate through in order to migrate toward the wound tissue (Gonzalez et al., 2007). Activated neutrophils are attracted by the gradient of cytokines, such as IL-8 and IFN-γ to the wound site (Ellis & Beaman, 2004; Hammond et al., 1995). Neutrophils act as a double-edged sword during wound repair. If neutrophils are over-activated or neutrophil infiltration is not controlled, tissues will be damaged by the proteases

released from neutrophils. However, if neutrophils are not present at wound site, spreading of bacteria will cause infection that strongly slows wound healing time (Smith, 1994). Neutrophils phagocytize bacteria at the infection site. They release different types of protein through a process called degranulation. Four types of granules, azurophilic granules (primary granules), specific granules (secondary granules), tertiary granules, and secretory vesicles are stored in neutrophils upon activation and released in sequential order after arrival at the infection site. The primary granules contain most toxic mediators, such as elastase, cathepsins, and defensins. The secondary granules store lactoferrin and metrix metalloprotease 9 (MMP9) (Borregaard & Cowland, 1997). Degranulation of neutrophils is activated by fMLP or IL-8 induced GPCR activation, which sequentially triggers several signal pathways including Rho guanosine triphosphatase Rac2, β-arrestins, and src family of tyrosine kinases (C. X. Chen et al., 2011). The activated granules translocate to plasma membrane and fuse with it to release the contents (Lacy, 2006). Activated neutrophils can also release fragments of DNA which contains several proteases to kill bacteria. The released DNA fragments form web-like structure to trap the microbes (Brinkmann et al., 2004).

PKM2 is expressed in neutrophils. Activated neutrophils in inflammation diseases had enhanced pyruvate kinase expression and activity. Several reports have shown that PKM2 could be used as serum or faecal markers in various inflammatory diseases. For example, pouch inflammation had increased PKM2 level in stool samples that could be used as indicator. Mycosis fungoides upregulated PKM2 in blood that plasma PKM2 was considered as potential marker (Hapa et al., 2011). A recent proteomic study suggested that PKM2 represented in human neutrophil granules, which provides good evidence of PKM2 release from neutrophils in inflammatory diseases (Lominadze et al., 2005).

1.4.3 Angiogenesis

Angiogenesis is the process of generating new blood vessels from existing ones. It is a sequential and complicated process. Several different types of cells and growth factors are involved. To start angiogenesis, growth factors and cytokines are released from cancer cells, embryonic cells fibroblasts, and immune cells. The factors and cytokines then activate the endothelial cells on the pre-existing vessels through interacting with specific receptors locating on the cell membrane. Meanwhile, mural cells such as smooth muscle cells and pericytes dissociate from the blood vessels to leave space for endothelial cells to migrate. The activated endothelial cells proliferate and sprout out towards the tumor or wound areas to form new vessel tubes which will be stabilized by mural cells afterwards. During the angiogenesis process, endothelial cells also release protease to degrade extracellular matrix in favor of their migration (Risau, 1997).

Angiogenesis is regulated by a variety of pro-angiogenic and anti-angiogenic factors. In quiescent situation, the two types of factors are balanced to prevent unnecessary angiogenic effect. When angiogenesis is needed for embryonic development, wound recovering or cancer progression, pro-angiogenic factors such as vascular endothelial growth factor (VEGF), fibroblast growth factor (FGF), and (platelet-derived growth factor) PDGF, are upregulated that can cause balance to lean towards pro-angiogenic side, which will initiate the angiogenesis process (J. Li et al., 2003).

Angiogenesis involves in several physiological and pathological processes, such as wound healing, tumor growth and metastasis. After blood clot by platelets and clean of wound site by immune cells, angiogenesis takes place at early stage of proliferation and together with fibrogenesis to construct granulation tissues to support wound healing process. Capillary vessels

built through angiogenesis can provide nutrient to fibroblast proliferation and maturation. FGF2 is a 155 amino acids length heparin-binding protein belongs to FGFs family. It regulates angiogenesis by stimulating proliferation and migration of endothelial cells, smooth muscle cells and fibroblasts (Powers et al., 2000). FGF2 is widely expressed in the wound area and FGF2 null mice show delayed healing and thicker scabs when compared with wild-type mice. FGF2 may play a major role in promoting angiogenesis and granulation tissue formation during wound healing (Ortega et al., 1998). It is important to have angiogenesis to "feed" granulation tissues and assist the wound recovering steps. However, the angiogenic effects cannot be overstimulated at later stage of wound healing. It needs to be shut down for the remodeling process.

In pathological conditions, e.g. cancer progression, angiogenesis functions in two processes. In process of tumor growth, cancer cells need angiogenesis to recruit blood vessels for oxygen and nutrient supply. Solid tumor cannot grow beyond 1 mm^3 without the support of blood vessels. To favor tumor growth, cancer cells generate various pro-angiogenic factors to promote angiogenesis. These pro-angiogenic factors stimulate the angiogenesis through activating endothelial cell proliferation and migration, and also mural cell dissociation. The newly divided endothelial cells migrate to the tumor site and form the vessel tubes. Inside the tumor tissues, blood vessel formation is not well regulated due to genetic errors of cancer cells and tumor endothelial cells. The disorganization of tumor blood vessel reduces the anti-therapy efficiency because unregulated vessel network causes resistance to blood flow, which reduces delivery to all cancer cells. Unregulated vessels also generate local hypoxia in tumor which continuously activates angiogenesis. In addition, angiogenesis plays an important role in cancer metastasis. At the late stage of cancer progression, cancer cells gain ability to penetrate to surrounding tissues to form secondary tumors, or even to invade into the blood vessels and

circulate with the blood flow to other tissues and organs. Newly formed tumors can stimulate neovascularization to recruit nutrient supply for rapid growth. Studying angiogenesis in cancer progression can provide targets for anti-angiogenic therapy to restrain tumor growth in early stage and prevent metastasis (Bergers & Benjamin, 2003; Weis & Cheresh, 2011).

1.4.4 Myofibroblast differentiation

Fibroblasts differentiate to myofibroblasts during wound healing and tissue repair. The differentiated myofibroblasts gain high contractile ability to help wound healing process. After the wound is healed, myofibroblasts undergo apoptosis to prevent excessive stress in the tissue. If myofibroblast differentiation is not well controlled, it causes fibrotic diseases and supportive matrix in tumor growth (Eckes et al., 2000).

The differentiation from fibroblast to myofibroblast is divided into two main steps. The first step is from fibroblast to proto-myofibroblast. Fibroblasts are recruited to the wound site and acquire minor stress fibers by influence of mechanical force. The second step is from proto-myofibroblast to differentiate myofibroblast. Proto-myofibroblasts are activated by growth factors such as TGFβ to stimulate the expression of α-SMA. α-SMA binds with stress fiber bundles to further increase contractile activity of myofibroblasts (Hinz et al., 2001; Masur et al., 1996).

Myofibroblasts have various origins other than fibroblasts. Fibroblasts are the major resources of myofibroblasts which are attracted to the inflammation site during wound repair. Pericytes and smooth muscle cells from blood vessels can also be transformed into myofibroblasts. Fibrocytes generated from bone marrow are found to be another important origin in the wound case. It is also discovered that fibrocytes take place in fibrosis and tumors to play a role of myofibroblast differentiation (Baum & Duffy, 2011).

To identify myofibroblasts, three structural features are important: stress fiber bundles, high attachment force, and increase cell-cell interaction. α-SMA is the most commonly used myofibroblast marker. However, α-SMA is also expressed in other cells such as smooth muscle cells. In addition to the stress features and α-SMA expression in myofibroblasts, induced extracellular matrix is found in differentiated myofibroblasts. Collagens type I, III, IV, and V are secreted by differentiated myofibroblasts to build up the matrix network surrounding myofibroblasts and strengthen the tissue contractile (Hinz, 2007).

The major pathway to activate myofibroblast differentiation is TGFβ-Smad pathway. TGFβ interacts with to activate TGFβ receptor type II which subsequently recruits TGFβ receptor type I. Association of TGFβ receptor heterodimer activates its serine/tyrosine kinase activity, and phosphorylates Smad2/Smad3. Phosphorylated Smad2/Smad3 binds to Smad4 and translocates into the nucleus to activate α-SMA transcription through interacting with α-SMA promoters (Engler et al., 2011; Midgley et al., 2013). A few of Smad independent pathway has been revealed under activation of TGFβ. PI3K is activated by TGFβ signal and transfers the signal to downstream p21-activated kinase-2 (PAK2), which induces the expression of α-SMA to promote myofibroblast differentiation (Wilkes et al., 2005; Wilkes et al., 2003). Connective tissue growth factor and gelectin-3 are cooperatively worked with TGFβ in some circumstances. Integrin is also found to cooperate with TGFβ receptor in the TGFβ-Smad signal pathway (Ding et al., 2008; Thannickal et al., 2003). IL-6 and nerve growth factor are discovered to activate myofibroblast differentiation without the presence of TGFβ, but inhibition of TGFβ signal is not ruled out in the study (Gallucci et al., 2006). Thus, the independent of TGFβ signal pathway may still need the downstream of TGFβ pathway.

1.4.5 From immune response to proliferation

Neutrophils and macrophages are recruited to wound site after injury. They clean bacteria and damaged cell debris to provide a clean wound for closure. Another important function of immune cells is to initiate and promote proliferation, including angiogenesis, fibrogenesis and re-epithelialization. Neutrophils and macrophages secrete numbers of growth factors and cytokines to activate endothelial cells and fibroblasts (Barrientos et al., 2008).

Macrophage is considered the major resource of growth factors and cytokines to activate angiogenesis and fibrogenesis. TGFβ is released from macrophage and activates both angiogenesis and fibrogenesis during proliferation stage. A chicken chorioallantoic membrane (CAM) model showed that TGFβ-1 induced the formation of large blood vessels and also increased fibroblast density. TGFβ-1 activates both proliferation and migration ability of endothelial cells (E. Y. Yang & Moses, 1990). A study revealed that tumor necrosis factor α (TNFα) secreted from activated macrophages blood vessel formation in a rat cornea model. TNFα stimulated chemotaxis of endothelial cells and enhanced tube formation (Leibovich et al., 1987). Granulocyte/macrophage colony-stimulating factor (GM-CSF) is another growth factor secreted by macrophages. GM-CSF is found to induce early stage of endothelial tube formation and late stage of new vessel maturation by regulating VEGF and Ang-Tie expressions (Zhao et al., 2014).

Functional study of neutrophil during wound repair is mainly focused on anti-microorganism. A group claimed that activated neutrophils increased VEGF expression and released VEGF to promote angiogenesis (Gong & Koh, 2010). IL-1 and IL-6 are also correlated with proliferation stage during wound healing. IL-1α and IL-1β upregulated the expression of keratinocyte growth factor (KGF) in fibroblasts (Tang & Gilchrest, 1996). IL-6 deficient and IL-

6 antibody treated mice showed delayed wound closure (X. L. Zhang et al., 2005). In addition, infiltrating neutrophils functioned in tumorigenesis to switch the pro-angiogenesis (Nozawa et al., 2006). Given the fact that neutrophils arrive at wound site in the early inflammation, they may play a role of initiating angiogenesis and fibrogenesis during wound repair.

1.4.6 Treatment of wound

For treatment of wound to facilitate repair, different aspects are considered. Collagen dressings, hydrogels, and growth factors are used to enhance epithelialization. Some drugs are used to enhance granulation tissue formation. To prevent infection, antimicrobials are always combined with other drugs in severe wound cases. Several growth factors are released during wound healing to facilitate the process. Thus, applications of growth factors are proved to have positive effect on wound healing (Falanga, 2004). Topical application of EGF was first found to enhance wound healing (Brown et al., 1989). PDGF is also approved by FDA for treatment of wound (Pierce et al., 1991). However, the application of growth factors is not recommended in clinical treatment. Different stages of wound are well organized in a sequential order. For each reaction, it needs to be switched on and off at certain time point. Excessive application of growth factors may cause prolonged angiogenesis and granulation tissue growth which will inhibit wound healing by postponing the maturation process.

1.5 Liver fibrosis and cirrhosis

1.5.1 Introduction of liver fibrosis and cirrhosis

Liver fibrosis is characterized by the accumulation of extracellular matrix, especially collagen in liver. Chronic liver damages induced by alcohol abuse, hepatitis virus, and obesity are the main causes of liver fibrosis. The accumulated extracellular matrix proteins disrupt the architecture of liver tissue by forming scar-like network. Advanced liver fibrosis leads to

cirrhosis which is defined as separation of the hepatocyte nodules by scar tissue. In the late stage of cirrhosis, scar tissue gradually replaces original liver structure, and finally causes the block of portal blood flow, and portal hypertension (Bataller & Brenner, 2005; Friedman, 2003).

Liver fibrosis is not easy for diagnosis until development of late stage cirrhosis. Chronic liver damage takes several years to progress of liver fibrosis to cirrhosis. Cirrhosis is often correlated with other complications such as ascites, esophageal variceal bleeding, and hepatocellular carcinoma. Biopsy is the standard method for diagnosis of liver fibrosis. Histology staining of biopsy can be graded by pathologist in order to identify the stage of liver fibrosis. Given that collagen expression is the key feature of liver fibrosis, Sirius red staining of biopsy is another convenient method to identify fibrotic status. However, biopsy is an invasive method with high error. One time biopsy examination is not suitable for detection of progression of fibrosis (Thampanitchawong & Piratvisuth, 1999). Serum markers of fibrosis are used as a noninvasive detection for liver fibrosis. Liver fibrosis patients show high serum level of aminotransferase, total proteins, collagen, and TIMP-1 (Arthur, 2000). Although serum marker screening is not invasive method compared with biopsy, it is still not able to identify the progression of liver fibrosis. Imaging techniques, such as ultrasonography, computed tomography, and MRI, are also applied in the diagnosis of liver fibrosis due to their noninvasiveness and good vitalization (Hirata et al., 2001; Popper & Uenfriend, 1970).

1.5.2 Pathogenesis of liver fibrosis

Liver fibrosis starts with inflammation caused by hepatic injury. In regular case, fibrogenesis starts after hepatic injury and ends when injury is healed, so the inflammatory response is stopped afterwards. However, in the fibrosis case, the hepatic injury persists overtime, which leads to prolonged inflammation and subsequent fibrogenesis. Ultimately,

hepatocytes are replaced with various ECM and eventually the liver fails to heal back. During the progression of liver fibrosis, ECM accumulation first occurs around portal tracts or perisinusoidal areas, then elongates to form bridges between the portal tracts, and finally expands to large area and disrupts liver structure. This is so called frank cirrhosis. Several ECM are involved in liver fibrosis, including collagens (type I, III, and IV), fibronectin, elastin, laminin, and proteoglycans. The accumulation of ECM is caused by inhibition of protease such as MMPs, and activation of TIMPs, specific inhibitors of MMPs.

Hepatic stellate cells (HSCs) are the main player in liver fibrosis development and progression. In the normal liver, quiescent HSCs reside in liver and function to store vitamin A. In fibrotic liver, HSCs are activated by different types of factors and migrate to the injury site to secrete larger amounts of ECM. Platelets are the first cells coming to the injury site. They release PDGF, TGFβ, and also EGF to activate HSCs including proliferation, migration and differentiation (Marra, 1999). Activated Kupffer cells at the fibrotic site also secrete large amounts of cytokines to stimulate HSCs (Naito et al., 2004). Since hepatic injury results in inflammatory response, infiltrated leukocytes also join with Kupffer cells to activate HSCs. Neutrophils produce ROS to stimulate the collagen synthesis of HSCs. It was found that co-culture of neutrophils with HSCs induced collagen production up to three-fold in vitro. In addition, several interleukins released by Th1 and Th2 lymphocytes also play a role in HSCs activation and differentiation. Activated HSCs acquire several behaviors to favor fibrogenesis. Activated HSCs are attracted by chemoattractants, and their migration activity is upregulated. ECM production is increased in the activated HSCs. Activation transforms HSCs to myofibroblasts under stimulation of TGFβ. Induction of collagen expression is the most typical feature in TGFβ activation of HSCs. On the other hand, ECM degradation is another important

phenomenon of activation of HSCs. MMPs secreted by HSCs is first upregulated in early stage of fibrosis to degrade pre-existing ECMs. As long as the fibrosis goes on, the activity of MMPs is reduced by increase tissue levels of TIMP. Increase in TIMP prevents MMP from degrading the newly formed ECM network, and maintains progression of fibrosis. Activated HSCs also acquire high contractile ability due to expression of α-SMA and formation of fiber bundles. Endthelin-1 is another activator to stimulate contractile ability besides TGFβ (Sato et al., 2003).

1.5.3 Reverse of liver fibrosis

Liver fibrosis and cirrhosis was considered as "irreversible" for many years. However, more and more experiments and clinical evidences have shown that liver fibrosis and cirrhosis are reversible. One of the most critical keys in those discoveries is the apoptosis of activated HSC. One group showed that rats with liver fibrosis induced by CCl_4 were able to recover by removing activated HSCs through apoptosis. Both generator of new ECM and protector of ECM degradation were eliminated by removal of activated HSCs. The group followed tests with another model, bile duct ligation, and found that the activated HSCs apoptosis was significantly enhanced during recovery stage (Benyon & Iredale, 2000; Elsharkawy et al., 2005).

The survival and apoptosis of HSCs is regulated by several mediators. ECM is the main source to support growth and migration of HSCs. One study suggested that collagen type I played a role in maintaining the activation of HSCs and mutation of collagen type I resulted in activated HSCs apoptosis (Bataller & Brenner, 2001). Integrin is also critical for the survival of HSC. The activated HSCs express integrin αvβ3 on cell membrane. Knockdown integrin αvβ3 by RNAi or inhibition by antibody against the integrin was found to induce HSCs apoptosis (Iwamoto et al., 1999; Zhou et al., 2004). Several growth factors have been shown to inhibit HSCs proliferation or induce HSCs apoptosis. Nerve growth factor (NGF) is a growth factor

secreted by hepatocytes. Treatment of activated HSCs by NGF leads to inhibition of proliferation. Fas and FasL have been studied for the induction of HSCs apoptosis (Trim et al., 2000). The activated HSCs have increased expression of both Fas and FasL. Treatment of activated HSCs with FasL or Fas antibody causes apoptosis in vitro. TNF-related apoptosis – inducing ligand (TRAIL) is another apoptotic mediating factor of activated HSC. The TRAIL and TRAIL receptor expression is also upregulated in the activated HSCs in the similar manner as of Fas and FasL. TRAIL and TRAIL receptor agonists can induce HSCs apoptosis in vitro (Anan et al., 2006). Nuclear factor kappa B (NF-κB), a well-studied DNA transcription regulator in several inflammatory events, is involved in the protection of activated HSCs from apoptosis by upregulating several anti-apoptotic factors including, TRAF-1, TRAF-2, c-IAP1 and c-IAP2. A study suggested that treatment of NGF induced apoptosis of HSCs and also reduced the transcriptional activity of NF-κB (Luedde & Schwabe, 2011; Qu et al., 2007; Takahra et al., 2004). In summary, liver fibrosis and cirrhosis have potential to be reversible. Therapy targeting activated HSCs apoptosis is proved to be a promising method for treatment of liver fibrosis and cirrhosis.

1.6 Rational and Aims

Previous studies from our laboratory demonstrated that extracellular PKM2 released from cancer cells promoted tumor growth through activating angiogenesis. PKM2 promoted tumor angiogenesis by stimulating endothelial cell proliferation, migration, and adhesion. Angiogenesis plays an important role in proliferation stage of wound healing. It connects granulation tissue formation with inflammatory response. Cytokines and growth factors are released from immune cells during inflammation stage, and then activate angiogenesis. The newly formed vessels provide blood flow and nutrient supply for growth of granulation tissue. Given that PKM2 is a

protein expressed and secreted in both cancer cells and neutrophils, and the facts that cancer progression and wound healing share surprisingly high similarity in many features, it is very reasonable to hypothesize that PKM2 may play a similar role of promoting angiogenesis in wound healing. Therefore, we hypothesize that extracellular PKM2 released by neutrophils promotes angiogenesis to facilitate wound healing process.

In our laboratory, we found that extracellular PKM2 activated endothelial cells via integrin αvβ3. Fibroblasts upon differentiation have increased expression of integrin αvβ3. Integrin αvβ3 involves in the myofibroblast differentiation. Given the fact that fibroblasts are the main source in proliferation stage, it is very likely that extracellular PKM2 at wound site can stimulate fibroblasts and myofibroblast differentiation through integrin αvβ3.

In our preliminary study of liver fibrosis, we found that the level of extracellular PKM2 is gradually increased in the liver fibrosis and cirrhosis patients. The expression level of integrin αvβ3 is correlated with the level of extracellular PKM2. The activated HSCs express high level of integrin αvβ3 during liver fibrosis. Given that the activation of integrin αvβ3 mediate the survival pathway, we hypothesizes that extracellular PKM2 released by neutrophils prevents HSCs from apoptosis, thus worse liver fibrosis.

In this dissertation, the aim is divided into three parts. First, I examine the effect of extracellular PKM2 during wound healing process. Second, I study the interaction between PKM2 and fibroblasts in the case of myofibroblast differentiation. Last, I test the function of extracellular PKM2 against HSCs in liver fibrosis. Here, I demonstrated that topical application of PKM2 promoted wound healing process through activating angiogenesis. The extracellular PKM2 at wound site was released from neutrophils under the influence of degranulation. On the other hand, neutralization of extracellular PKM2 during wound healing inhibited the process. I

claimed that PKM2 activated myofibroblast differentiation through "αvβ3-PI3K-PAK2" pathway, which was independent of the classical "TGFβ-Smad" pathway. I also demonstrated that extracellular PKM2 protected HSCs from apoptosis via integrin αvβ3 survival pathway during liver fibrosis. Neutralization of extracellular PKM2 during liver fibrosis relieved the stress of liver fibrosis. Therefore, I established a connection between inflammatory response and differentiation in physiopathological condition that extracellular PKM2 released from neutrophils activates endothelial cells and fibroblasts in both wound healing and liver fibrosis.

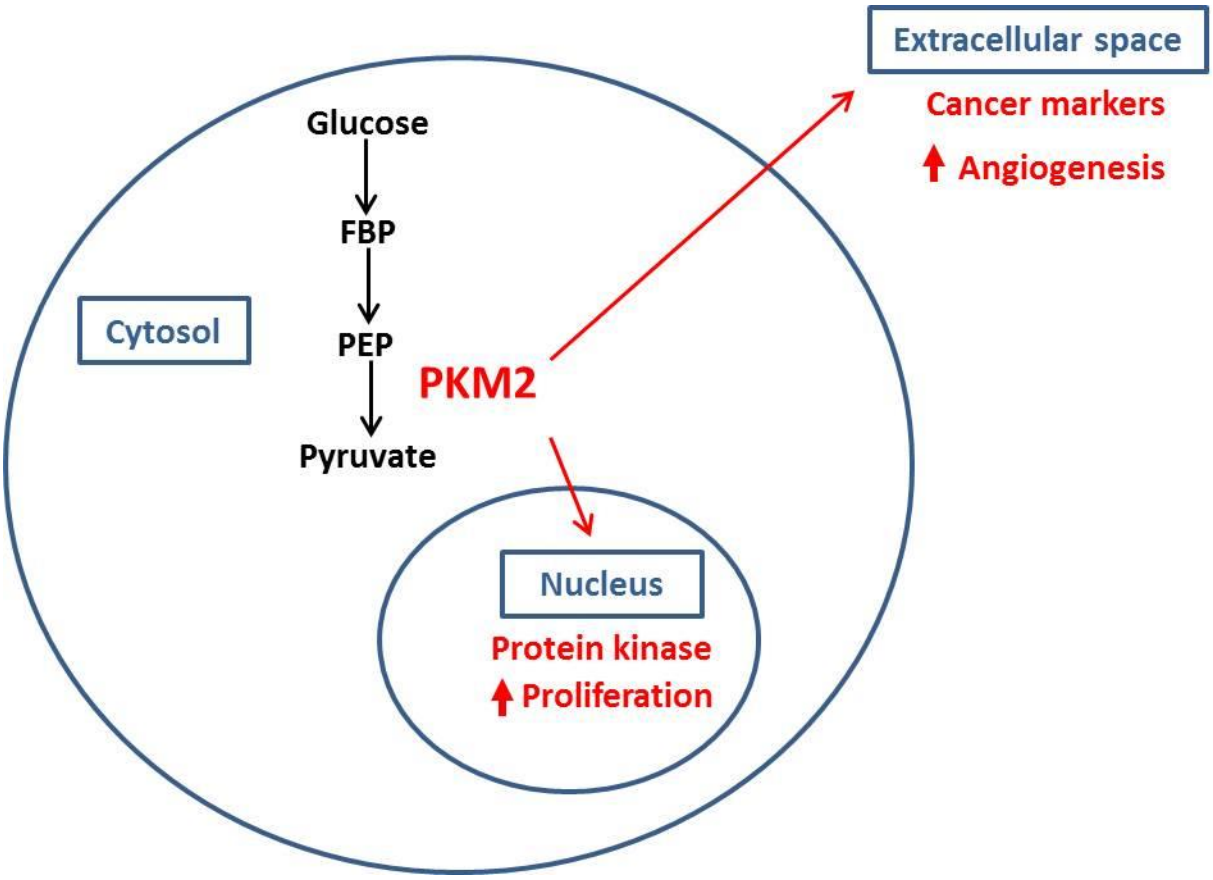

Figure 1.1 Locations and functions of PKM2

PKM2 converts PEP to pyruvate in cytosol. PKM2 can translocate in to cell nucleus and extracellular space. Nuclear PKM2 acts as protein kinase to phosphorylate histone H3 and STAT3. PKM2 also interacts with transcription factors to induce cell proliferation. Extracellular PKM2 is used as serum marker for multiple cancers and immune diseases. Cancer cells secrete PKM2 to promote angiogenesis by activating endothelial cell proliferation and migration.

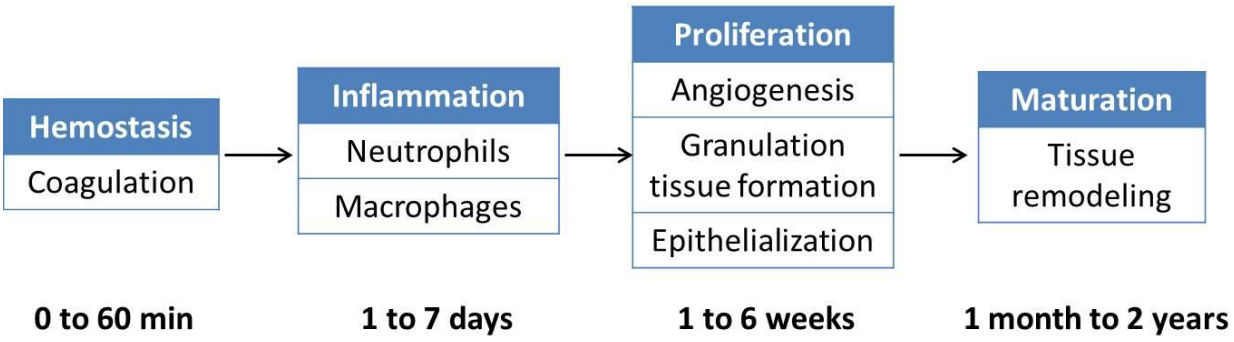

Figure 1.2 Wound healing process

Wound healing process is divided into four stages, hemostasis, inflammation, proliferation and maturation. Each stage is well regulated by different factors in order. The whole wound healing process takes months to years to heal.

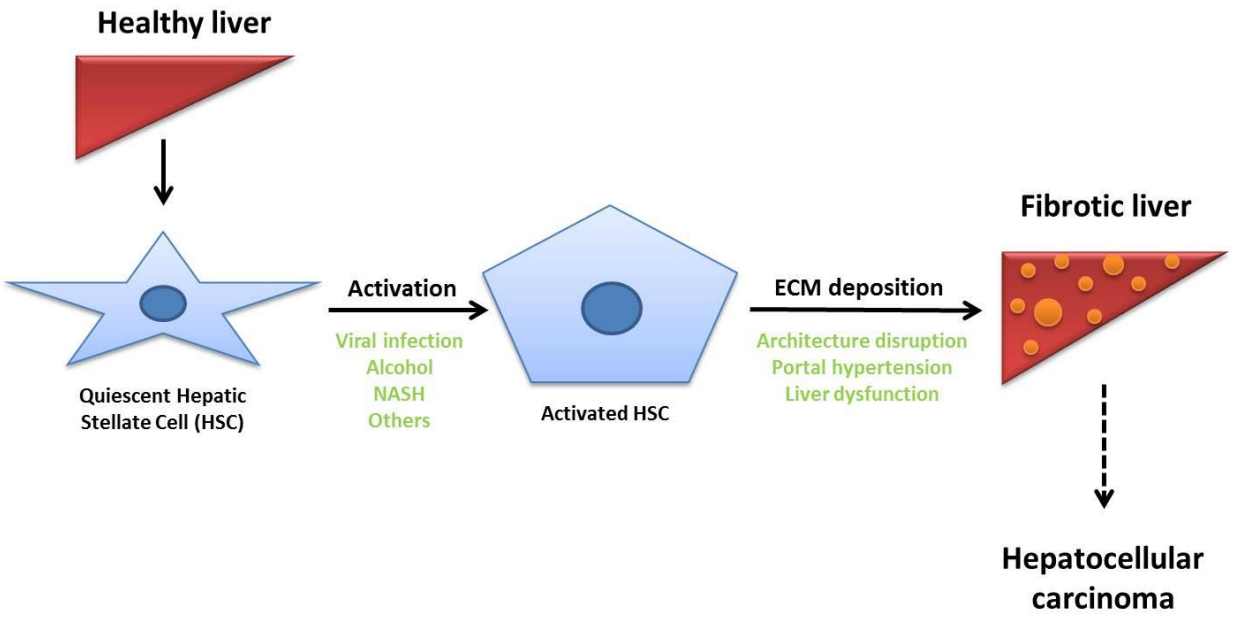

Figure 1.3 Liver fibrogenesis

After activation by different stimulators, quiescent HSCs transform into activated HSCs and secret large amount of extracellular matrix. If this is unsolved and lasts for several years, healthy liver is damaged and becomes fibrotic. Advanced liver fibrosis develops into cirrhosis, and has higher incidence of hepatocellular carcinoma.

CHAPTER 2 EXTRACELLULAR PYRUVATE KINASE M2 RELEASED FROM NEUTROPHILS FACILITATES EARLY WOUND HEALING BY PROMOTING ANGIOGENESIS[1]

[1] This chapter was published in Wound Repair and Regeneration.

2.1 Abstract

During wound healing, neutrophil infiltration represents the early inflammation response to function in cleaning microbes. However, the role of activated neutrophil in tissue regeneration is still not well understood. Here, we report that the activated neutrophils at wound site release PKM2 through degranulation at the early stage of wound healing. Extracellular PKM2 facilitates wound healing by promoting angiogenesis. Our study reveals a new molecular connection between early inflammation response and proliferation phase in wound repair.

2.2 Introduction

Cutaneous wound healing is a complex process that skin tissue repairs itself after injury. After wound induction, hemostasis first occurs and broken blood vessels are clotted by platelets. Different types of immune cells infiltrate into wound site to clean microorganisms and stimulate the later proliferation stage. Macrophage is considered the major source of activating angiogenesis, whereas neutrophil mainly plays a role in cleaning microbes and dead cell debris. However, several studies have showed that the function of infiltrated neutrophil is still controversial, that neutrophil is found to inhibit re-epithelialization, but also promote angiogenesis during wound healing (Singer & Clark, 1999).

Pyruvate kinase is an enzyme acts at the last step of glycolysis that converts PEP to pyruvate to generate ATP. There are four isoforms of pyruvate kinases, L/R and M1/M2. PKM1 and PKM2 are transcribed from the same mRNA with alternative splicing. PKM2 is expressed in

highly proliferating cells with low pyruvate kinase activity compared with other pyruvate kinases. The inactivation of PKM2 slows the process of glycolysis, that more biosynthesis building blocks are accumulated in favor of cell proliferation. In addition to the role in glycolysis, PKM2 is involved in other biological processes, such as transcription regulation, immune response, and metabolism control (Mazurek et al., 2005).

High level of PKM2 is found in the blood stream of cancer patients. Serum and stool PKM2 levels have been used as diagnostic marker for various cancers. The level of PKM2 in blood circulation is strongly correlated with progression of cancer (Mazurek, 2007). Our laboratory previously discovered that extracellular PKM2 promoted tumor growth by activating angiogenesis. Extracellular PKM2 interacted with integrin αvβ3 on cell surface and stimulated proliferation and migration of endothelial cells. PKM2 is also detected in the blood stream of various inflammation diseases. Given that PKM2 is expressed in the immune cells, the function of extracellular PKM2 might be correlated with inflammation.

2.3 Results

2.3.1 rPKM2 facilitates wound healing by activating angiogenesis.

We previously found that recombinant PKM2 (rPKM2) plays an important role in tumor angiogenesis. Since angiogenesis is a key stage during wound healing, we first tested the topical application of rPKM2 mixing with cream in the wound healing CD-1 mouse model. Buffer and rPKM1 were used as controls. After wound induction, the size of wound was measured on day 0, day 3, day 6, and day 8 (Figure 2.1 A). The quantitative curve showed that rPKM2 group had smaller wound area on day 3 and day 6 compared with rPKM1 and buffer groups. The differences among three groups were not significant on day 8 (Figure 2.1 B). From skin wound pictures, the wound size was smaller in rPKM2 group, compared with rPKM1 and buffer groups

on day 3. The difference was more significant on day 6. The wound size in all groups on day 8 looked similar (Figure 2.1 C). In a word, topical application of rPKM2 facilitates wound healing process.

To test the angiogenic effect during wound healing, skin tissue at wound site was stained with CD-31 (endothelial cell marker) using immunofluorescence staining. rPKM2 group showed more condensed signal compared with the staining in rPKM1 and buffer groups (Figure 2.2 A). To quantify the immunofluorescence staining, we analyzed the micro vesicular density (MVD) and the area covered by CD31 positive staining. rPKM2 group showed significant increase in both MVD and CD31 positive area (Figure 2.2 B&C). As a result, topical application of rPKM2 promotes wound healing by activating angiogenesis.

2.3.2 rPKM2 promotes granulation tissue growth during wound healing

Angiogenesis and the growth of granulation tissue are strongly connected with the proliferation stage of wound healing. Since topical application of rPKM2 promotes angiogenesis, we pursued the effect of rPKM2 on the growth of granulation tissue. Granulation tissue is formed during the proliferation stage of wound healing. It consists of connective tissue and capillary networks that build up from the bottom of the wound and fill the whole wounded area. It also protects the wound from further infection. After proliferation stage, granulation tissue gradually remodels to normal skin or tissue. It is important to have the proper granulation tissue growth during wound healing. The growth of granulation tissue at early time of wound healing indicates a start of the proliferation stage. By measuring the thickness of granulation tissue (distance from bottom to top of the granulation tissue), we can analyze the process of wound healing, and how the wound is healed.

We first examined the inner side of wound skin. rPKM2 group had complex capillary structure and thick granulation tissue, whereas rPKM1 and buffer groups had thin granulation tissue, or even transparent membrane structure (Figure 2.3 A). To quantify the thickness of granulation tissue, the slides with vertical cut were stained by H&E staining. The thickness of granulation tissue was measured from the outside to the inside of wound skin. As a result, the thickness of granulation started to increase as early as day 3 in rPKM2 group. This effect continuously maintained till the end of the experiment (Figure 2.3 B). To further analyze the growth of granulation tissue, fibroblast was stained in the frozen section of wound skin using fibroblast marker (ER-TR7). rPKM2 group had more condensed fibroblast signal compared with rPKM1 and buffer groups. The quantified result showed that the fibroblast positive area was doubled in rPKM2 group (Figure 2.3 C). In summary, Topical application of rPKM2 stimulates the growth of granulation tissue during wound healing.

2.3.3 Application of PKM2 antibody slows wound healing process

Given the effect of rPKM2 during mouse cutaneous wound healing, we generated a new mouse wound healing model using PKM2 antibody to neutralize extracellular PKM2 during wound healing. Buffer and IgGCon were used as controls. The rabbit monoclonal PKM2 antibody was first I.P. injected into CD-1 mice one day before wound induction to let it circulate in the blood system. The following procedure was similar as in the previous wound healing experiment (Figure 2.4 A&B). The healing speed of wound was slower in IgGPK group compared with buffer and IgGCon groups (Figure 2.4 C). From the quantitative curve, IgGCon and buffer groups were at the same trend, compared with IgGPK group with a slow start from day 2. This inhibition effect continued till day 8 (Figure 2.4 B).

To determine the effect of PKM2 antibody in angiogenesis, we performed the same CD31 staining and quantified with MVD and CD31 positive area. We clearly saw the capillary structure in buffer and IgG groups, even tube structure in buffer group. The density and length of vessels were significantly decreased in IgGPK group. The quantified data showed that both MVD and CD31 positive area were reduced under the treatment of PKM2 antibody (Figure 2.5 B&C).

2.3.4 PKM2 was released from neutrophils in wound healing

To find out whether PKM2 is endogenous in wound healing, we collected the skin samples on day 3 of wound healing in both rPKM2 treated and non-rPKM2 treated groups. Samples were paraffin embedded and stained with PKM2 antibody for IHC. The non-wound tissue did not have any positive signal of PKM2. In wound tissue, compared with rPKM2 treated sample, non-rPKM2 treated one had light signal of PKM2 positive staining (Figure 2.6 A). This indicated that PKM2 was endogenous during wound healing. In cancer progression, PKM2 is secreted by cancer cells and locates in the extracellular space. After observation under higher magnification, we found that most PKM2 located in the extracellular space (Figure 2.6 B). The cells containing intracellular PKM2 had similar polymorphonuclear phenomenon like neutrophils. We suspected that neutrophils are the resource of extracellular PKM2 during wound healing. To test the correlation between extracellular PKM2 and neutrophils, we generated a time-series wound skin samples from day 0 to day 5 and stained the samples with PKM2 and Ly6G antibody (neutrophil marker). By quantifying the positive signal in each staining, we observed a similar pattern of increase and decrease in PKM2 and Ly6G staining (Figure 2.6 C&D). This meant that the presence of neutrophils is highly correlated with extracellular PKM2.

We used in vitro system to study the release of PKM2 from neutrophils. Neutrophils were isolated from mouse bone marrow and activated with fMLP and damnacanthal for 15 min. Both culture medium and cell lysates were collected for immunoblot. The medium PKM2 level was increased in the fMLP and damnacanthal treatments (Figure 2.7 A&B). We also obtained a sucrose gradient sample of neutrophil fractionation from Dr. Yuan Liu's lab. Two sets of samples, inactivated neutrophils and fMLP activated neutrophils were examined by immunoblot using PKM2, β-actin (represents cytosolic part) and CD11b (represents granule part) antibodies. In the inactivated neutrophils, PKM2 located in the cytosol as β-actin. In the fMLP activated neutrophils, PKM2 had another fraction in granules as CD11b. In summary, we revealed that PKM2 is released from activated neutrophils.

2.3.5 Inhibition of neutrophil infiltration reduces extracellular PKM2

To further test the correlation between extracellular PKM2 and neutrophils, we used beige-J mouse, a mouse strain with neutrophil infiltration defect, as the model in wound healing study. At day 3 after wound induction, wild-type group had reduced wound size compared with beige group (Figure 2.8 A). On the other hand, wild-type group had thicker granulation tissue (Figure 2.8 B). IHC staining of wound sites showed that wild-type group had both Ly6G and PKM2 positive signals, but beige group had no signal (Figure 2.8 C). This indicated that beige-J mice had reduced extracellular PKM2 at wound site as a result of defective neutrophil infiltration. To further confirm the correlation between extracellular PKM2 and neutrophils, we also applied rPKM2 to the wound of beige-J mouse to test whether this application can overcome the defect. Reasonably, rPKM2 application increased the speed of wound healing, but it was still slower compared with wild-type mouse (Figure 2.8 D).

2.3.6 Identification of PKM2 release from neutrophil degranulation

To test whether degranulation is the way to release PKM2, we used several degranulation inhibitors. PP1, SB 203580, and piceatannol were pre-treated before fMLP activation. Compared with fMLP activation of PKM2 level in the culture medium, the inhibitors treated ones had different degrees of reduction. Piceatannol had the best inhibitory effect among three inhibitors (Figure 2.9 A). We also examined the time-series of fMLP activation in PKM2 release. We picked up 5 min, 10 min, and 30 min to test the level of released PKM2 in the culture medium, which showed gradually increasing (Figure 2.9 B&C). In summary, in vitro cell analysis demonstrated that PKM2 is released by neutrophils through degranulation.

2.4 Discussion

Wound healing is a slow and complex process. Opened wound area causes several infection problems. To prevent infection and seal wound at an early time is the major goal of fast wound healing. Different immune cells function in cleaning microorganisms and promoting granulation tissue formation. A major question in wound healing process is what is role of immune cells during the early stage of wound healing. Here we found that neutrophils as the early resources of immune cells release PKM2 to facilitate granulation stage of wound healing. It fills a gap between early inflammation and proliferation stage. We demonstrated that PKM2 is released from neutrophils via degranulation process. The extracellular PKM2 activates angiogenesis and promotes the growth of granulation tissue in proliferation stage. We followed up to use PKM2 antibody to inhibit the connection between neutrophil infiltration and granulation tissue growth. The wound healing was significantly slowed and the angiogenic effect was reduced.

Another question is why and how neutrophils release PKM2. Neutrophil is one of the earliest immune cells arrive at wound site. Neutrophil infiltration reaches to a peak around 48 to 72 hours in mouse cutaneous wound. High density of neutrophils accumulates at wound site and release large amount of PKM2 to stimulate angiogenic activity. The induced angiogenesis supports the later coming fibroblasts to build up granulation tissue. Extracellular PKM2 plays an important role in early wound healing process as the connection between inflammation and proliferation stage. Neutrophils have several secretory pathways for protein transportation. Since PKM2 is a cytosolic protein, the classic secretory pathway which needs membrane recognition peptide is not the proper transporting method. Our experiments showed that the release of PKM2 was highly correlated with degranulation. PKM2 level was gradually increased in the culture medium of activated neutrophils and was significantly reduced under the effect of degranulation inhibitors. We thought PKM2 in cytosol was interacted with the protein in or on the granules and was coupled transported out of the cells during degranulation.

2.5 Materials and Methods

2.5.1 Mouse Wound Healing Model

All animal experiments were carried out in accordance with the guidelines of IACUC of Georgia State University. CD-1 mice were anesthetized with 3% isoflurane and kept under anesthesia during the whole surgery process. The furs on back of mice were shaved with electronic hair shaver and further cleared with Nair (Church & Dwight Co Inc.). The shaved areas were cleaned and aseptically prepared with cotton swabs soaking in antiseptic surgical scrub solution and 70% alcohol alternatively for three times. The body temperature of mouse was maintained by using a circulating water bed. The surgical areas were kept sterile throughout the surgery process. The wounds were induced by using a 6 mm diameter dermatology biopsy

punch. The photo of wound was taken and the size was measured by caliper. Vanicream (Stacy's Compounding Pharmacy) mixed with buffer, rPKM1 or rPKM2 was applied on the wound. The wounds were then dressed with transparent adhesive films, and wrapped with adhesive tapes. The mice were carefully monitored during surgery and 30 min after, and then single housed to prevent scratching. The wounds were re-opened and same procedure of cream application and dressing were performed on day 3, day 6. The mice were euthanized on day 8 by CO_2. Skin wound samples were collected and put in frozen section or paraffin embedded. The slides were cut vertically across the wound area.

2.5.2 Tissue Sample Preparation

The wounded areas were cut off for sample preparation. For the frozen tissue, the samples were immersed in the OCT solution and snap-frozen in liquid nitrogen. The frozen section slides were cut with cryostat. For paraffin embedding tissue, the samples were incubated in the formalin solution at room temperature for two days, and then stored at 4 ˚C in 70% ethanol. The paraffin embedding process was done by using Citadel with the standard protocol, and then embedded with Histostar. The paraffin embedding section slides were cut with microtome.

2.5.3 H&E Staining

The paraffin slides were baked at 60 ˚C for 2 hours, and then incubated with the following solutions 5 min each in order (three times xylene, twice 100% ethanol, 90% ethanol, 70% ethanol, 50% ethanol, 30% ethanol, and distilled water). The slides were incubated with 0.1% Mayers Hematoxylin for 5 min and washed with running water. The slides were dipped in 0.5% Eosin for 1 min and then washed with water. The slides were dehydrated by incubated with

the previous solutions reversely. At last, the slides were mounted with mounting medium and covered by coverslip. The coverslips were sealed with nail polish and waited for one day to dry.

2.5.4 Measurement of Granulation Thickness

The pictures shown in the figure were taken by camera. The wound skin samples were cut off and flipped over. The H&E staining slides from buffer and rPKM2 group at different time points were observed under microscope. The distance between out-layer and inner-layer of skin was measured for each slide. All results were averaged and normalized with the result of buffer group on day 3.

2.5.5 Neutrophil Isolation

CD-1 mice were killed, and the femur and tibia were removed and cleaned. HBSS-EDTA was injected through the bone to push out cell clumps. The cells were washed once with HBSS, laid on a three-layer Percoll gradient (78%, 69%, and 52% from bottom to top), and then centrifuged at 1500 g for 30 min. The upper part of 78% and interface between 78% and 69% were collected and washed twice with HBSS-EDTA. The cells were resuspended in HBSS-EDTA for later experiment.

2.5.6 Activation of Neutrophils

To evaluate the release of PKM2 to culture medium, isolated neutrophils were treated with 1 μM fMLP at 37 ˚C for 20 min or 1 μM damnacanthal at 25 ˚C for 20 min in HBSS, and then centrifuged to collect the medium for following ELISA and Western blot. Cell pellets were lysed with RIPA buffer for the analysis of cytosol components. For the inhibitor assay, cells were pretreated with PP1 (10 μM), SB 203580 (1 μM), and piceatannol (20 μM) for 15 min, followed by same fMLP stimulating procedure. For the time series assay, cells were treated with 1 μM fMLP at 37 ˚C for 5, 10, and 30 min, respectively.

2.5.7 Beige Mice Wound Healing Protocol

The beige mutant and wildtype mice were purchased from The Jackson Laboratory. The wound was generated same as in the CD-1 mice previously. Generally, mice were anesthetized and kept under anesthesia during the whole surgical procedure. The furs on back of mice were shaved and the surgical site on mouse back was cleaned and aseptically prepared. The wounds were induced by using a 6 mm diameter dermatology biopsy punch, and then dressed with transparent adhesive film (3M), and wrapped with adhesive tape. The mice were euthanized on day 3, and the wounded skins were cut off and processed for paraffin embedding.

2.5.8 Sucrose Gradient Centrifugation

Freshly isolated neutrophils were lysed and loaded onto a prepared sucrose gradient from 50% at bottom to 20% at top. After centrifugation at 66000 x g for 90 min, fractions were collected and prepared for immunoblot.

Figure 2.1 Topical application of rPKM2 facilitates wound healing.

(A). Diagram of mouse wound healing experiment. Cutaneous wounds were induced on the back of three groups of mice on day 0, and applied with cream mixing buffer, rPKM1, and rPKM2 respectively. The cream mixing with reagent was re-applied on day 3 and day 6. All mice were euthanized on day 8. (B). Quantitative analysis of wound size. Wound size was measured on day 0, day 3, day 6, and day 8. The size of day 0 was set as 100%, and gradually reduced by healing. (C). Pictures of wound. Pictures were taken by camera on day 0, day 3, day 6, and day 8.

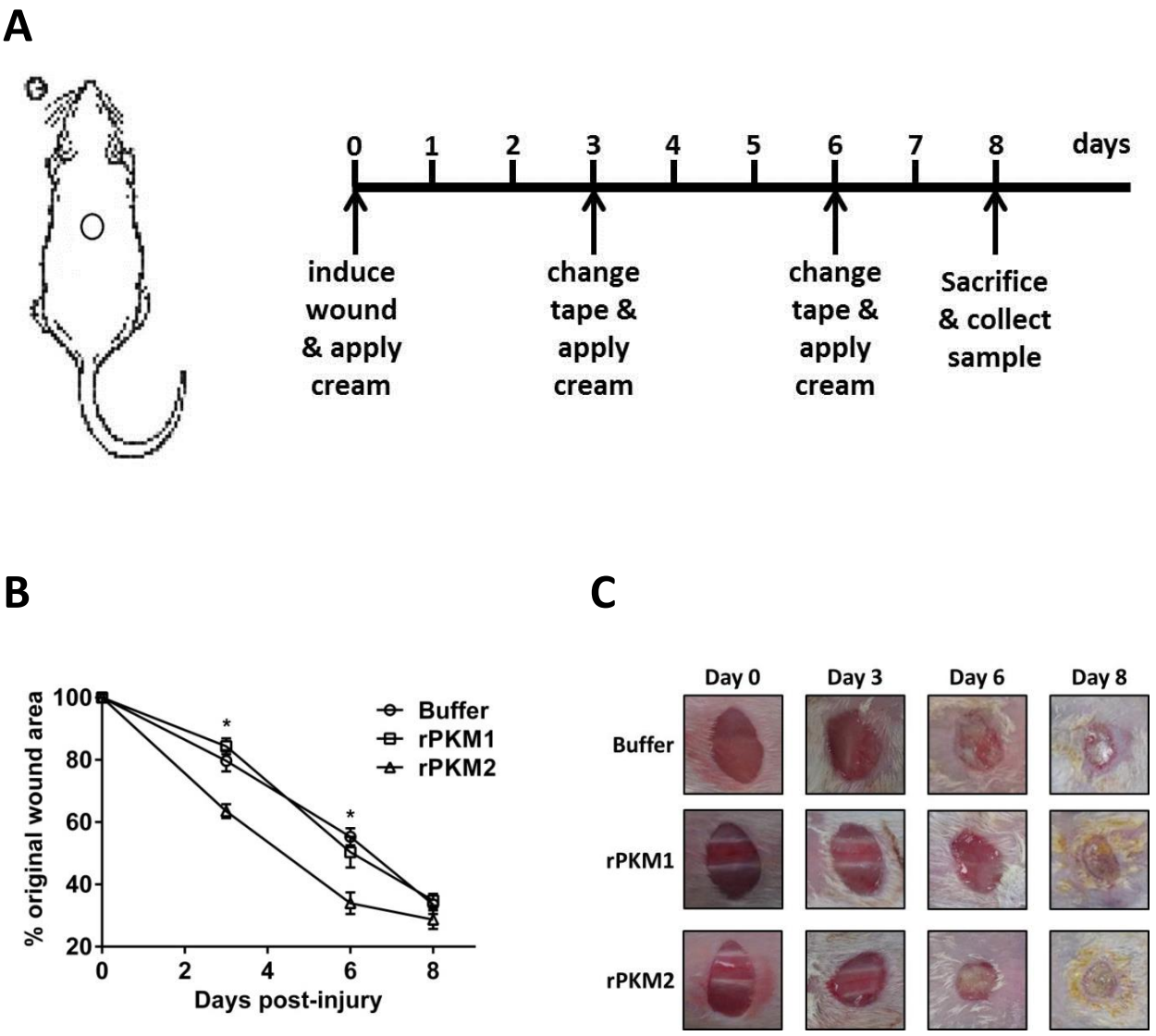

Figure 2.1 Topical application of rPKM2 facilitates wound healing.

Figure 2.2 Topical application of rPKM2 activates angiogenesis during wound healing.

(A). Immunofluorescence staining of CD31. Wound skin samples were cut off and snap-froze in opti medium in liquid nitrogen. Frozen sections were cut vertically through the wound area. CD31 was stained in green and DAPI was in blue. (B). Quantification of CD31 staining. Quantification was processed by ImageJ. Microvescular density was quantified by counting each staining pattern. CD31 positive pixel was quantified by calculating the area of CD31 staining.

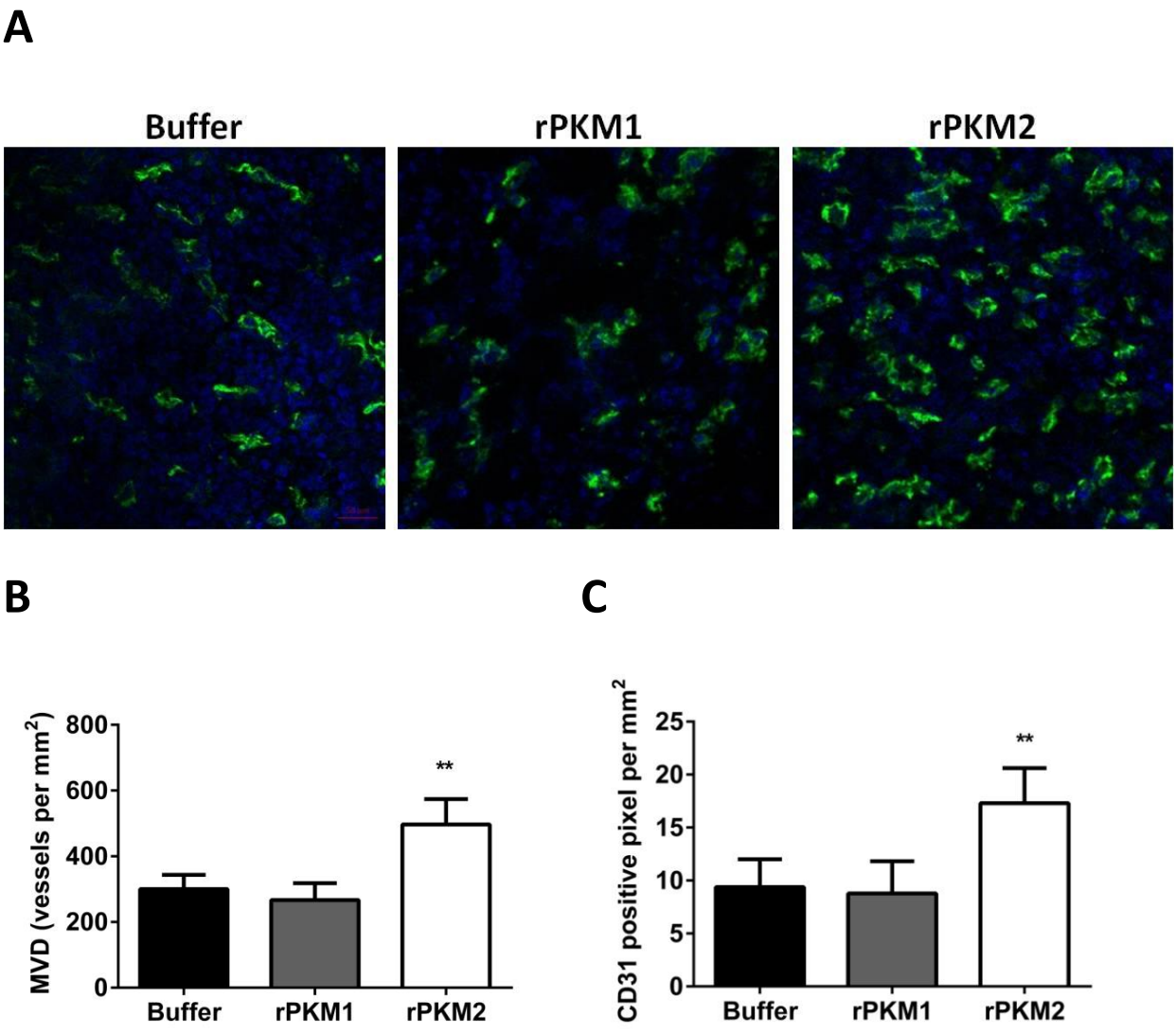

Figure 2.2 Topical application of rPKM2 activates angiogenesis during wound healing.

Figure 2.3 Topical application of rPKM2 induces granulation tissue growth during wound healing.

(A). Pictures of inner side of wounded skin. The wounded skin was cut off at day 8. The pictures were taken after flipping and spreading the wounded skin. (B). Quantification of thickness of granulation tissue. The wounded skin was cut off at day 3, day 6, and day 8, and embedded in paraffin for vertical sliding. The slides were performed with H&E staining. The thickness was measured by the length from the outside to the inside of wounded skin on H&E stained slide. The measurements were averaged and compared between buffer and rPKM2 groups. (C). Immunofluorescence staining of fibroblast and quantification. The fibroblast was stained in green with fibroblast marker ER-TR7, and DAPI was in blue. Quantification was processed by ImageJ. ER-TR7 positive pixel was quantified by calculating the area of staining.

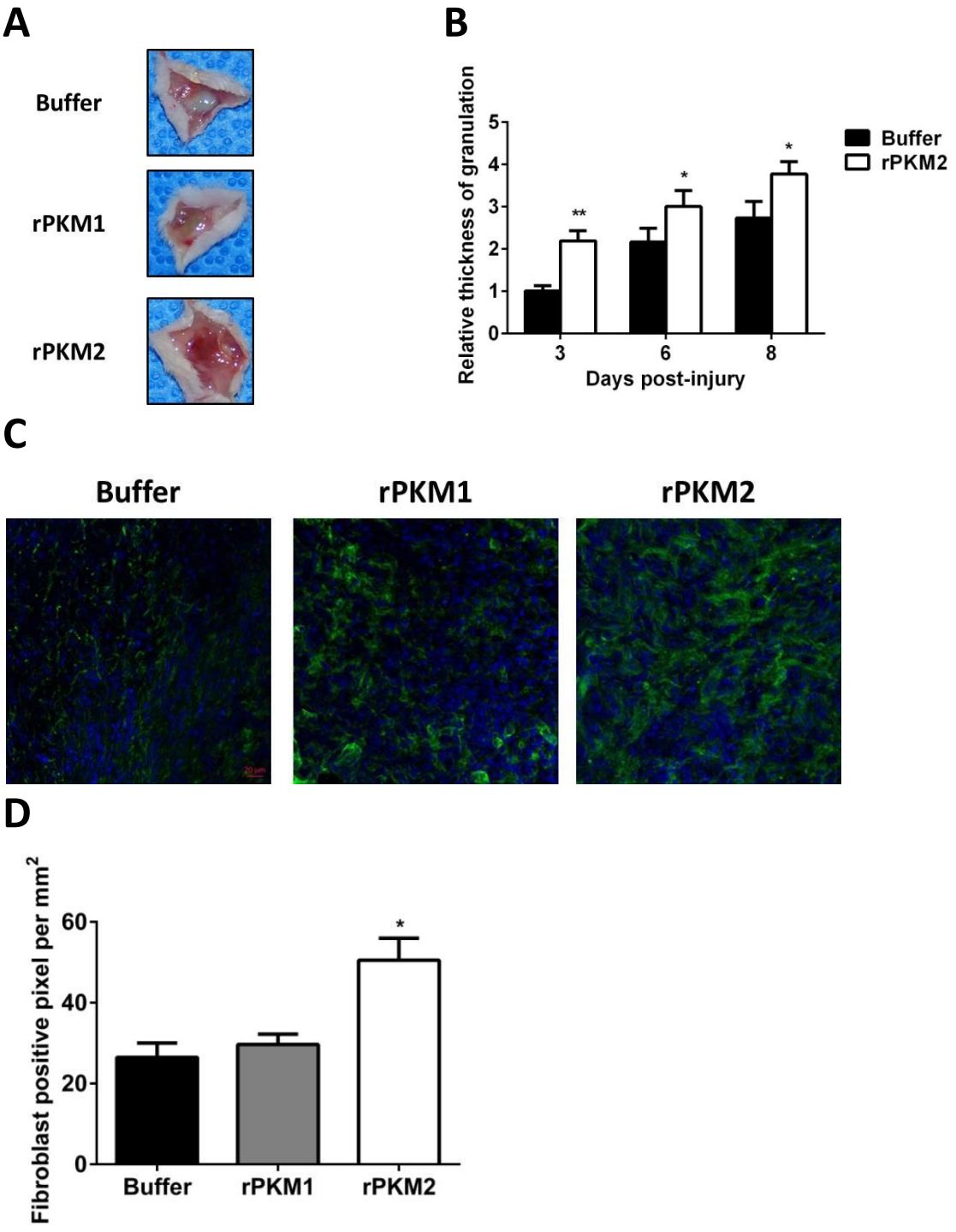

Figure 2.3 Topical application of rPKM2 induces granulation tissue growth during wound healing.

Figure 2.4 Neutralization of extracellular PKM2 inhibits wound healing process.

(A). Diagram of mouse wound healing experiment. Cutaneous wounds were induced on the back of three groups of mice on day 0, and applied with cream mixing buffer, IgGCon, and IgGPK respectively. The cream was re-applied on day 2 and day 4. All mice were euthanized on day 8. (B). SDS-PAGE of antibody pair, IgGCon vs IgGPK. Immunoblot of IgGPK on whole cell lysate of SW480 cell. (C). Quantitative analysis of wound size. Wound size was measured on day 0, day 2, day 4, day 6, and day 8. The size of day 0 was set as 100%, and gradually reduced by healing. (D). Pictures of wound. Pictures were taken by camera on day 0, day 2, day 4, day 6, and day 8.

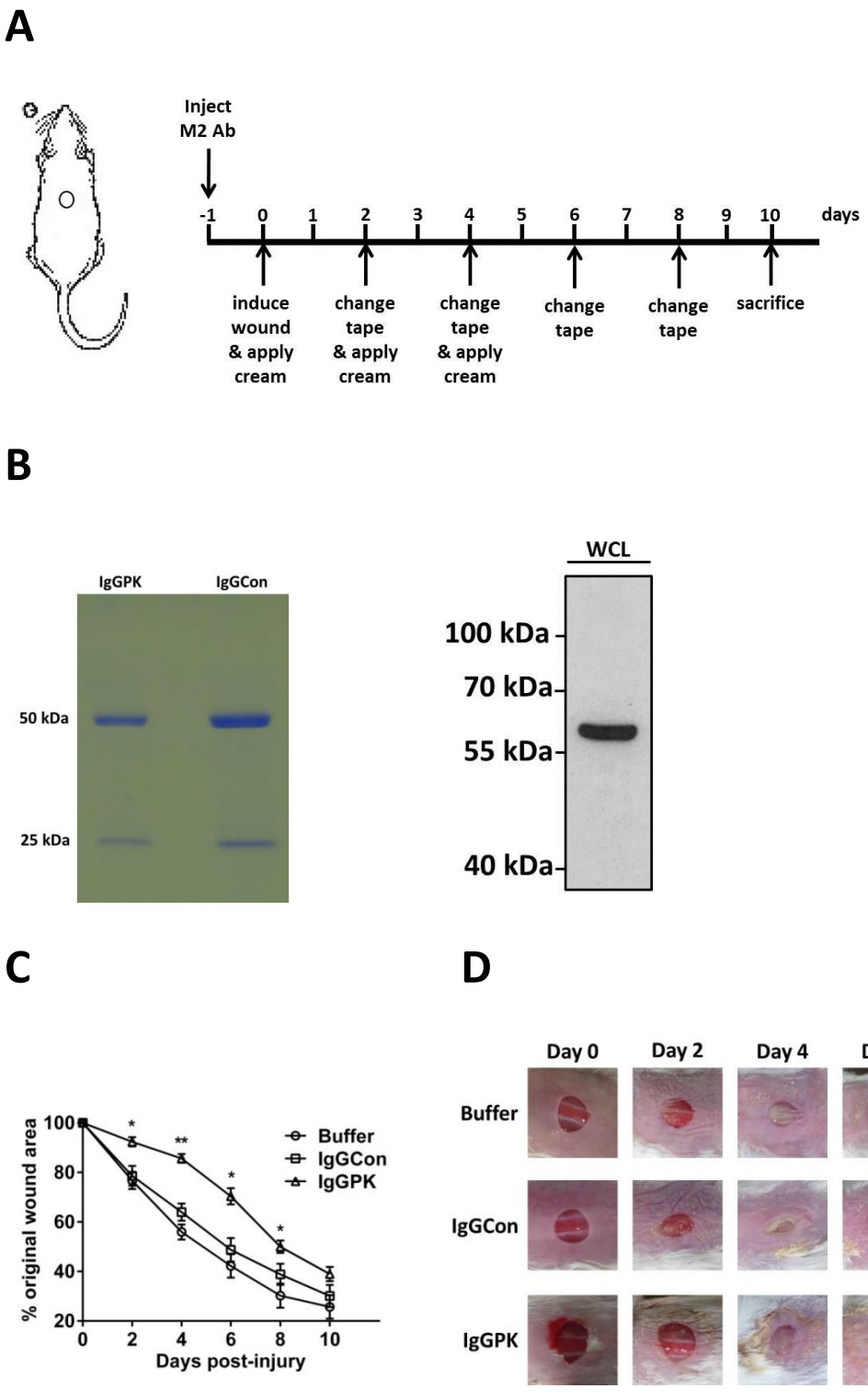

Figure 2.4 Neutralization of extracellular PKM2 inhibits wound healing process.

Figure 2.5 Neutralization of extracellular PKM2 reduces angiogenesis.

(A). Immunofluorescence staining of CD31. Wound skin samples were cut off and snap-froze in opti medium in liquid nitrogen. Slides were cut vertically through the wound area. CD31 was stained in green and DAPI was in blue. (B). Quantification of CD31 staining. Quantification was processed by ImageJ. Microvescular density was quantified by counting each staining pattern. CD31 positive pixel was quantified by calculating the area of CD31 staining.

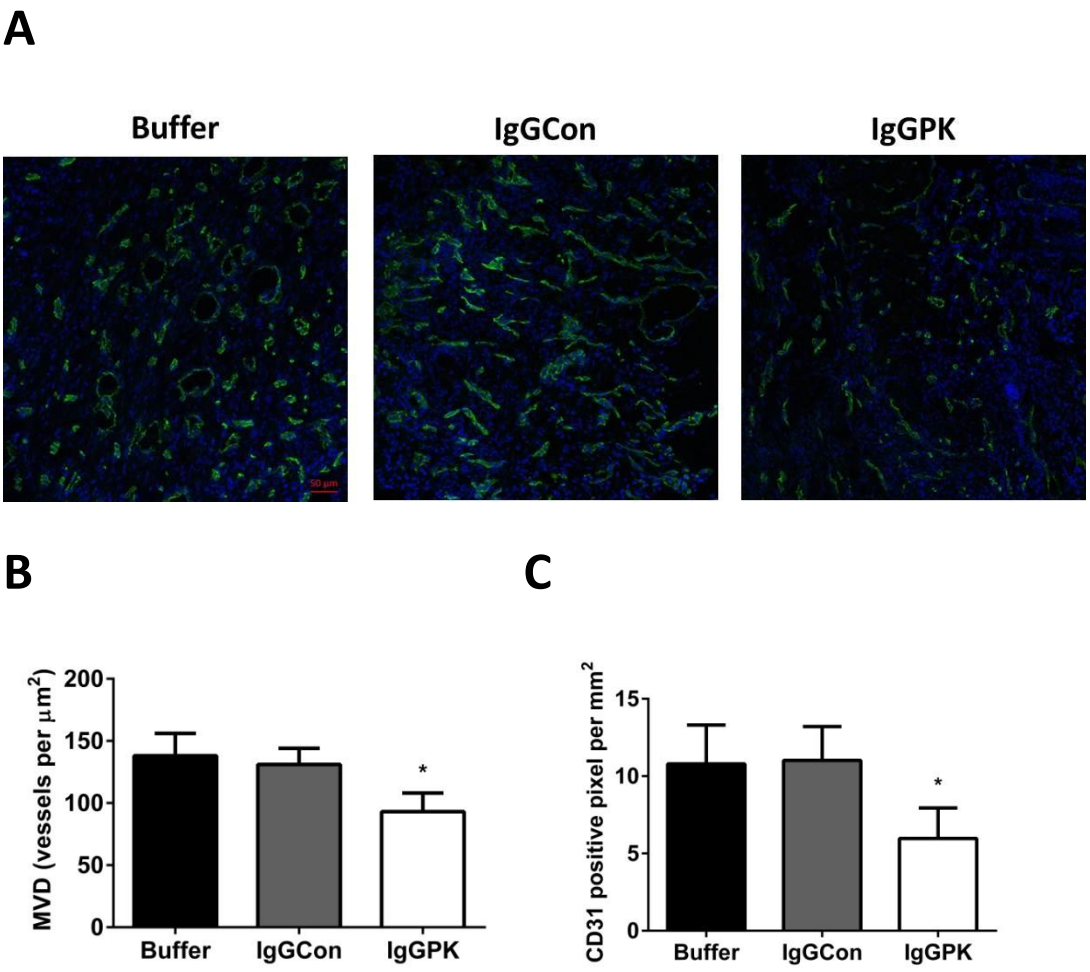

Figure 2.5 Neutralization of extracellular PKM2 reduces angiogenesis.

Figure 2.6 Identification of extracellular PKM2 in wound healing.

(A). Immunohistochemistry staining of PKM2 in wounded skin samples. Wounded skin at day 2 were cut and embedded in paraffin. Samples were cut vertically and stained with PKM2 antibody. The results were compared between non-wound tissue, wound tissue and wound tissue treated with rPKM2. (B). Identification of extracellular PKM2 in 10X and 40X magnification. (C). Time series of PKM2 and Ly6G staining. Mouse wounded skin samples from day 0 to day 5 were cut and embedded in paraffin. Samples were cut vertically and stained with PKM2 or Ly6G respectively. (D). Quantification of time series of PKM2 and Ly6G staining. Quantification was processed by FRamework for Image Dataset Analysis (FRIDA).

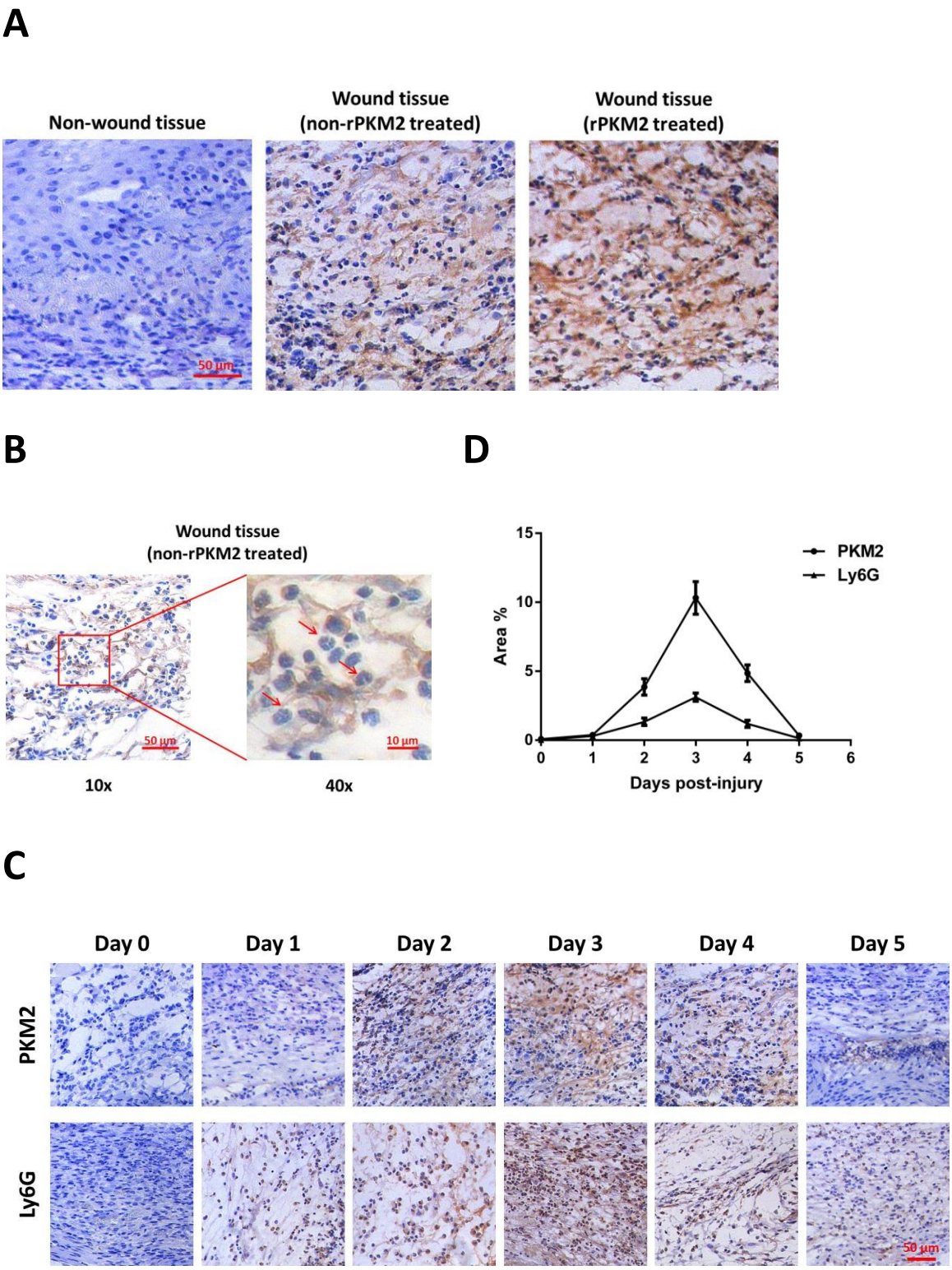

Figure 2.6 Identification of extracellular PKM2 in wound healing.

Figure 2.7 In vitro analysis of extracellular PKM2 released by neutrophils.

(A). Release of PKM2 by neutrophils under degranulation stimulation. Neutrophils were isolated from mouse bone marrow and activated with fMLP and damnacanthal. Whole cell lysate and concentrated culture media were analyzed by Western blot using PKM2 and β-actin antibody. (B). Quantification of released PKM2 by ELISA. Isolation and activation of neutrophils were performed the same as in Western blot. Culture media were added into ELISA plate coated with PKM2 antibody. Level of released PKM2 was measured with another PKM2 antibody and then recorded by spectrophotometer. (C). Presence of PKM2 in sucrose gradient fractions of activated neutrophils. Sucrose gradient fractions of neutrophils were analyzed with PKM2, β-actin, and CD11b antibodies using Western blot.

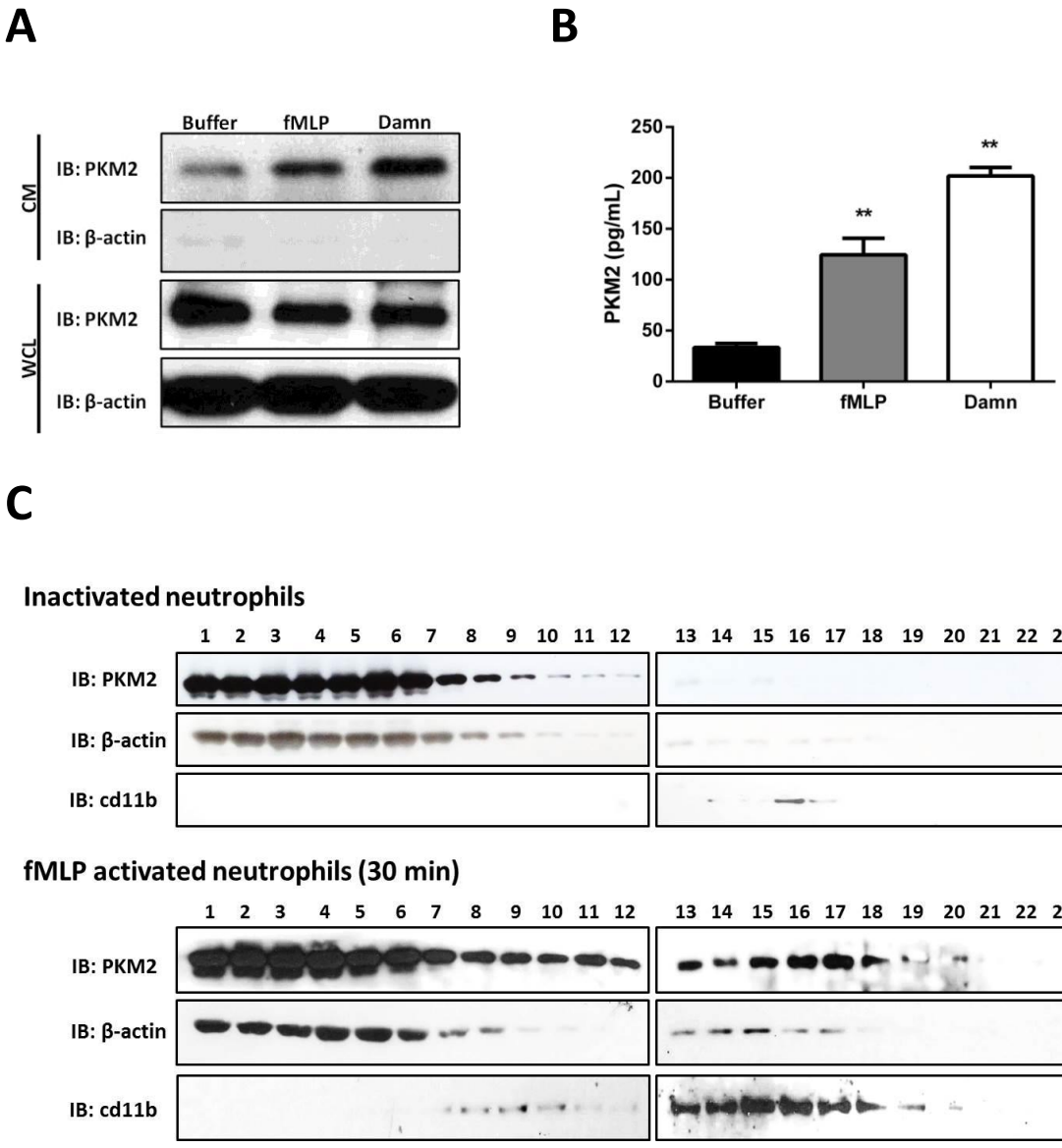

Figure 2.7 In vitro analysis of extracellular PKM2 released by neutrophils.

Figure 2.8 Identification of extracellular PKM2 in wounded beige-J mouse.

(A).Wound size comparison between beige and WT mice at day 3. Wound was induced the same as in CD-1 mice. (B). Granulation in beige and WT mice at day 3. Wounded skin was cut off and processed with H&E staining to measure the thickness of granulation. (C). Representative images of IHC staining of wound tissue sections from beige-J and WT mice. Wound skin tissue was collected at day 3.

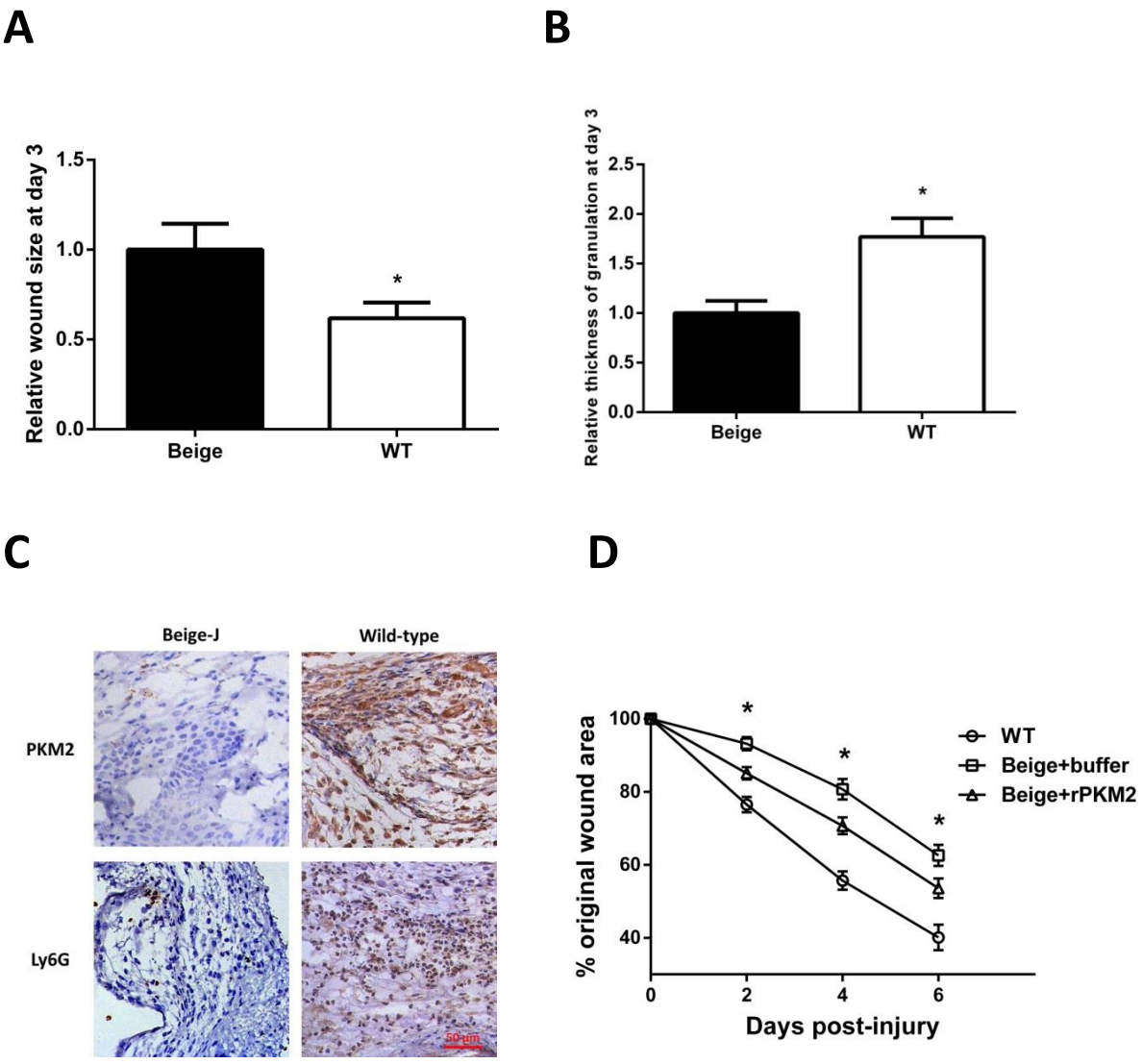

Figure 2.8 Identification of extracellular PKM2 in wounded beige-J mouse.

Figure 2.9 Inhibition and time series of extracellular PKM2 released from neutrophils.

(A). Inhibition of PKM2 release by degranulation inhibitors. Neutrophils were isolated and activated by fMLP. PP1, SB 203580, and piceatannol were tested under fMLP stimulation. Whole cell lysate and culture media were analyzed using Western blot. (B). Time series of PKM2 release in neutrophils. Neutrophils were activated by fMLP and culture media were collected at different time points for Western blot analysis. (C). Quantification of time series released PKM2 by ELISA. Culture media were added into ELISA plate coated with PKM2 antibody. The level of released PKM2 was measured with another PKM2 antibody and then recorded by spectrophotometer.

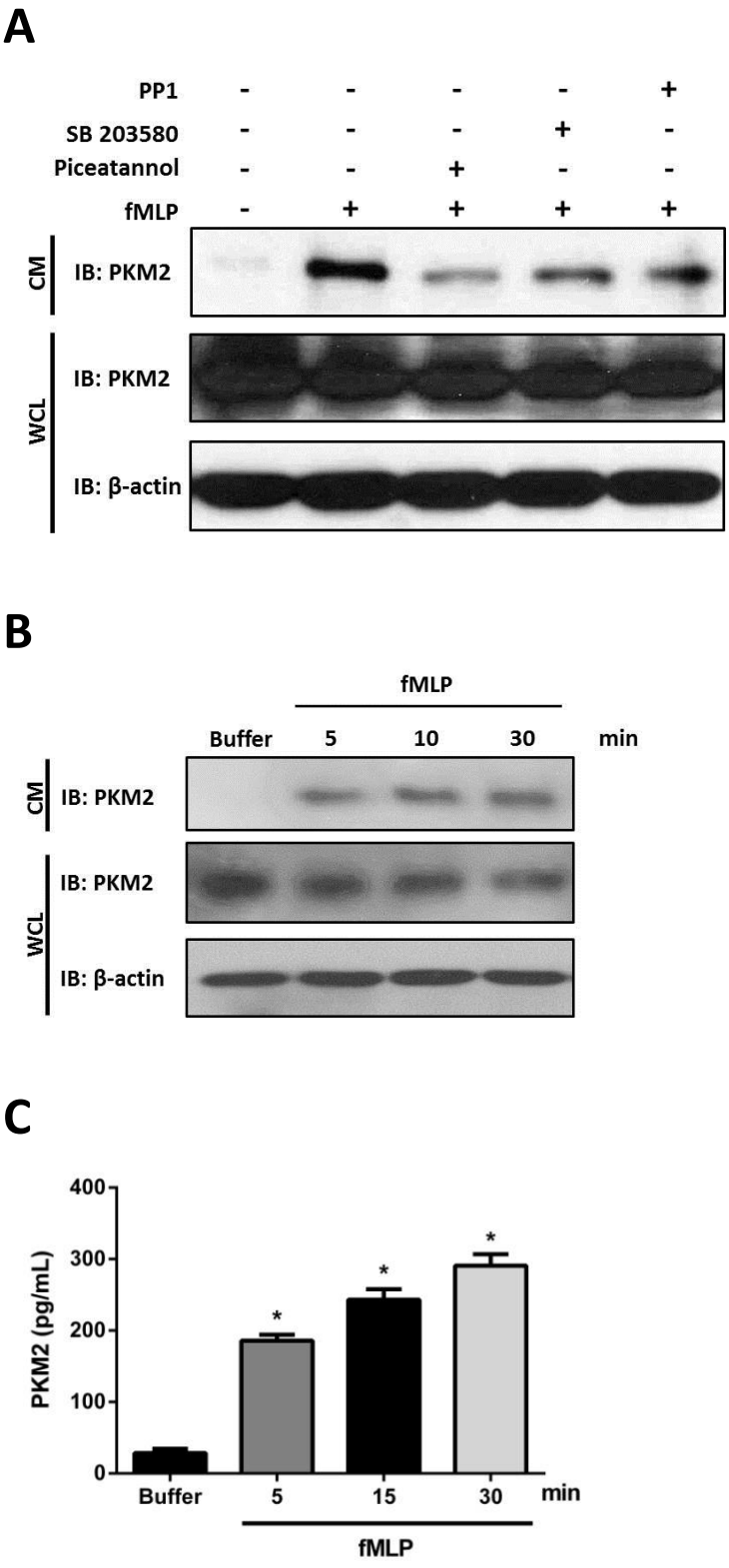

Figure 2.9 Inhibition and time series of extracellular PKM2 released from neutrophils.

CHAPTER 3 EXTRACELLULAR PYRUVATE KINASE M2 ACTIVATES DERMAL MYOFIBROBLAST DIFFERENTIATION

3.1 Abstract

Extracellular PKM2 released from neutrophils promotes wound healing by activating angiogenesis. In addition, we claim that extracellular PKM2 can also activate dermal fibroblasts to undergo myofibroblast differentiation. PKM2 facilitates the formation of early granulates at wound site by promoting fibroblast migration and myofibroblast differentiation. We demonstrate that extracellular PKM2 promotes myofibroblast differentiation through a TGFβ independent pathway via activation of integrin αvβ3 signaling. Our studies discover another function of extracellular PKM2 during wound healing to link early inflammation response with proliferation stage. Our studies also uncover a novel mechanism of stimulating myofibroblast differentiation.

3.2 Introduction

Myofibroblast differentiation is a key process during the proliferation stage of wound healing. Fibroblasts are recruited to the wound site by growth factors and cytokines released from immune cells. Together with endothelial cells, fibroblasts build up the granulation tissue to fill up wound area. After wound closure, fibroblasts convert to myofibroblasts to further contract the wound and secret extracellular matrix to support wound repair (Hinz, 2007).

TGFβ is the major ligand to activate myofibroblast differentiation. TGFβ activates TGFβ receptor on the plasma membrane fibroblasts. The activated TGFβ receptor heterodimer phosphorylates Smad complex to induce the nuclear translocation of Smad complex that leads to the upregulation of several fibroblast differentiated gene transcription, including α-SMA. Integrin αvβ3 also involved in myofibroblast differentiation (Gressner et al., 2002). Previously

we found that extracellular PKM2 promotes endothelial cells migration and attachment through integrin αvβ3.

3.3 Results

3.3.1 Myofibroblast differentiation is activated in rPKM2 treated wound

After examining the inside of wounded skin, we found that granulation tissue was grown much thicker in rPKM2 group. We questioned whether other effects of extracellular PKM2 existed besides activation of endothelial cells. Given that both endothelial cells and fibroblasts have integrin αvβ3 expression, we hypothesized that extracellular PKM2 also activated dermal fibroblasts during wound healing. We first checked myofibroblast differentiation in the wound skin sample. Frozen sections were stained with α-SMA antibody via immunofluorescence staining. The rPKM2 treated mice had increased level of α-SMA at wound site (Figure 3.1 A&B). Three time points as in granulation tissue thickness measurement were picked up for staining of α-SMA expression. On day 3, day6, and day 8, the rPKM2 treated mice all showed elevated levels of α-SMA (Figure 3.1 C). The PKM2 antibody treated group was also tested and the α-SMA level was reduced (Figure 3.1 D). Since other type of cells in skin also had αvβ3 expression, such as smooth muscle cells. To exclude the possibility of smooth muscle cells and also confirm the fibroblast staining, frozen sections were co-stained by α-SMA and smooth muscle cell marker myosin or fibroblast marker ER-TR7. Myosin and α-SMA had different staining pattern, on the other hand, ER-TR7 staining was overlapped with α-SMA expression pattern (Figure 3.2 A). In summary, myofibroblast differentiation is activated in the PKM2 treated mice during wound healing.

3.3.2 Effect of extracellular PKM2 on HDFa

To test the effect of PKM2 on fibroblasts, human dermal fibroblasts adult (HDFa) were treated with rPKM2 and tested in proliferation and migration assays. In BrdU proliferation assay, rPKM2 treated HDFa had a little bit increase compared with the controls, but it was not significant (Figure 3.2 B). In boydem chamber assay, rPKM2 treated cells had three-fold increase compared with the controls (Figure 3.2 C). After 48 hours of rPKM2 treatment, HDFa cells had increased expression of α-SMA in the immunoblot test. It was slightly less compared with the TGFβ treatment. Combination of rPKM2 and TGFβ treatment had enhanced α-SMA expression (Figure 3.3 A). To detect the differentiating features, HDFa were treated with rPKM2 or TGFβ, and then stained with phalloidin, α-SMA, and DAPI. HDFa cells in buffer group still remained the spindle shape, and the expression level of α-SMA was low. Both rPKM2 and TGFβ treated cells had the typical myofibroblast spreading shape and the signal α-SMA expression was stronger. Actin (Red) and α-SMA (green) formed bundles in yellow. In rPKM2 group, HDFa cells had more protrusions structures (Figure 3.3 B). Collagen level in culture medium was also increased in rPKM2 and TGFβ treated cells (Figure 3.3 C).

3.3.3 Extracellular PKM2 activates HDFa cells through integrin αvβ3

In the previous study, we found that extracellular PKM2 activates endothelial cells through integrin αvβ3 signaling. Since HDFa also have integrin αvβ3 on the cell surface, we questioned whether it was the same cell surface receptor on HDFa for extracellular PKM2. First, in vitro cell attachment assay was used to test the interaction between integrin αvβ3 and PKM2. HDFa only attached on rPKM2 coated plate and this effect was eliminated by the pretreatment of αvβ3 antibody (Figure 3.4 A). We carried out chemical crosslinking with rPKM2 and the membrane extracts of HDFa using glutaraldehyde as a crosslinker. The crosslinked proteins were

separated by His-tag pull-down and subsequently digested by trypsin. The digested integrin αvβ3 peptides were found in the mass spectrometry result (Figure 3.4 C). To further confirm the interaction between PKM2 and integrin αvβ3, we also tested the pull-down assay by PKM2 antibody and control antibody in western blot. Integrin β3 was detected in PKM2 antibody group, but not in control antibody group (Figure 3.4 B). Furthermore, in the migration activity assay, the αvβ3 antibody reduced the level of migration down to the buffer level (Figure 3.4 D).

TGFβ pathway is the well-known pathway to activate myofibroblast differentiation. We then asked whether PKM2-αvβ3 signaling was independent of TGFβ signaling pathway. Two additional treatments were used. TGFβ antibody was pretreated to neutralize the possible TGFβ residue in culture medium, and TGFβ receptor inhibitor was used to block TGFβ signaling pathway. Both of them were added into rPKM2 and TGFβ treatments respectively. As shown in the immunoblot, rPKM2 or TGFβ treatments induced the expression of α-SMA. Phospho-Smad2, the downstream signal of TGFβ signaling, was activated in TGFβ treatment, but not in rPKM2 treatment. Upon addition of TGFβ antibody or TGFβ receptor inhibitor, both α-SMA and p-Smad2 signal were lost in TGFβ treated cells. However, rPKM2 treatment was still able to induce α-SMA expression (Figure 3.5 A). Since PKM2 interacts with integrin αvβ3 on the cell surface of HDFa, we pretreated integrin αvβ3 antibody and the expression of α-SMA was reduced (Figure 3.5 B). FAK activation is the major downstream target of integrin αvβ3. If extracellular PKM2 activates HDFa through integrin αvβ3, then FAK should be activated. Phospho-FAK was detected as the signal of FAK activation. The rPKM2 treatment stimulated both expression α-SMA and phosphorylation of FAK, which were abolished after the treatment of FAK inhibitor (Figure 3.5 C).

Then we questioned what the downstream signal pathway of PKM2-αvβ3-FAK was. We first screened with several FAK downstream pathway inhibitors. PI3K, Src, and MEK inhibitors were applied and PI3K inhibitor showed the strongest inhibition in α-SMA expression (Figure 3.6 A). To further confirm this effect, we tested PI3K activity with treatment of rPKM2. Buffer treatment was normalized to baseline, and rPKM2 treatment had three-fold increase with or without addition of TGFβ receptor inhibitor. In addition, pretreatment of FAK inhibitor brought PI3K activity down to the baseline level (Figure 3.6 B). It is reported that PAK2 is activated by PI3K and plays a role in myofibroblast differentiation. We followed this track to test activation of PAK2 with the treatment of rPKM2. The rPKM2 treated HDFa cells stimulated the phosphorylation of PAK2 compared with rPKM1 and buffer controls (Figure 3.6 C).

3.4 Discussion

Myofibroblast differentiation is a critical pathophysiology process involved in different circumstances, including wound healing and fibrosis. We first noticed the granulation tissue was very thick in the previous wound healing experiment. Only by angiogenesis is not enough to grow such level of granulation tissue. Given the similar features between endothelial cells and fibroblasts, we tested the effect of extracellular PKM2 on dermal fibroblasts. Extracellular PKM2 activated the differentiation of myofibroblast through integrin αvβ3 and PI3K signaling pathway during wound healing.

One question is why extracellular PKM2 is the stimulator in addition to TGFβ. TGFβ is the well-known major growth factor to activate myofibroblast differentiation via Smad family signaling pathway. We found that rPKM2 activated dermal fibroblasts independent of TGFβ through integrin αvβ3. It is reported that only TGFβ is not enough to transit quiescent fibroblast to myofibroblast and TGFβ activation can change the transcription profile of fibroblast, such as

increase of integrin αvβ3 expression level. Thus, during wound healing, fibroblasts are attracted to wound area and activated by TGFβ first. After the increase of integrin αvβ3 level, extracellular PKM2 further converts myofibroblast differentiation. That was why the combination of rPKM2 and TGFβ had the strongest effect in α-SMA stimulation.

3.5 Materials and Methods

3.5.1 Induction of HDFa Differentiation

HDFa were cultured to reach 70% confluency, and starved with serum-free medium overnight before differentiation induction. The cells were treated with TGF-β (10 ng/mL) or rPKM2 (0.1 μM) for 2 days. After treatment, the cells were lysed with RIPA buffer and medium was collected for further analysis. Cell lysates prepared with RIPA buffer and culture media were collected and analyzed with western blot.

3.5.2 Cells Immunofluorescence Staining

HDFa seeded on the coverslips were fixed with 4% paraformaldehyde for 15 min and then permeabilized with 0.1% Triton X-100 in PBS for 15 min. HDFa were washed twice with PBS and blocked with 5% BSA solution at room temperature in humidity box for 30 min. HDFa were incubated with primary α-SMA antibody with 1:500 dilutions in 5% BSA solution at 4 ˚C overnight. HDFa were washed with PBST three times each time 5 min and then incubated with secondary antibody conjugated with fluorescence dye at room temperature for 30 min. If another fluorescence dye was needed, the slides were incubated with another primary antibody at room temperature for 2 hours and secondary antibody conjugated with fluorescence dye for 30 min. The slides were washed and mounted with Prolong Gold Antifade Mountant with DAPI. The coverslips were sealed by nail polish. The results of immunofluorescence staining were acquired by using Zeiss LSM 700 Confocal.

3.5.3 Cell Attachment Assay

HDFa were cultured in good condition. rPKM1, rPKM2 or BSA was coated on the 24-well plate at 4 ˚C overnight. The wells were washed with PBS twice and then blocked with 5% BSA at room temperature for 1 hour. HDFa were trypsinized and pre-treated with LM609 or BSA as control. HDFa were seeded on the plate and incubated for 2 to 4 hours. After wash twice with PBS, the unattached cells were washed and the attached cells were stained with crystal violet. The cell number in each well was counted for comparison of the cell attachment.

3.5.4 Crosslink

HDFa were harvested and washed with PBS. The membrane proteins were extracted by using a membrane protein extraction kit. The membrane protein lysates were incubated with rPKM2 at room temperature for 2 hours. Glutaraldehyde (1:100) was added in the reaction and incubated for another 30 min. 1 M Tris/glycine was added into to the reaction to reach a final concentration of 100 mM to stop the crosslink reaction. The magnetic Ni^{2+} beads were added in to the lysate and incubated at room temperature for 1 hour. The beads were washed 3 times with PBS, and then eluted by imidazole. The elution was dialyzed in ammonium bicarbonate at 4 ˚C twice each time 4 hours. The sample was concentrated using lyophillizer and trypsinized using the kit from Sigma. The sample was desalted using C_{18} tip. The final samples were sent to mass spectrophotometer for analysis.

3.5.5 Immunoprecipitation

HDFa membrane proteins were extracted using the membrane protein extraction kit. The membrane protein lysates were incubated with rPKM2 at room temperature for 2 hours and the PKM2 antibody was added into the lysate and incubated at 4 ˚C overnight. The protein G Agarose beads were added into the lysate and incubated at 4 ˚C for 2 hours. The beads were

collected by centrifugation at 13000 rpm and washed three times with PBS. The beads were resuspended in the sample loading buffer and boiled for 5 min. The samples were loaded for SDS-PAGE and later for western blot analysis.

3.5.6 PI3K Activity Assay

The PI3K activity was measured by ADP-Glo^{TM} Lipid Kinase Systems from Promega followed the instruction. Generally, the cells were inducted first with TGF-β or rPKM2 for two days and cell lysates were made using RIPA buffer. The lysates were pulled-down by Pi3K antibody and incubated with ATP and lipid substrate. The PI3K activity was measured by monitoring the increase of ADP level.

3.5.7 PAK2 Activity Assay

The PAK2 activity was measured by in vitro protein kinase reaction and then western blot to test the phosphorylation. The cells were inducted first with TGF-β or rPKM2 for two days and cell lysates were made using RIPA buffer. The lysates were pulled-down by PAK2 antibody. The in vitro protein kinase reaction consisted with PAK2 antibody pulldown lysate, 25 mM Tris pH 7.4, 10 mM $MgCl_2$, 1 mM DTT, 5 μM ATP, and 5 μg of myelin basic protein. The reaction was preceded at 37 ˚C for 30 min. The reaction was stopped by adding loading buffer and boiled for 5 min. The samples were loaded for SDS-PAGE and phospho-myelin basic protein antibody was used in the western blot.

Figure 3.1 Identification of α-SMA in wound healing.

(A). IF staining of α-SMA in wound skin. Frozen section of wound skin were cut and stained with α-SMA antibody in green. (B). Quantification of α-SMA staining. IF staining of α-SMA were quantified with ImageJ for the area of positive pixel. (C). Quantification of α-SMA staining in PKM2 antibody treated group. IF staining of α-SMA were quantified with ImageJ for the area of positive pixel. (D). Quantification of α-SMA in time series wound. Wound skin was collected at day 3, day 6 and day 8. Staining of α-SMA was quantified with ImageJ for the area of positive pixel.

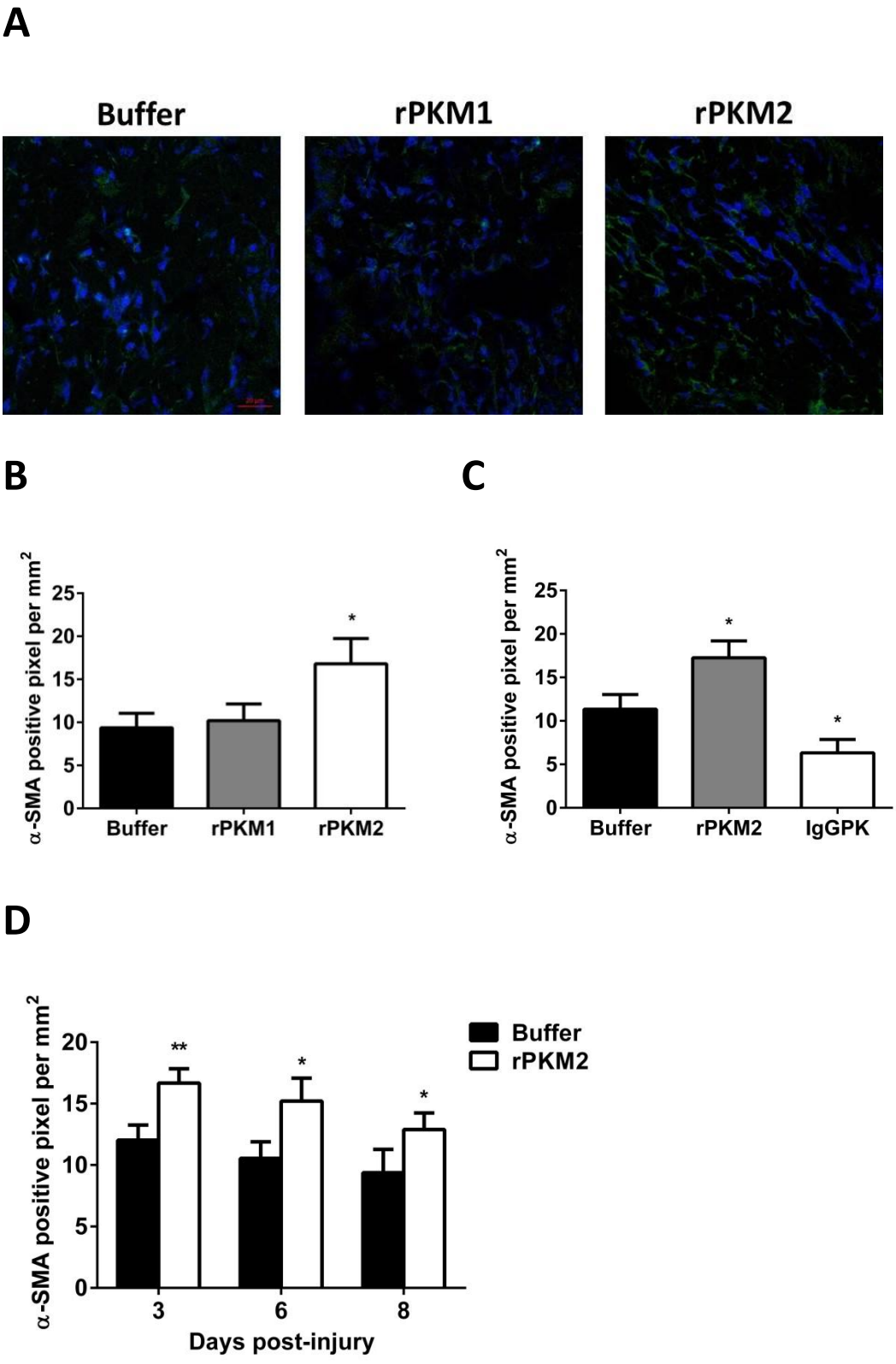

Figure 3.1 Identification of α-SMA in wound healing.

Figure 3.2 Verification of myofibroblast and in vitro analysis of PKM2 effect on HDFa.

(A). Verification of myofibroblast. Myofibroblast was verified with myosin and ER-TR7 staining. (B). In vitro analysis of PKM2 effect on HDFa. Cell proliferation assay was analyzed with BrdU proliferation assay. Cell migration assay was analyzed with boydem chamber assay. Both assays were tested in buffer, rPKM1, and rPKM2 groups.

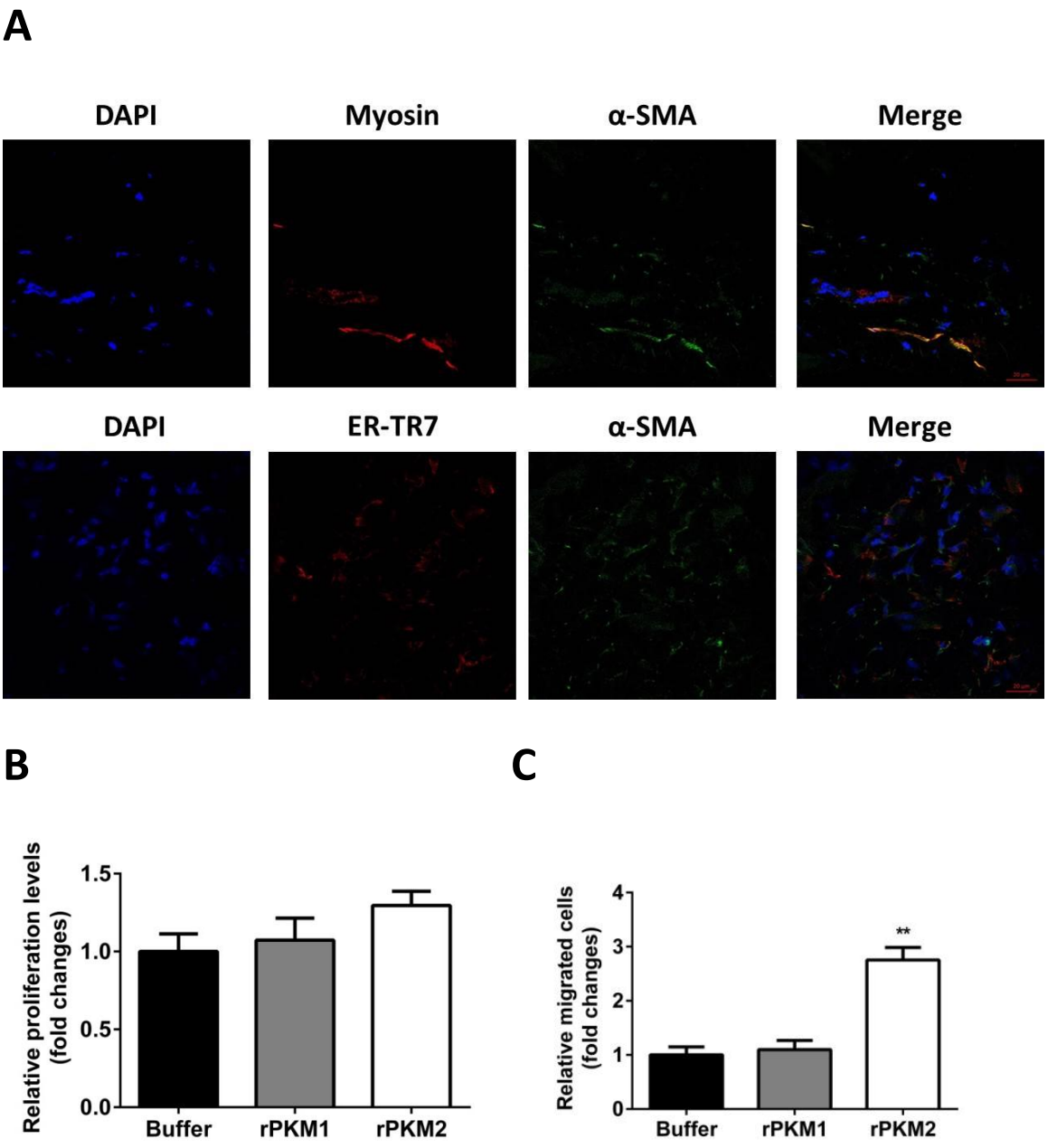

Figure 3.2 Verification of myofibroblast and in vitro analysis of PKM2 effect on HDFa.

Figure 3.3 Effect of PKM2 on HDFa.

(A). In vitro analysis of PKM2 in HDFa differentiation. HDFa differentiation was induced with rPKM2 or TGFβ as positive control. Combination of rPKM2 and TGFβ was also applied. Western blot was performed to test α-SMA level. (B). IF staining of differentiated HDFa cells. rPKM2 and TGFβ were applied on HDFa cells. α-SMA was stained in green and phalloidin as actin indicator was stained in red. (C). Collagen level in culture media. Collagen level was test using antibody in Western blot.

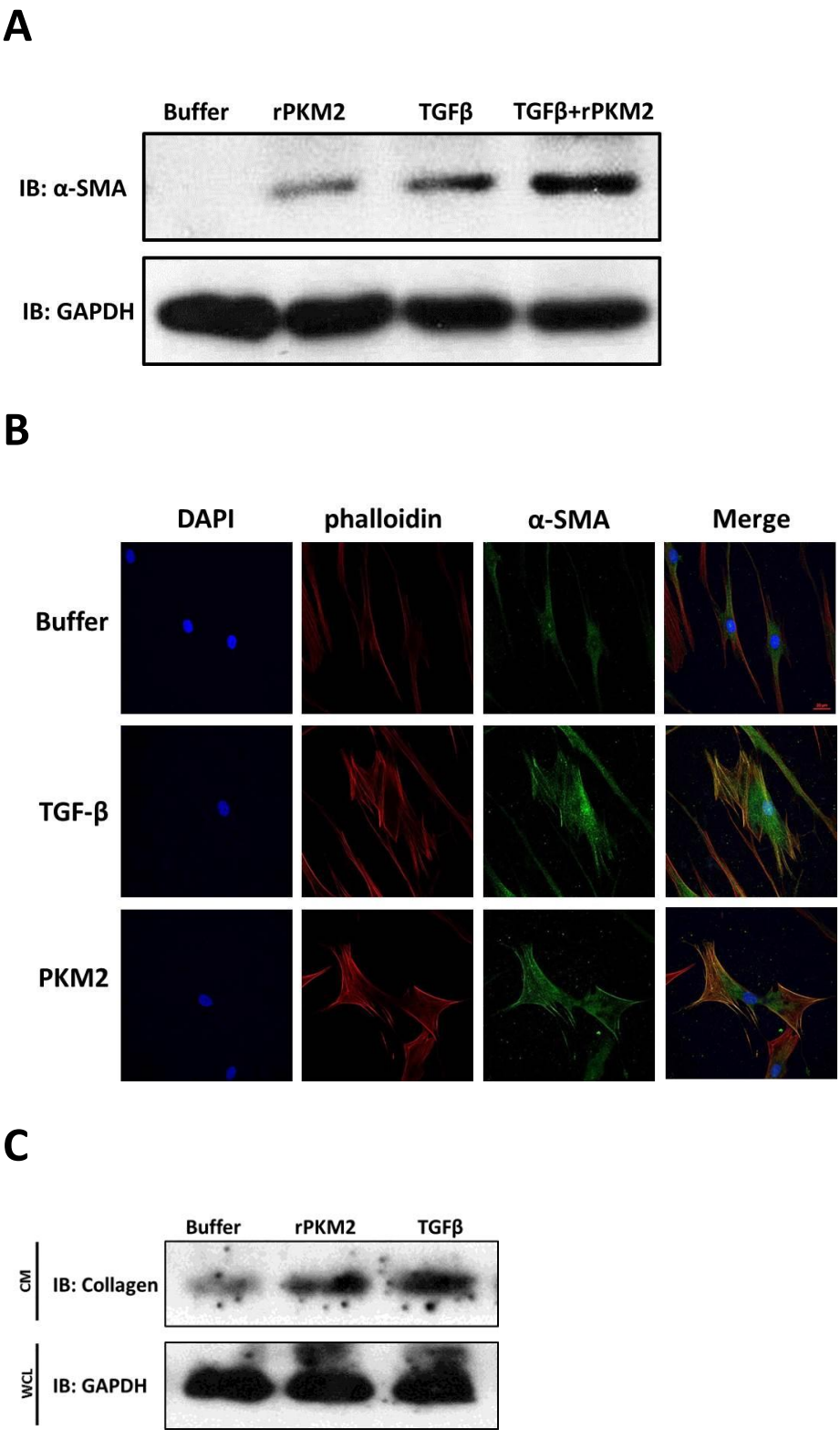

Figure 3.3 Effect of PKM2 on HDFa.

Figure 3.4 Extracellular PKM2 activates integrin αvβ3 signaling.

(A). Cell attachment assay of HDFa cells. rPKM2 and rPKM1 were coated on plate and HDFa cells were added in with αvβ3 antibody or BSA. (B). Immunoprecipitation of rPKM2 with HDFa membrane protein lysate. PKM2 antibody and IgG were used for IP. β3 antibody was used to test αvβ3 in the IP result. (C). The highlighted peptide fragments from trypsin digestion of rPKM2-HDFa crosslinks and MALDI-tof/tof analyses that match the amino acid sequence of integrin αvβ3. (D). rPKM2 enhanced migration ability of HDFa was inhibited by αvβ3 antibody.

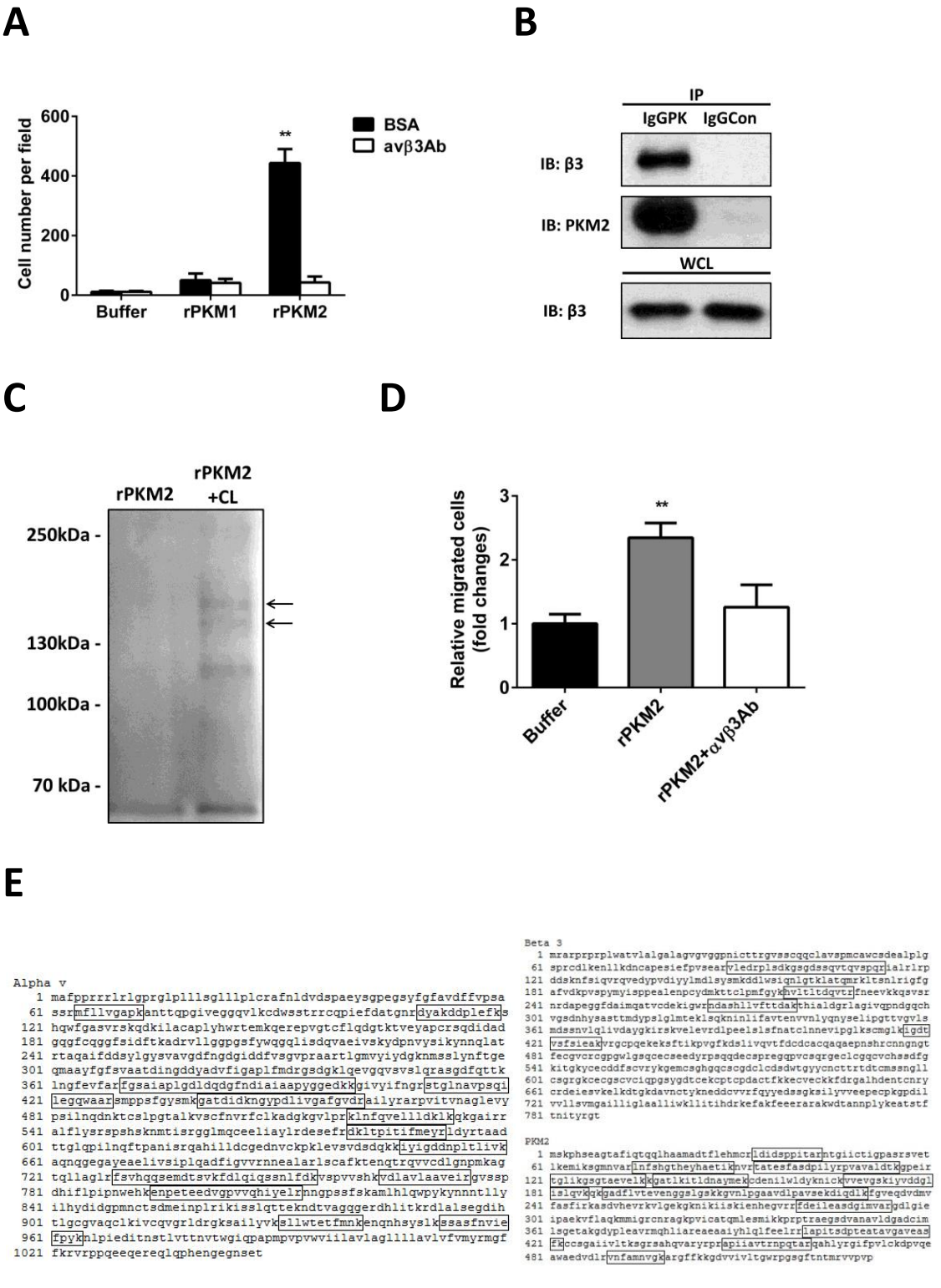

Figure 3.4 Extracellular PKM2 activates integrin αvβ3 signaling.

Figure 3.5 Extracellular PKM2 activates HDFa through integrin αvβ3.

(A). Signaling pathway of extracellular PKM2 activating HDFa differentiation is independent of TGFβ pathway. TGFβ receptor inhibitor and TGFβ antibody were used to test the effect of rPKM2. P-Smad2 was used to represent as the classical signaling pathway of TGFβ. (B). αvβ3 antibody eliminates the effect of rPKM2 on activation of α-SMA expression in HDFa. (C). FAK inhibitor reduces the effect of rPKM2 on activation of α-SMA expression in HDFa.

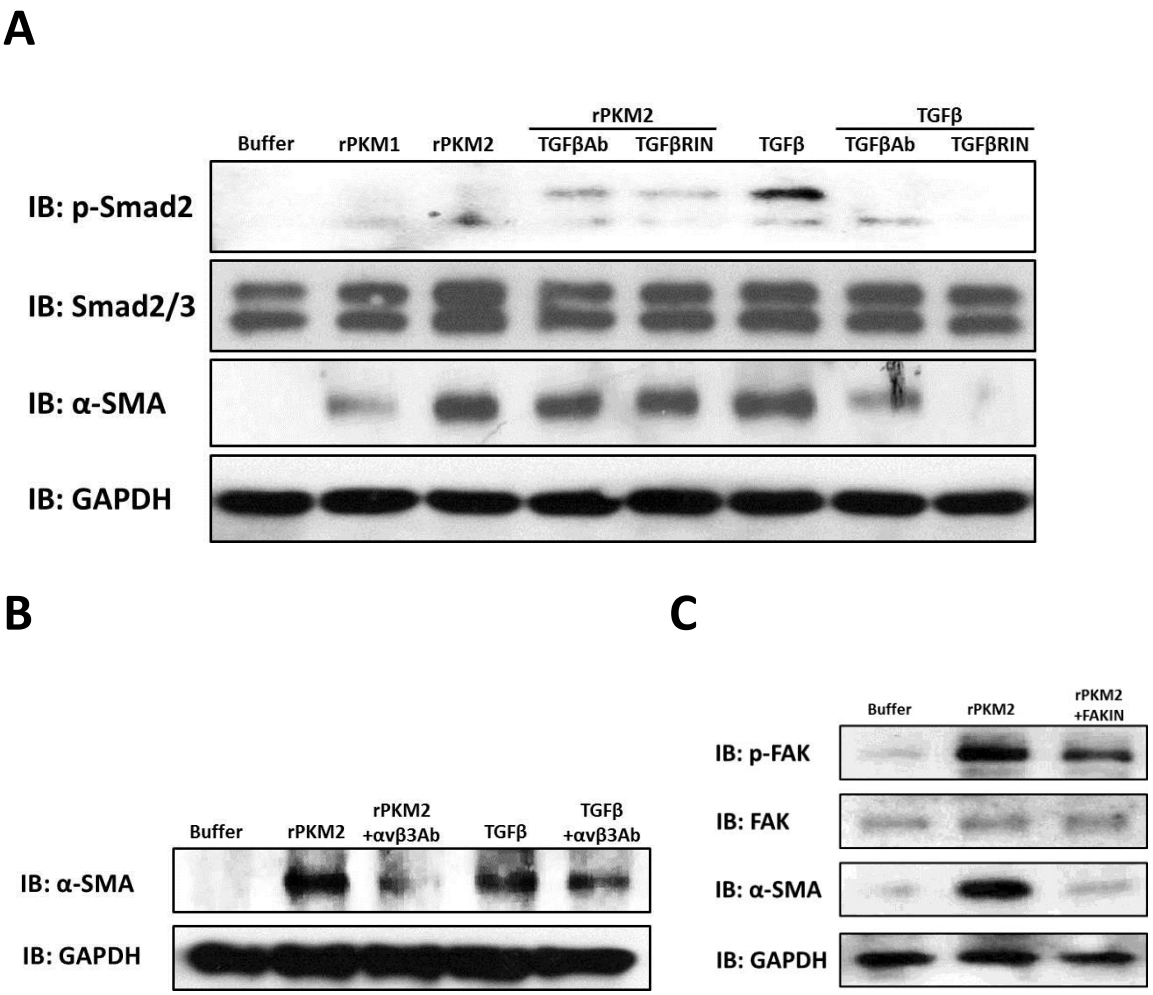

Figure 3.5 Extracellular PKM2 activates HDFa through αvβ3.

Figure 3.6 Extracellular PKM2 activates HDFa differentiation via PI3K.

(A). PI3K activity is upregulated in the rPKM2 treated HDFa. TGFβ receptor inhibitor and FAK inhibitor was used as controls. (B). Phosphorylation of PAK2 was used as an indicator to test the downstream pathway of extracellular PKM2 activating α-SMA expression. (C). Inhibitor screening of extracellular PKM2 effect. PI3K inhibitor, Src inhibitor, and MEK inhibitor were tested.

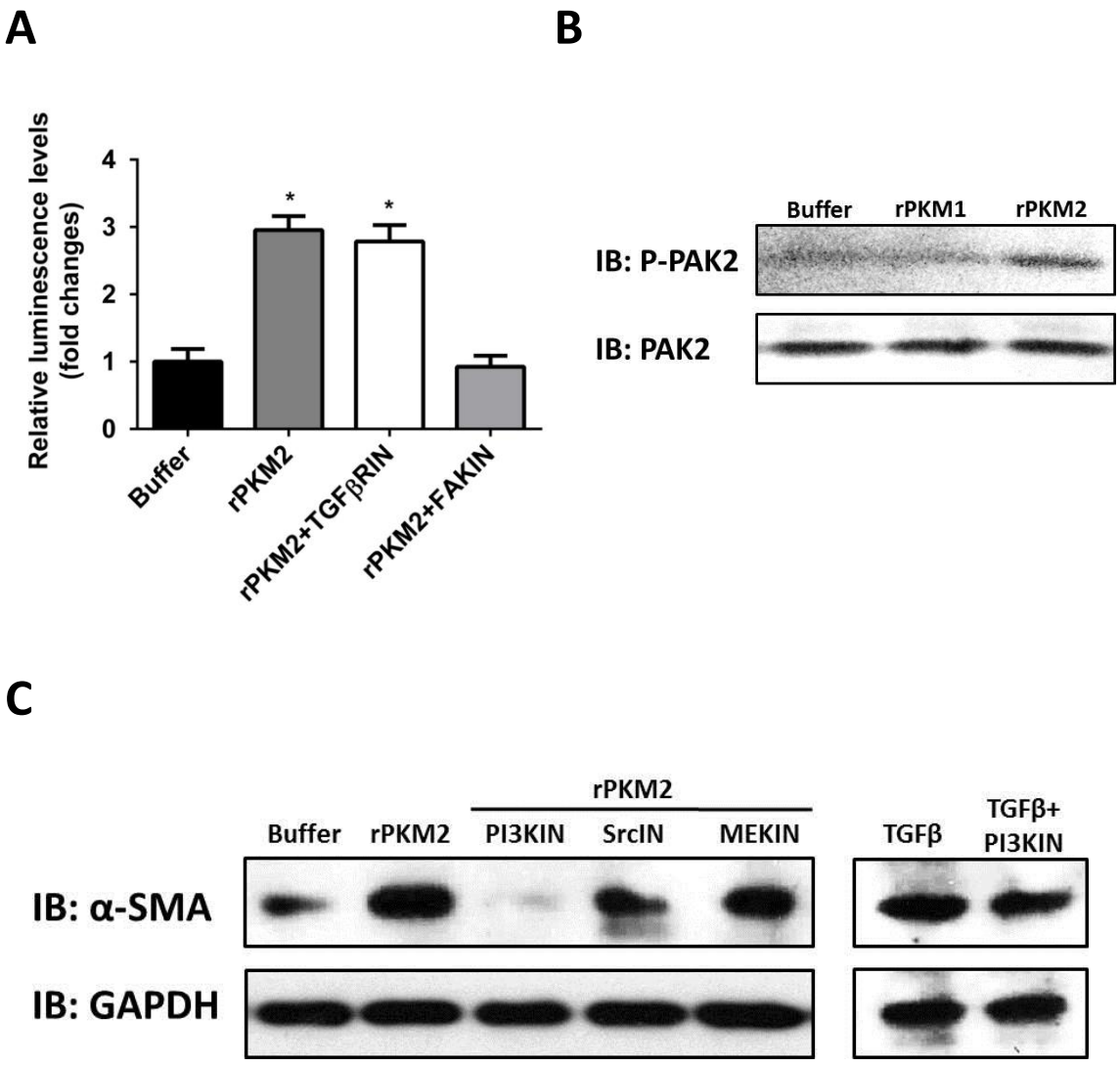

Figure 3.6 Extracellular PKM2 activates HDFa differentiation via PI3K.

CHAPTER 4 EXTRCELLULAR PKM2 PLAYS A ROLE IN LIVER FIBROSIS

4.1 Abstract

Liver fibrosis is caused by chronic inflammation and activation of Hepatic Stellate Cells (HSCs). The resistance of HSCs to apoptosis is the main reason for non-reversal of liver fibrosis. However, the molecular mechanism of how activated HSCs are prevented from apoptosis is still not well understood. Here, we report that extracellular PKM2 exists in the liver tissue of liver fibrosis patients. Extracellular PKM2 promotes progression of liver fibrosis by protecting activated HSCs from apoptosis. PKM2 interacts with integrin αvβ3 on the cell surface of HSCs and activates FAK-PI3K pathway to stimulate survival signal. Neutralization of extracellular PKM2 by a specific antibody relieves the process of liver fibrosis. Our study uncovers a novel mechanism of activated HSCs survival during liver fibrosis. The positive effect of PKM2 antibody treatment also suggests a possible therapeutic method for liver fibrosis.

4.2 Introduction

Liver fibrosis is the result of chronic liver damage which causes persistent inflammation at injury site. Inflammatory response continuously activates HSCs to differentiate into myofibroblast. Activated HSCs secret large amounts of extracellular matrix proteins that disrupt the architecture of liver tissue and restrains the normal liver function (Friedman, 2003). Liver fibrosis is considered “irreversible” because apoptosis of activated HSCs is reduced under the effect of chronic inflammation. However, a few studies have shown that low degree of liver fibrosis was reversible in certain circumstances. The study focusing on the apoptosis of activated HSCs is still the major target of liver fibrosis recover (Benyon & Iredale, 2000; Elsharkawy et al., 2005).

The serum and stool level of PKM2 is highly correlated with several immune diseases with strong inflammatory response. In the previous study, we found that extracellular PKM2 releases from activated neutrophils and facilitates wound healing by activating angiogenesis and granulation tissue formation. PKM2 activates myofibroblast differentiation through an integrin αvβ3-PI3K signal pathway.

4.3 Results

4.3.1 Identification of PKM2 in liver diseases

To explore whether extracellular PKM2 plays a role in liver injury repair, we carried out IHC analysis of human liver disease tissue array using PKM2 antibody. High level of extracellular PKM2 was detected in viral hepatitis and liver cirrhosis (Figure 4.1 A). PKM2 level was gradually increased as the degree of liver disease progression. It showed a small increase in viral hepatitis samples, and had a significant increase in liver cirrhosis samples. As control, no PKM2 was detected in normal hepatic tissue sample. We classified the degree of staining into three categories, weak, medium, and strong. It showed that most of the normal hepatic tissue had weak PKM2 level, and viral hepatitis shifted to the medium level. Liver cirrhosis had huge increase in the strong category. (Figure 4.1 B). To confirm our tissue array analysis, we analyzed several freshly collected tissue samples from patients of liver cirrhosis. In consistent with the tissue array analysis, we observed strong extracellular PKM2 staining with tissue sample of liver cirrhosis, compared with normal hepatic tissue and viral hepatitis. The classified categories represented similar portion as in the tissue array (Fig. 4.1 C&D). ELISA assay of patient blood sample showed that PKM2 was detected in the blood circulation of patients with viral hepatitis and liver cirrhosis (Fig. 4.1 E). These results indicate that PKM2 is released to extracellular space of liver cirrhosis patients.

4.3.2 Extracellular PKM2 promotes liver fibrosis

To study the function of extracellular PKM2 during liver fibrosis, a TAA/alcohol induced liver fibrosis mouse model was established. TAA/alcohol treatment is commonly used to induce liver fibrosis in mouse and rat model. TAA (Thioacetamide) is an organic molecule with sulfate group and is known as a potent centrilobular hepatotoxicant to induce liver injury with certain dosage (LD50, 300 mg/kg in mouse and rat). After administration of TAA, it undergoes a two-step process from TAA to thioacetamide sulphoxide (TASO), and then thioacetamide-S, S-dioxide (TASO2), which is an active metabolite. This process releases inducible nitric oxide synthase (iNOS) and nuclear factor-κB that causes apoptosis and necrosis (T. M. Chen et al., 2008). Liver undergoes inflammation after injury caused by TAA. Long time treatment of TAA induces chronic inflammation and continuously activates HSCs to develop liver fibrosis.

In our experiment, TAA was treated for two and a half weeks, and then buffer, rPKM1, and rPKM2 were added into the treatment respectively for three and a half weeks (Figure 4.2 A). Mouse body weight was measured though out the whole experiment. Starting from the injection of TAA at day 1, the average body weight of control group elevated compared with that of in the groups of TAA treatment. After rPKM2 was combined into the TAA injection, the body weight of TAA+rPKM2 group began to decrease and showed a significant difference at day 26. Body weights of TAA+rPKM2 group went to a steady level at day 34, and maintained a 2 grams difference compared with TAA+rPKM1 and TAA+buffer groups. Since the mice in control group kept growing, the final body weight difference between TAA and non-TAA groups was 5 grams (Figure 4.2 B). After 6 weeks, livers were dissected and liver weight was measured. TAA treatment significantly increased liver weight, and the addition of rPKM2 had even more enhancement (Figure 4.2 C). Liver pictures were taken after six weeks of the treatment. TAA

treatment resulted in the increase of liver size. Some livers in TAA+rPKM2 groups had obvious bigger size compared with the livers in other groups (Figure 4.3 A) Close look of the liver surface showed typical fibrotic features on the liver of TAA treated groups. The liver from TAA+rPKM2 group had more white and yellow dots on the surface, considered as the typical liver fibrotic signs (Figure 4.3 B)

4.3.3 Combination of rPKM2 and TAA causes more damage to liver function and architecture

To study the liver function in different groups, serum markers (albumin, ALT, and AST) reflecting liver function were screened. In albumin test, TAA treatment significantly increased the serum level of albumin, but there was no difference between TAA+buffer, TAA+rPKM1, and TAA+rPKM2. In ALT and AST tests, TAA treatment had three-fold increase compared with control, and TAA+rPKM2 treatment doubled the effect of TAA treatment (Figure 4.4 A). To observe the architecture of liver tissue, we used Sirius Red to stain collagen in liver tissue. Control group did not have much collagen signal. Only a little was stained around blood vessels. TAA+buffer and TAA+rPKM1 groups showed increased collagen staining, that thin collagen bridges were formed between portal tracts. TAA+rPKM2 groups had extensive level of collagen with thick band and collagen bridges crossing portal tracts. (Figure 4.4 B) Quantification of collagen staining using FRIDA software revealed that TAA treatment induced the expression of collagen, and addition of rPKM2 resulted in dense collagen pattern and disrupted tissue structure (Figure 4.4 C). Other serum markers reflecting liver function were screened. All TAA treatments elevated the levels of cholesterol and total protein compared with control group.

Only TAA+rPKM2 group had increased total bilirubin level (Figure 4.5 A). Liver fibrosis induces apoptosis of hepatocytes and generates apoptotic bodies in the liver tissue. The

number of apoptotic bodies is another way to analyze liver fibrosis. We stained the liver sections by H&E staining. The apoptotic bodies were marked with arrows. Control group did not have any apoptotic body, whereas TAA treatment damaged liver and showed typical apoptotic bodies in the liver sections. In addition, TAA+rPKM2 revealed more apoptotic bodies, indicating more damage to the liver tissue (Figure 4.5 B&C).

To test whether extracellular PKM2 can induce liver fibrosis, rPKM2 treatment without injection of TAA was compared with TAA treatment and control. We performed the same procedure as in the previous model. rPKM2 only group did not have any change in body weight and liver weight compared to control group (Figure 4.6 A&B). The liver size in rPKM2 only group showed similar as in control group (Figure 4.6 C). Both rPKM2 only group and control group had no significant collagen staining compared with TAA+buffer group (Figure 4.6 D)

4.3.4 Extracellular PKM2 protects activated HSCs from apoptosis

Addition of rPKM2 to TAA treatment induced more activated HSCs in liver tissue, which was marked by α-SMA in red. Apoptotic cells around HSCs were stained in green with TUNEL. The number of apoptotic cells was decreased in the TAA+rPKM2 treatment (Figure 4.7 A&B). Given that HSCs apoptosis is involved in liver fibrosis, we questioned whether extracellular PKM2 can affect HSCs apoptosis to promote liver fibrosis. We first tested the effect of extracellular PKM2 in HSCs in vitro using MTT assay. Primary HSCs were purchased and cultured for at least 7 days to obtain α-SMA activation (Figure 4.7 C). FasL and TRAIL were applied to induce apoptosis which reduce the absorbance in MTT assay, but addition of rPKM2 brought it back (Figure 4.7 D). Similar experiment was done using LX-2 cells also showed that rPKM2 treatment reduced the apoptotic level of LX-2 after TRAIL induction (Figure 4.7 E).

4.3.5 PKM2 interacts with integrin αvβ3 on the cell surface of HSCs

Our laboratory found that extracellular PKM2 interacted with integrin αvβ3 on the cell surface of endothelial cells and HDFa cells. Activated HSCs has been shown to have enhanced integrin αvβ3 expression. We performed the same crosslinking experiment and mass spectrometry assay to detect what is the cell surface target of PKM2 on HSCs. Several protein bands were found in the crosslinked result (Figure 4.8 A). Integrin αvβ3 was identified (Figure 4.8 B&C). We confirmed this interaction with PKM2 antibody pull-down assay and cell attachment assay with rPKM2 coated on the plate (Figure 4.8 D&E)

4.3.6 PKM2 activates the survival signal of activated HSCs through integrin αvβ3, PI3K, and NFκB

To pursue the interaction between PKM2 and integrin αvβ3, we added integrin αvβ3 antibody to the MTT assay and found it disrupted the protecting effect of rPKM2 (Figure 4.9 A). Since FAK is the downstream pathway of integrin αvβ3, we then tested the effect of FAK inhibitor in the rPKM2 protection of LX-2 cell apoptosis. As expected, rPKM2 induced the viability of LX-2 cells back to normal level, but addition of FAK inhibitor eliminated its benefit (Figure 4.9 B). In the extracellular PKM2 activated HDFa case, we discovered that PI3K is activated. Since PI3K is an important factor in the survival signaling pathway, we revealed that PI3K was activated in LX-2 cells after treatment of rPKM2 and the activity was reduced when FAK inhibitor was added (Figure 4.9 C). Further apoptotic test found that PI3K inhibitor also disrupted the protection of rPKM2 for the TRAIL induced LX-2 cell apoptosis (Figure 4.9 D). NFκB is known as a downstream factor of PI3K mediated survival signaling pathway. We then examined whether NFκB play a role in the activation of PI3K by extracellular PKM2 in HSCs. NFκB activity was measured by NFκB transcription factor assay. rPKM2 treatment significantly

elevated the activity of NFκB compared with control. This activation was inhibited by both αvβ3 antibody and PI3K inhibitor (Figure 4.9 E).

4.3.7 Neutralization of extracellular PKM2 facilitates liver recovery from TAA/alcohol induced fibrotic damage

Since PKM2 is found extracellularly during liver fibrosis, we wondered whether neutralization of extracellular PKM2 can relieve the liver tissue damage. To find the appropriate PKM2 antibody for animal experiment, we tested the blocking ability of PKM2 antibody in LX-2 cell attachment assay. We first picked two antibodies recognizing only PKM2 but not PKM1 (Figure 4.10 A). We tested this pair of PKM2 antibody IgGPK16 and IgGPK21. IgGPK16 had very good effect of blocking the attachment of LX-2 cell on rPKM2 coated plate (Figure 4.10 B). This set of mouse liver fibrosis model was designed by treating TAA/alcohol for 12 weeks and then following 10 doses of PKM2 antibody and control antibodies (buffer, IgGCon, and IgGPK21) (Figure 4.10 C). Mouse body weights were measured through the experiment. During the 12-weeks of TAA/alcohol treatment, body weight of TAA treated groups was significantly lower compared with control group. After stop of TAA/alcohol treatment, body weight of IgGPK16 group had faster increase than other control groups (Figure 4.10 D). Final liver weights showed that buffer, IgGCon, and IgGPK21 group had about 0.5 g increase compared with control, and body weight of IgGPK16 group reduced close to control level (Figure 4.10 E).

Liver pictures clearly showed the liver size of buffer, IgGPK21, and IgGCon groups were bigger than IgGPK16 group (Figure 4.11 A). Close examination of liver surface revealed bigger size and typical fibrotic feature in buffer group. IgGPK16 group had similar liver size and surface features compared to control group (Figure 4.11 B). To test the effect of PKM2 antibody in liver function and architecture, we did both serum marker screen and Sirius Red staining to

stain collagen. In the serum albumin level, all treatments had increased compared with control, and there was no difference among them. In the serum ALT and AST levels, all treatments also increased compared with control, but IgGPK16 treatment reduced ALT and AST levels after the whole experiment (Figure 4.12 A). In the Sirius Red staining result, buffer, IgGCon, and IgGPK21 groups presented dense collagen with network structure. On the other hand, IgGPK16 group indicated reduction of collagen expression (Figure 4.12 B&C). In the H&E staining result, IgGPK16 treatment showed less numbers of apoptotic bodies indicating the relief of liver fibrosis (Figure 4.13 A). Double staining of α-SMA and TUNEL showed that IgGPK16 treatment had less α-SMA expression but more apoptotic cells compared with IgGCon treatment (Figure 4.13 C).

Previously, we reported that PKM2 can be released from infiltrated neutrophils during wound repair process. The released PKM2 promotes wound repair. Very similar to the case of cutaneous wound, liver injury would also trigger strong immune responses with neutrophil infiltration/activation. Thus, it is expected that high levels of infiltration neutrophils would be presented in fibrotic liver. Indeed, IHC staining of liver tissue array showed that neutrophils presented at high levels in liver cirrhosis tissue samples (Figure 4.14 A). The observation clearly supported the notion that activated neutrophils release PKM2. Extracellular PKM2 acts on integrin αvβ3 of HSCs to promote activated HSCs survival. A number of previous studies showed that activation of several pairs of integrin facilitates fibrosis progression, including αvβ6, αvβ8, and αvβ1. It is believed that the effects of these integrin pairs on fibrosis progression are mediated via activation of latent TGFβ. Thus, we asked whether extracellular PKM2 acted by a similar mechanism in facilitating liver fibrosis progression. We tested the effects of a TGF neutralize antibody and a TGFβ receptor inhibitor on the activity of extracellular PKM2. Clearly,

the function of extracellular PKM2 was TGFβ signaling independent (Figure 4.14 B). Furthermore, TGFβ receptor was not activated in LX-2 cells upon rPKM2 treatment (Figure 4.14 C). Cell attachment assays demonstrated that integrin αvβ6 and αvβ1 expressing CHO cells did not attach to rPKM2 coated plates (Figure 4.14 D), indicating that PKM2 did not interact with these integrins.

4.4 Discussion

We demonstrated that extracellular PKM2 promotes liver fibrosis by protecting activated HSCs from apoptosis. Our laboratory previously discovered that neutrophils releases PKM2 activated myofibroblast differentiation of dermal fibroblasts via integrin αvβ3 signaling pathway. By interacting with the same target on cell surface, extracellular PKM2 stimulates different reactions in dermal fibroblasts and HSCs. We questioned what could be the reason of this alternative function. Is extracellular PKM2 also involved in the transformation from HSCs to myofibroblasts? Integrin αvβ3 signaling is involved in several pathways. Multiple factors can activate integrin αvβ3 in addition to its natural ligand vitronectin. We cannot exclude the function of PKM2 activating differentiation in HSCs during liver fibrosis. More tests related with myofibroblast differentiation of HSCs should be done in the future.

PKM2 antibody treatment showed promising effect in the TAA/alcohol induced mouse fibrosis model. We questioned can PKM2 antibody treatment fully reverse liver fibrosis? In our experiment, after 12 weeks of TAA/alcohol treatment, PKM2 antibody was applied for 20 days. Body weight of IgGPK16 group was still about 2 grams smaller than control group. Extension of PKM2 antibody treatment might provide better result that IgGPK16 group can catch up control group. Collagen staining result showed that the IgGPK16 group still maintains certain amounts of collagen. The digestion of remaining collagen by MMPs would take longer time. In this

TAA/alcohol induced mouse liver fibrosis model, the stage of fibrosis was still considered in early or middle stage corresponding to the collagen staining pattern. At this stage, liver fibrosis could be still reversible, because of the high metabolism of mouse. Different mouse fibrosis models, such as CCl_4, dimethylnitrosamine (DMN), bile duct ligation, and concanavalin A should be tested with PKM2 antibody treatment to confirm the effect of reversing fibrosis.

4.5 Materials and Methods

4.5.1 Liver fibrosis induction and treatments

All animal experiments were carried out in accordance with the guidelines of IACUC of Georgia State University. Balb/c mice (6-7 week old male) were I.P. injected with 100 mg/kg TAA and gradually increased to 200 mg/kg TAA in two weeks. 10% alcohol was also fed to mice along with the TAA treatment. For rPKM2 experiment, 5 mg/kg of rPKM2 was mixed with TAA for injection starting at two and a half week, and lasted for total of seven weeks. TAA mixed with buffer or rPKM1 was the control. For the PKM2 antibody experiment, TAA was continuously treated for twelve weeks. After that, TAA and alcohol was stopped and 4mg/kg of PKM2 antibody was I.P. injected every other day for ten doses. Buffer and rabbit IgG was the control. The body weights were recorded every week or every four days. At the end of the experiments, animals were sacrificed. Livers, other organs, and blood samples were collected. Liver weights were measured and liver pictures were taken. Tissue sections were prepared and analyzed by IF, IHC, or H&E stains using commercially available antibodies as indicated. Serum samples were prepared from collected blood samples. The serum samples were analyzed by the service of Comparative Clinical Pathology.

4.5.2 Sirius Red staining and analysis for collagen

Sirius Red staining was used the NovaUltra^{TM} Sirius Red Stain Kit from IHCWORLD. The staining procedure was basically followed the protocol provided in the kit. In brief, the paraffin embedded slides were deparaffinized in xylene, 100% alcohol, 95% alcohol, 70% alcohol, 50% alcohol, 30% alcohol, and then distilled water. The slides were stained in Weigert's Hematoxylin Solution for 10 min, and washed with running tap water for 10 min. Then, the slides were incubated in Pico-Sirius Red Solution for one hour and followed with Acetic Acid Solution for 1 min. The cells were stained in light brown and collagen was stained in red. The slides were dehydrated through increased concentration of alcohol and mounted in a resinous mounting medium. The pictures of collagen staining were taken with microscope under X100 magnification. The density of collagen staining was quantified using FRIDA software.

4.5.3 MTT assay

MTT assay was used to measured HSCs and LX-2 cell viability. MTT was dissolved at 5 mg/ml in specific culture medium to make the stock solution. The solution was filtered through a 0.22 μm filter before adding into the culturing cells. MTT stock solution was added to each well at a 1:10 dilution and incubated for 3 to 4 hours. At the end of the incubation period, the culture media were removed and acidic isopropanol was added into each well to solubilize the dye. Absorbance of solubilized dye was measured at a wavelength of 570 nm with background subtraction at 690 nm.

4.5.4 NFκB transcription factor assay

Activity of NFκB was measured by an NFκB p50/p65 EZ-TFA transcription factor assay kit. The flanked DNA binding consensus sequence for NFκB was coated on the plate. After incubation with cell extracts, activated NFκB was captured by the plate. The bound NFκB

transcription factor unit p50 and p65 were detected by specific antibodies similarly as in ELISA procedure.

Figure 4.1 Identification of PKM2 in liver diseases.

(A) Immunohistochemistry staining of PKM2 in liver cirrhosis or hepatitis tissue microarray. Microarray is stained with PKM2 antibody. Samples are separated to three groups, normal hepatic tissue, viral hepatitis, and liver cirrhosis. (B) Quantification of PKM2 staining in microarray. PKM2 intensity is divided into three categories: weak (<2000), medium (2000-5000), and strong (>5000). Each core is examined and classified into one of the previous three categories. (C) IHC staining of PKM2 in hepatitis and cirrhosis patient liver samples. (D) Quantification of PKM2 staining fresh patient samples. PKM2 intensity is divided into three categories: weak (<2000), medium (2000-5000), and strong (>5000). Each section is examined and classified into one of the previous three categories. (E) Serum PKM2 levels of viral hepatitis and liver cirrhosis patients.

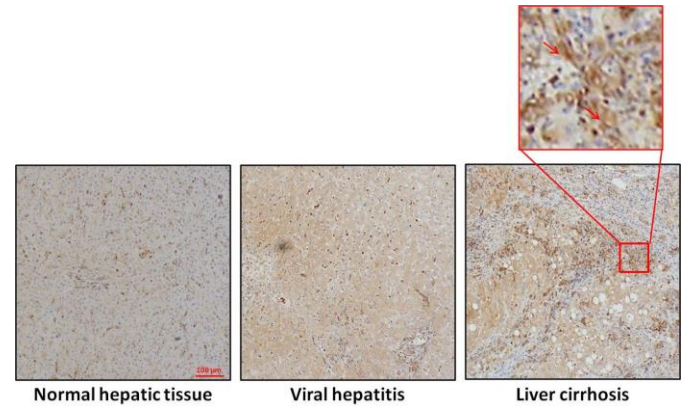

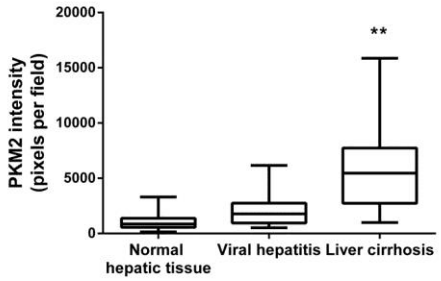

PKM2 intensity	Weak		Medium		Strong	
Normal hepatic tissue	24/30	80%	6/30	20%	0/30	0%
Viral hepatitis	3/10	30%	6/10	60%	1/10	10%
Liver cirrhosis	4/40	10%	14/40	35%	22/40	55%

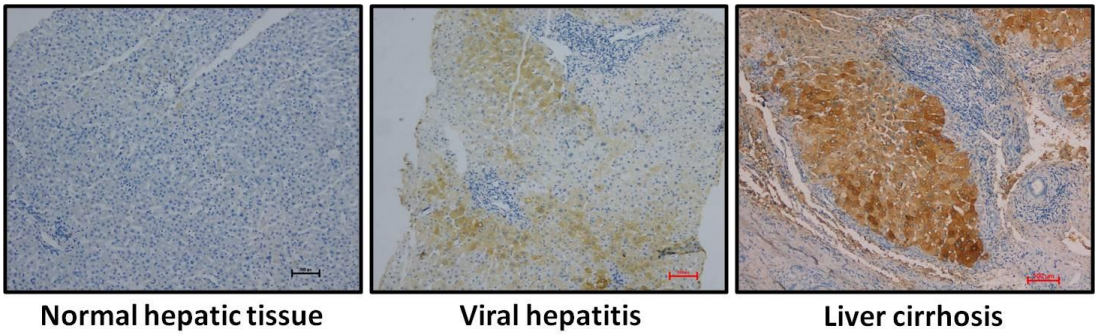

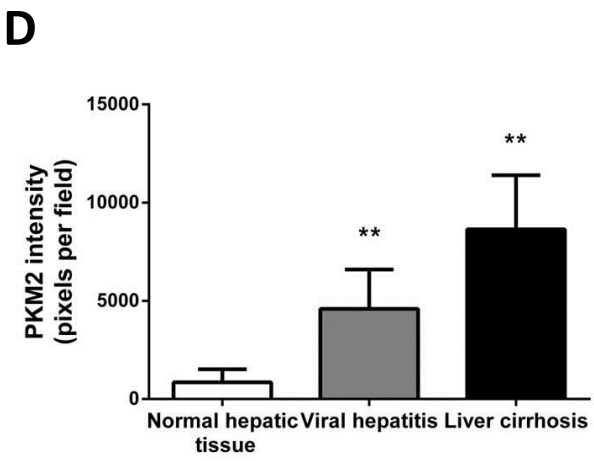

PKM2 intensity	Weak		Medium		Strong	
Normal hepatic tissue	80/80	100%	0/80	0%	0/80	0%
Viral Hepatitis	27/80	34%	29/80	36%	24/80	30%
Liver cirrhosis	2/80	3%	13/80	16%	65/80	81%

E

Serum PKM2 level (ng/mL)	Range	Mean
Normal (n=10)	0.12-0.55	0.393
Viral hepatitis (n=10)	0.79-1.46	1.099
Liver cirrhosis (n=10)	1.3-3.4	2.14

Figure 4.1 Identification of PKM2 in liver diseases.

Figure 4.2 Addition of PKM2 affects body weight and liver weight in the TAA/alcohol mouse model.

(A) Liver fibrosis mouse model diagram. (B) Average mouse body weight through the treatment (6 weeks). (C) Average mouse liver weight at the end of the experiment.

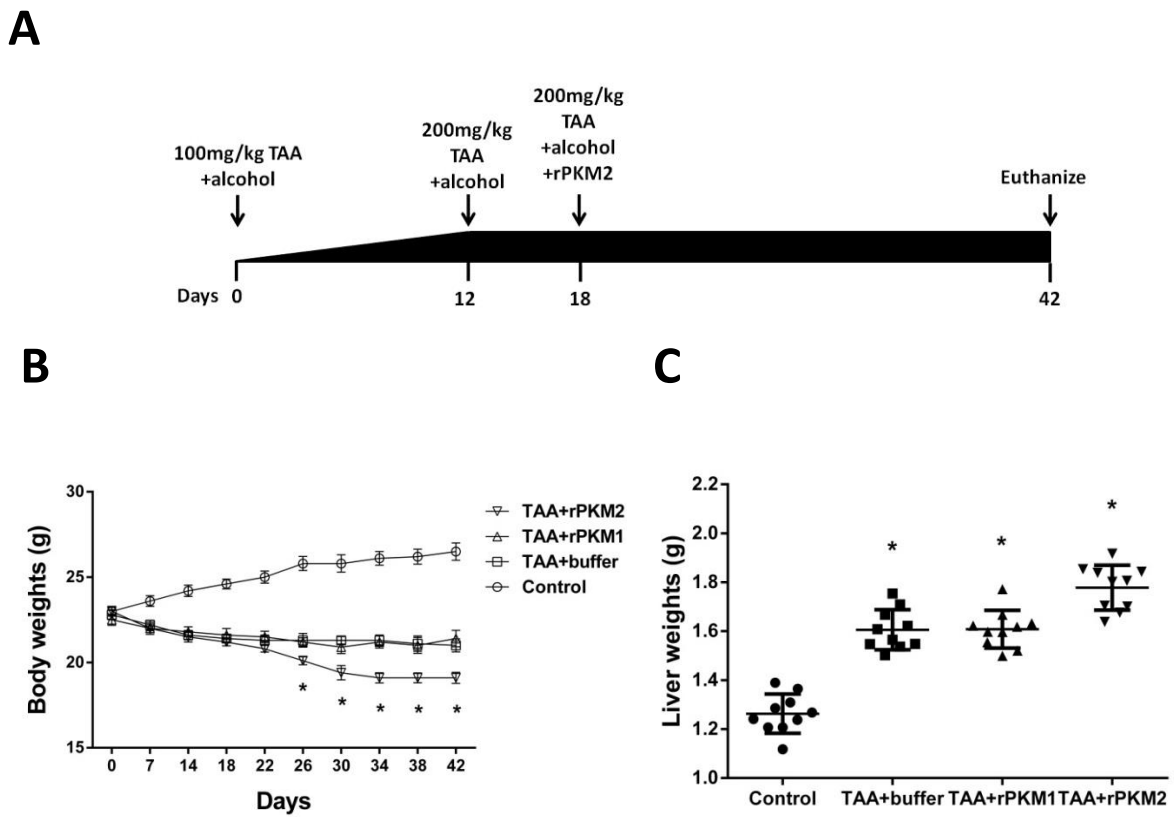

Figure 4.2 Addition of PKM2 affects body weight and liver weight in the TAA/alcohol mouse model.

Figure 4.3 Addition of PKM2 promotes liver fibrosis in the TAA/alcohol mouse model.

(A) Liver pictures of different groups. (B) Liver zoomed-in pictures of control, TAA+buffer, and TAA+rPKM2 groups.

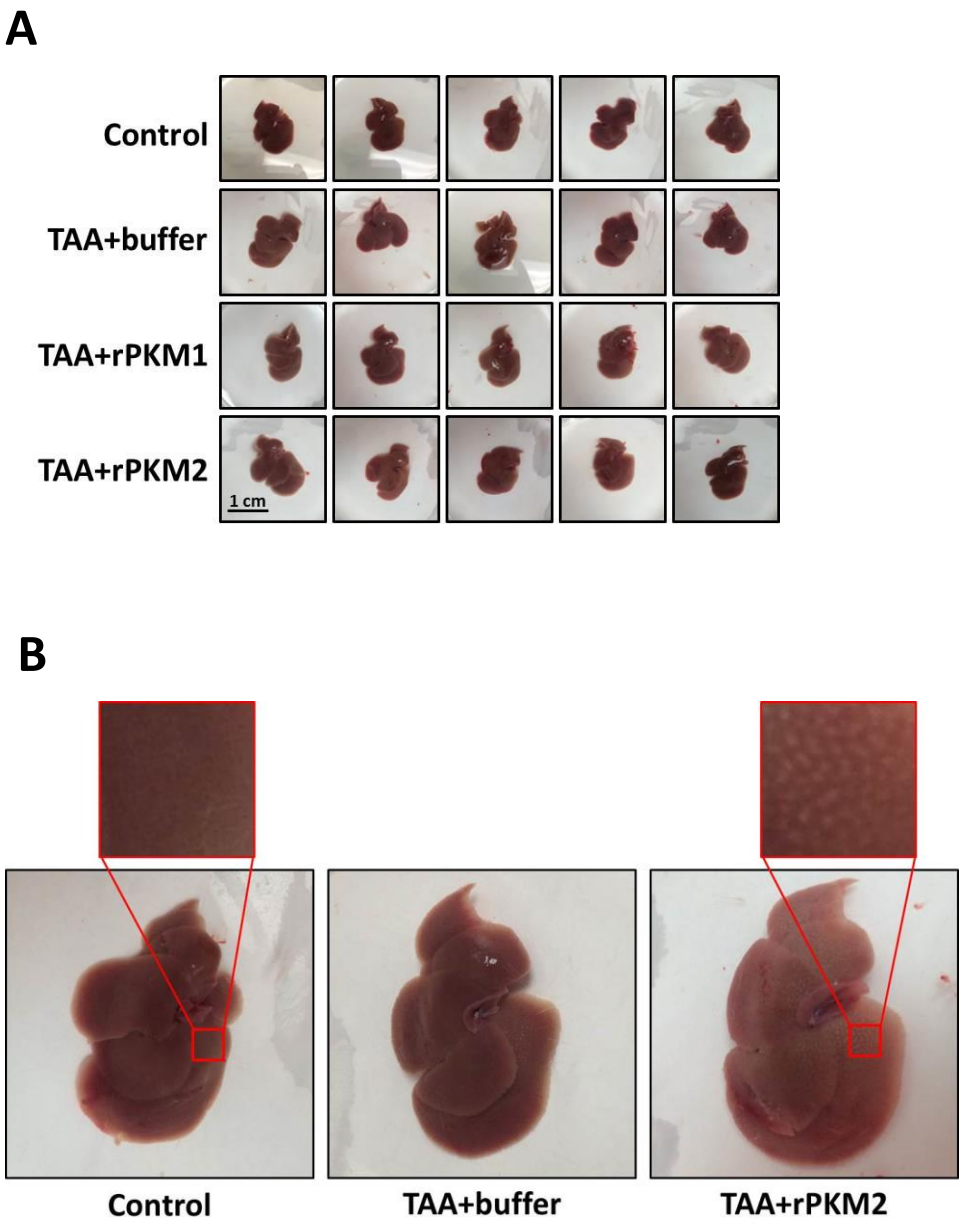

Figure 4.3 Addition of PKM2 promotes liver fibrosis in the TAA/alcohol mouse model.

Figure 4.4 Addition of PKM2 deals more liver damage in the TAA/alcohol mouse model.

(A). Serum marker analysis in different groups. (Albumin, ALT, and AST) (B). Sirius Red staining of paraffin embedded liver samples. Light brown color indicates background cell staining, and red color indicates collagen staining. (C) Quantification of Sirius Red staining for collagen.

A

	Albumin (mg/dl)	ALT (U/L)	AST (U/L)
Control	2.77±0.44	34.17±7.25	29.71±6.42
TAA+buffer	3.71±0.42	93.5±26.98	97.5±.47
TAA+rPKM1	3.86±0.34	92.38±23.31	98.38±36.07
TAA+rPKM2	3.74±0.31	169.13±22.76	207.88±50.66

B

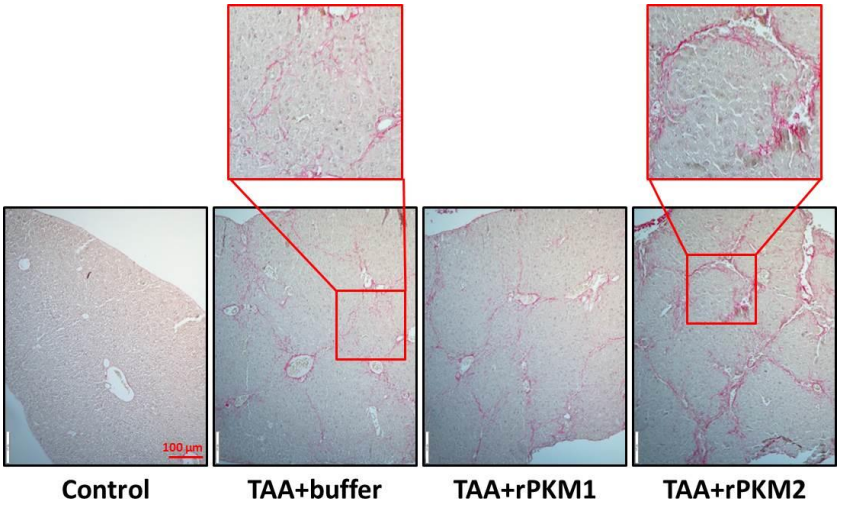

C

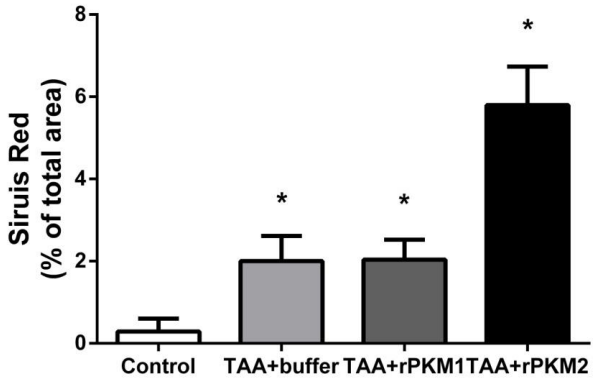

Figure 4.4 Addition of PKM2 deals more liver damage in the TAA/alcohol mouse model.

Figure 4.5 Addition of PKM2 induces apoptotic body number in the TAA/alcohol mouse model.

(A). Serum markers analysis in different groups (cholesterol, total protein, and total bilirubin). (B). H&E staining of paraffin embedded liver samples. Nucleus is stained in purple, and cytosol is stained in pink. Apoptotic bodies are marked with arrows. (C) Quantification of apoptotic bodies.

A

	Cholesterol (mg/dl)	Total Protein (g/dl)	Total Bilirubin (mg/dl)
Control	133.38±5.32	5.02±0.58	0.65±0.11
TAA+buffer	167.52±15.69	6.15±1.01	0.625±0.36
TAA+rPKM1	167.75±9.32	6.43±0.48	0.64±0.21
TAA+rPKM2	165.87±17.58	6.38±0.21	0.875±0.47

B

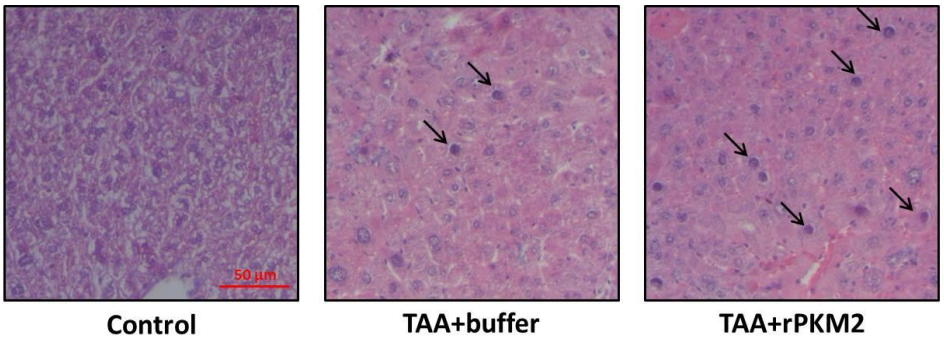

C

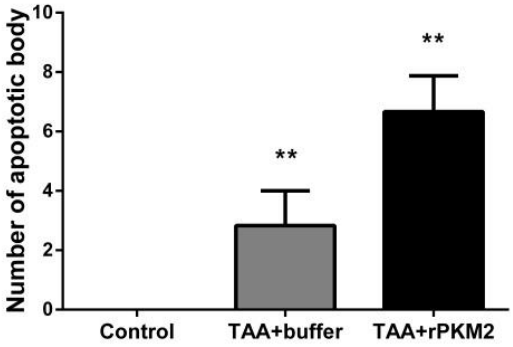

Figure 4.5 Addition of PKM2 induces apoptotic body number in the TAA/alcohol mouse model.

Figure 4.6 Treatment of PKM2 only does not induce liver fibrosis.

(A) Mouse body weights through the treatment (rPKM2 only). (B) Mouse liver weights at the end of the experiment (rPKM2 only). (C) Liver pictures of different groups (rPKM2 only). (F) Sirius Red staining of paraffin embedded liver samples (rPKM2 only).

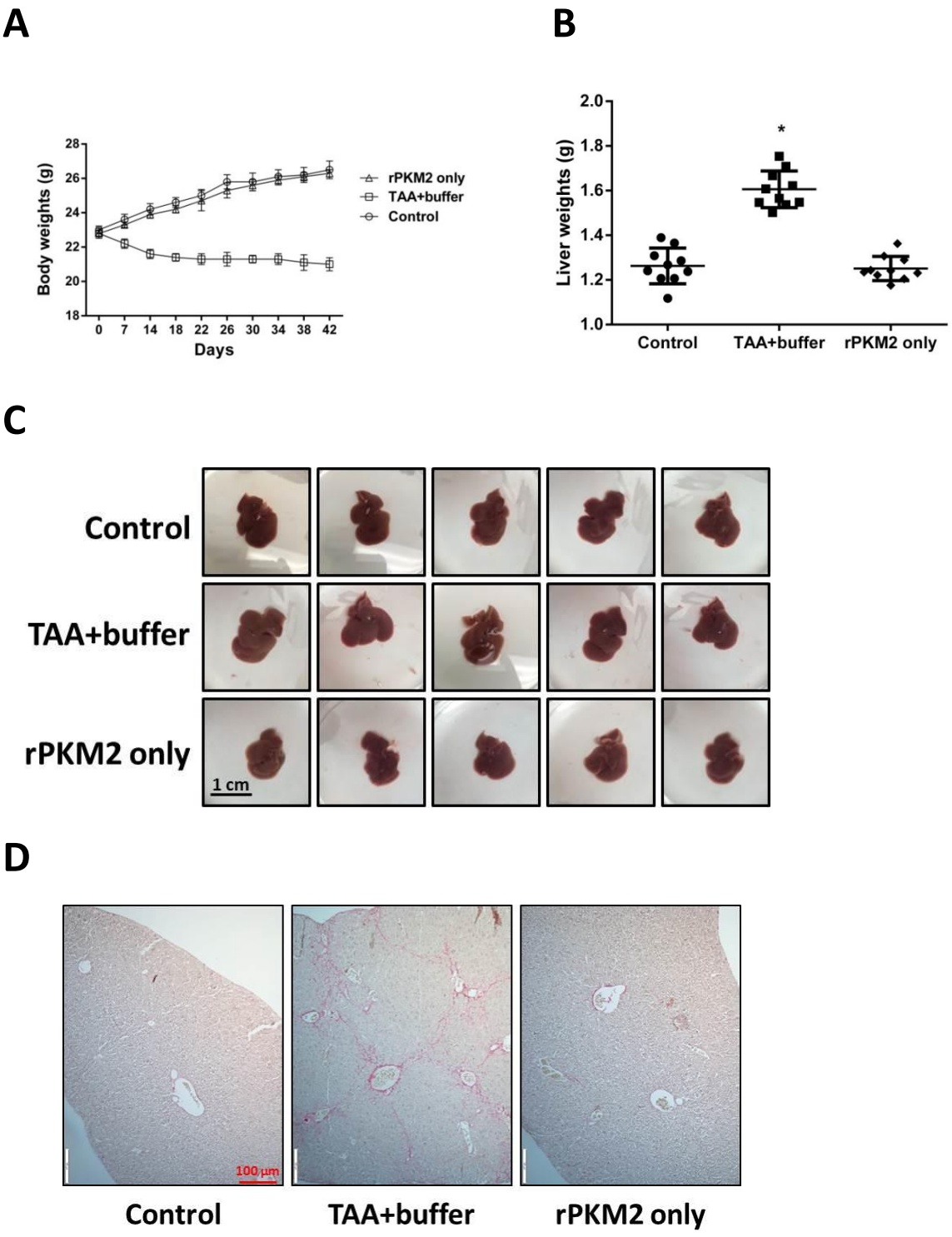

Figure 4.6 Treatment of PKM2 only does not induce liver fibrosis.

Figure 4.7 Extracellular PKM2 protects activated HSCs from apoptosis.

(A) Immunofluorescence staining of frozen liver samples. Green color indicates TUNEL, and red color indicates α-SMA. (B) Quantification of α-SMA intensity vs numbers of TUNEL nucleus. (C) Immunoblot of α-SMA in HSCs before and after activation. (D) rPKM2 treatment protects HSCs from FasL and TRAIL induced apoptosis. (E) rPKM2 treatment protects LX-2 cells from TRAIL induced apoptosis.

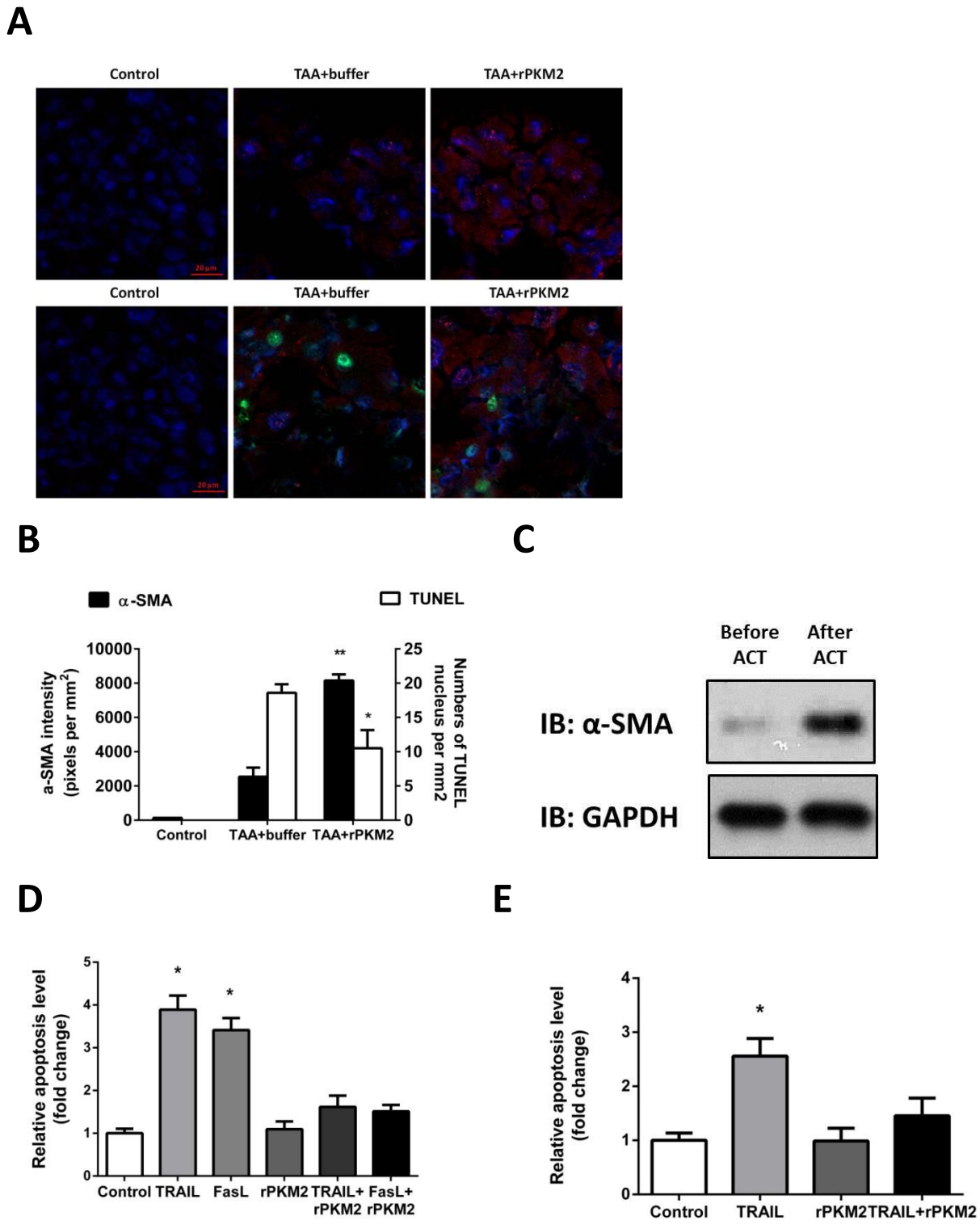

Figure 4.7 Extracellular PKM2 protects activated HSCs from apoptosis.

Figure 4.8 PKM2 interacts with integrin αvβ3 on the cell surface of LX-2 cells.

(A) SDS-PAGE of LX-2 cell membrane extract with or without crosslink. Arrows indicate possible integrin proteins. (B) Mass spectrometry analysis of digested protein bands showed integrin αv in the result. (C) Mass spectrometry analysis of digested protein bands showed integrin β3 and PKM2 in the result. (D) Attachment assay of LX-2 cells on different coatings. BSA or integrin αvβ3 antibody is pre-treated before the assay. (E) PKM2 antibody IP result of membrane extract of LX-2 cells.

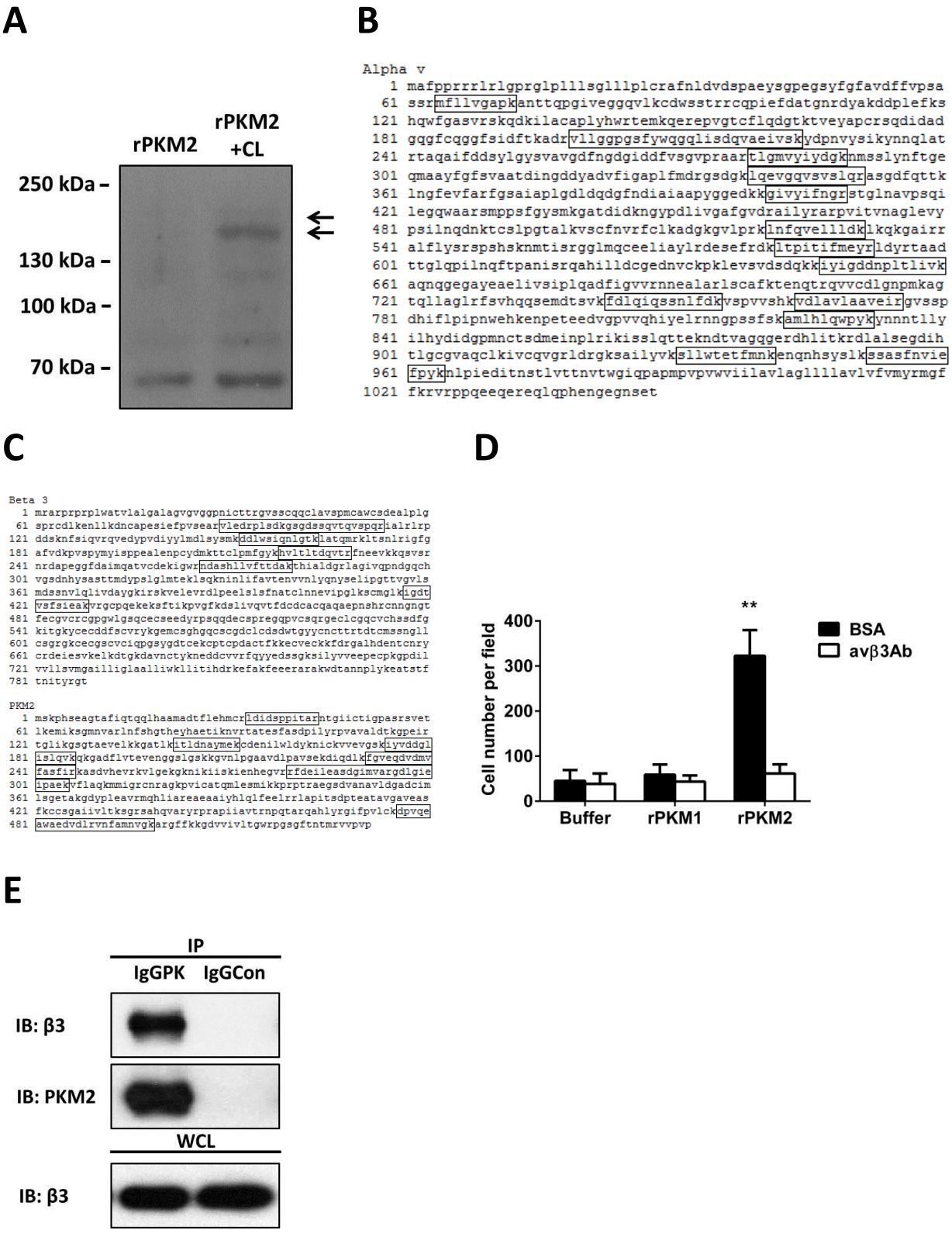

Figure 4.8 PKM2 interacts with integrin αvβ3 on the cell surface of LX-2 cells.

Figure 4.9 PKM2 activates the survival signal of activated HSCs through integrin αvβ3, PI3K, and NFκB.

(A) rPKM2 treatment protects LX-2 cells from apoptosis, which is disrupted by αvβ3 antibody in MTT assay. (B) FAK inhibitor diminishes the protection of PKM2 in LX-2 cell apoptosis in MTT assay. (C) PI3K activity assay of LX-2 cells. (D) PI3K inhibitor reduces the protection of PKM2 in LX-2 cell apoptosis in MTT assay. (E) NFκB activity assay. αvβ3 antibody and PI3K inhibitor decreases the NFκB activity induced by rPKM2 treatment in LX-2 cells.

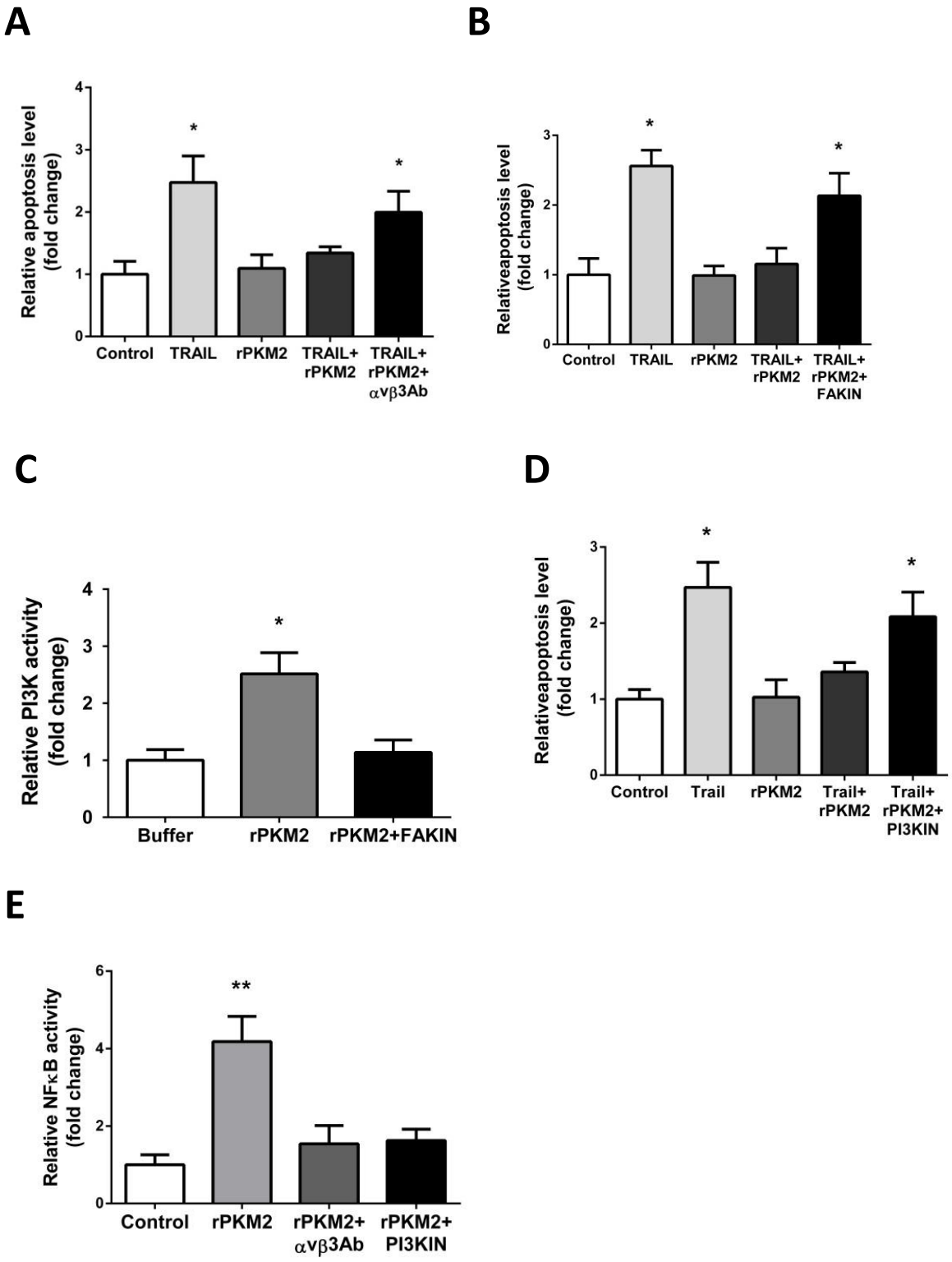

Figure 4.9 PKM2 activates the survival signal of activated HSCs through integrin αvβ, PI3K, and NFκB.

Figure 4.10 Neutralization of extracellular PKM2 in the TAA/alcohol mouse model.

(A) Attachment assay of LX-2 cells on rPKM2 coated plate with antibody blocking treatment. (B) Immunoblot of PKM2 antibody: IgGPK16 vs IgGPK21. (C) Diagram of liver fibrosis mouse model with antibody treatment (15 weeks). (D) Mouse body weights through the treatment. (E) Mouse liver weights at the end of experiment.

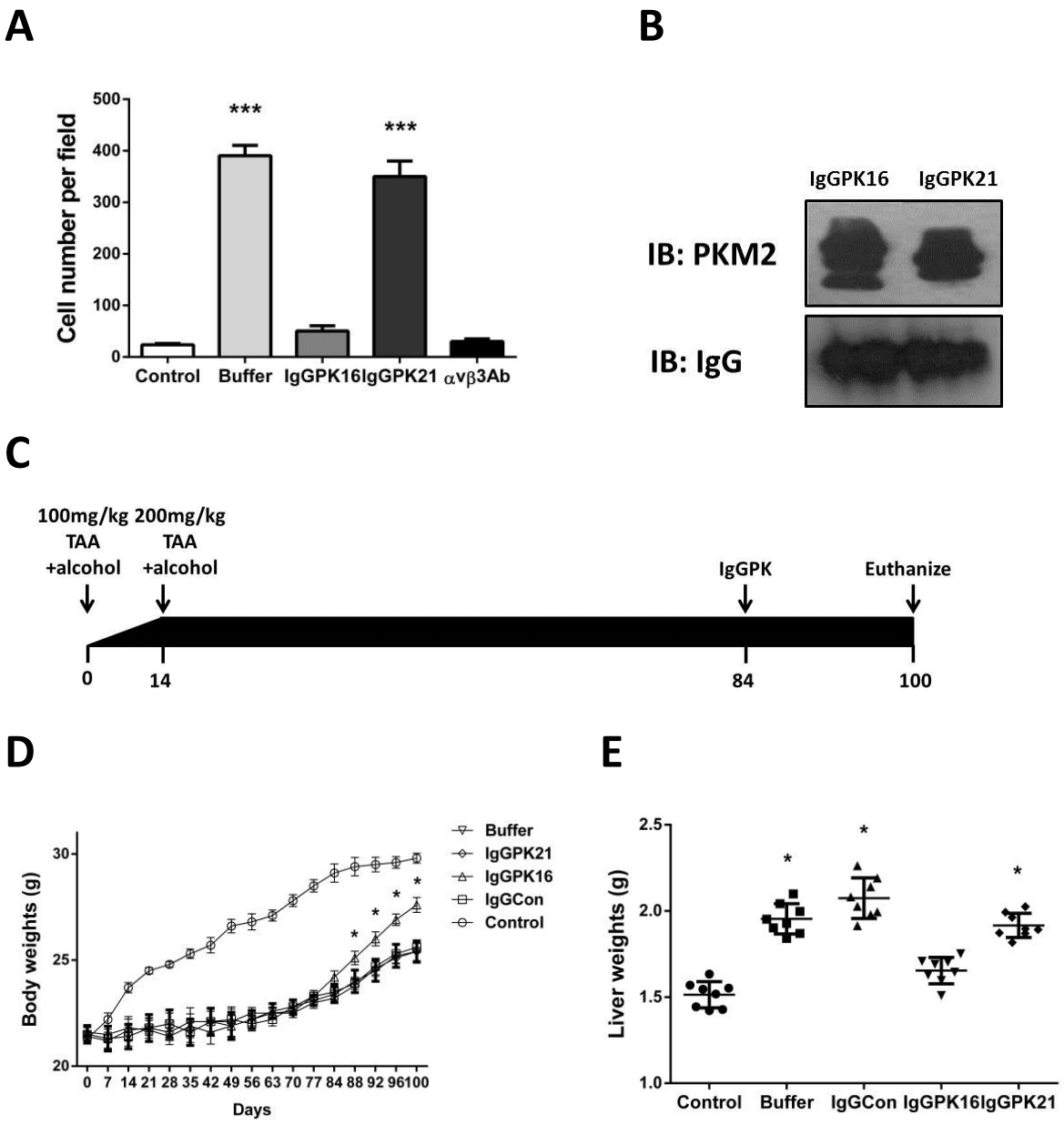

Figure 4.10 Neutralization of extracellular PKM2 in the TAA/alcohol mouse model.

Figure 4.11 Neutralization of extracellular PKM2 facilitates liver recovery from the TAA/alcohol induced fibrotic damage.

(A) Liver pictures of different groups. (B) Liver zoomed-in pictures of control, buffer, and IgGPK16 groups.

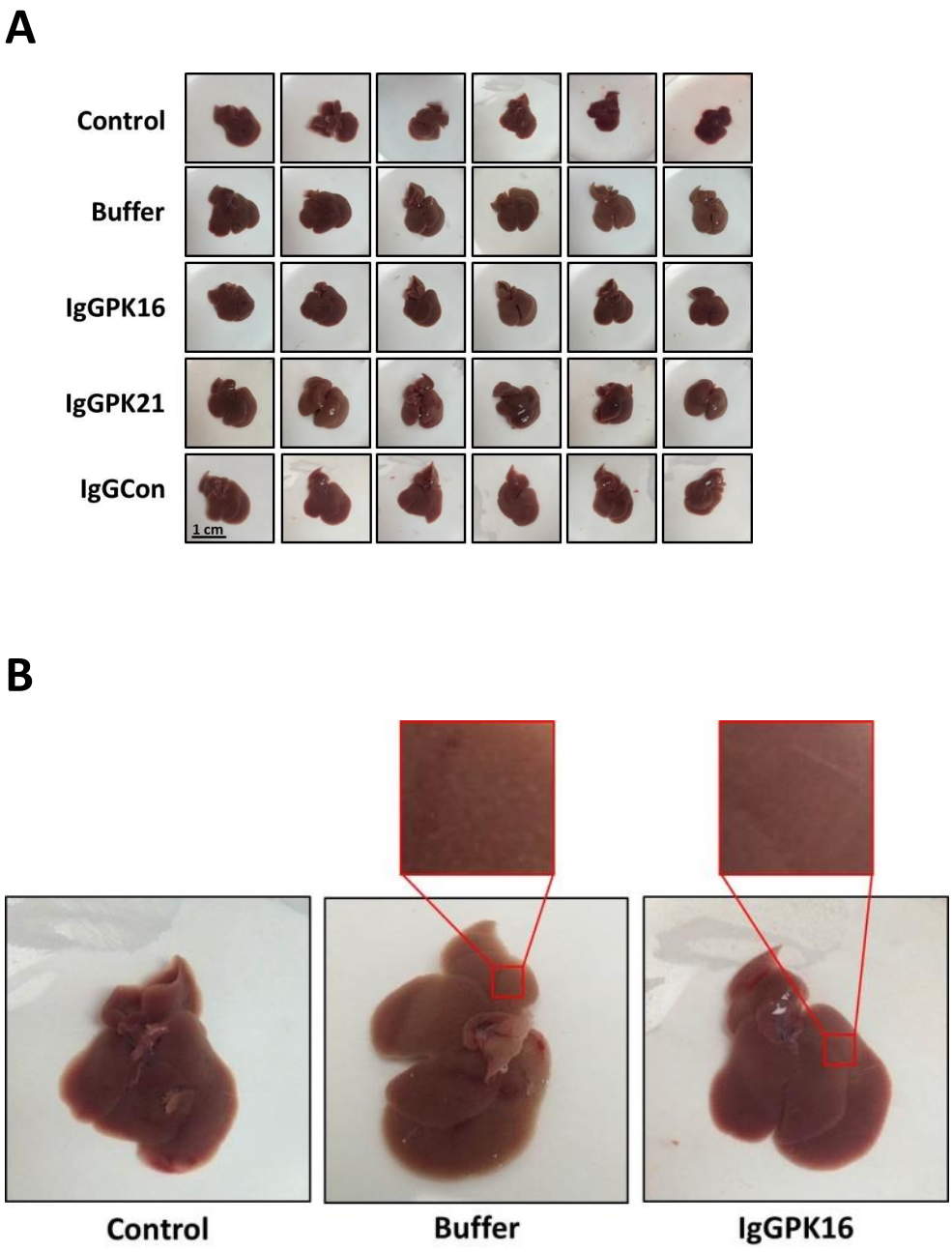

Figure 4.11 Neutralization of extracellular PKM2 facilitates liver recovery from the TAA/alcohol induced fibrotic damage.

Figure 4.12 Neutralization of extracellular PKM2 recovers liver function from the TAA/alcohol induced fibrotic damage.

(A) Serum markers reflecting liver function (albumin, ALT, and AST). (B) Sirius Red staining of paraffin embedded liver samples. (C) Quantification of Sirius Red staining for collagen.

A

	Albumin (mg/dl)	ALT (U/L)	AST (U/L)
Control	2.38±0.39	31.38±7.15	35.43±8.18
Buffer	3.25±0.37	198.88±40.19	195.86±47.84
IgGPK16	3.05±0.48	82.75±22.21	118.38±32.39
IgGPK21	3.16±0.24	180.63±37.83	174.25±23.74
IgGCon	3.14±0.23	195.25±46.69	189.12±31.71

B

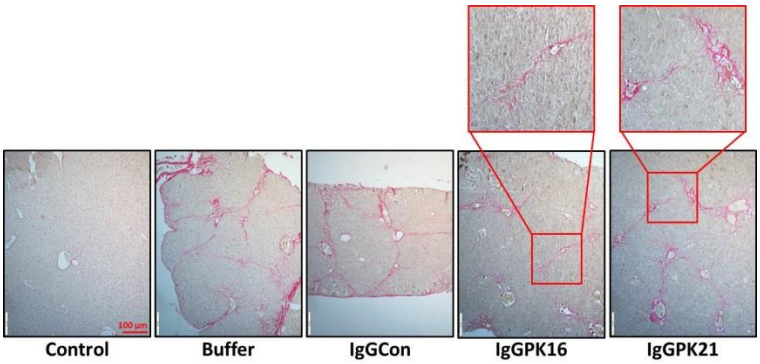

C

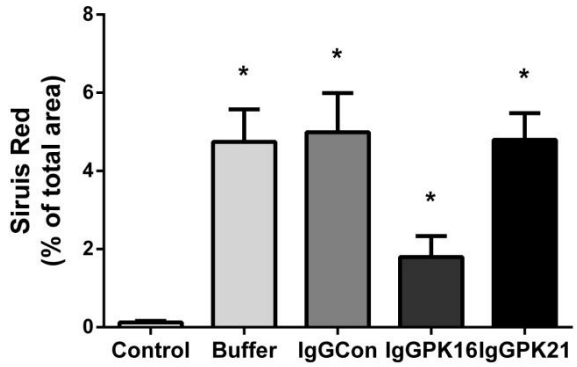

Figure 4.12 Neutralization of extracellular PKM2 recovers liver function from the TAA/alcohol induced fibrotic damage.

Figure 4.13 Neutralization of extracellular PKM2 affects apoptotic bodies and HSCs apoptosis in the TAA/alcohol mouse model.

(A) H&E staining of liver sections. (B) Immunofluorescence staining of frozen liver samples. (C) Quantification of α-SMA intensity vs numbers of TUNEL nucleus.

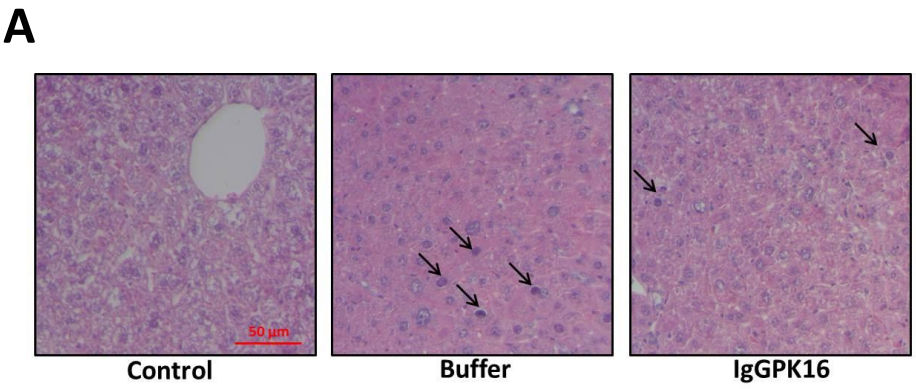

Figure 4.13 Neutralization of extracellular PKM2 affects apoptotic bodies and HSCs apoptosis in the TAA/alcohol mouse model.

Figure 4.14 PKM2 activated integrin αvβ3 signal is independent of TGFβ signal.

(A) Quantification of IHC staining of Ly6G in liver disease tissue microarray. (B) TGFβ antibody and TGFβ receptor inhibitor does not affect the activity of PKM2. (C) TGFβ receptor is not activated upon treatment of PKM2. (D) CHO cells expressing integrin αvβ3 attach to the rPKM2 coated plate, compared with integrin αvβ1 and αvβ6 expressions.

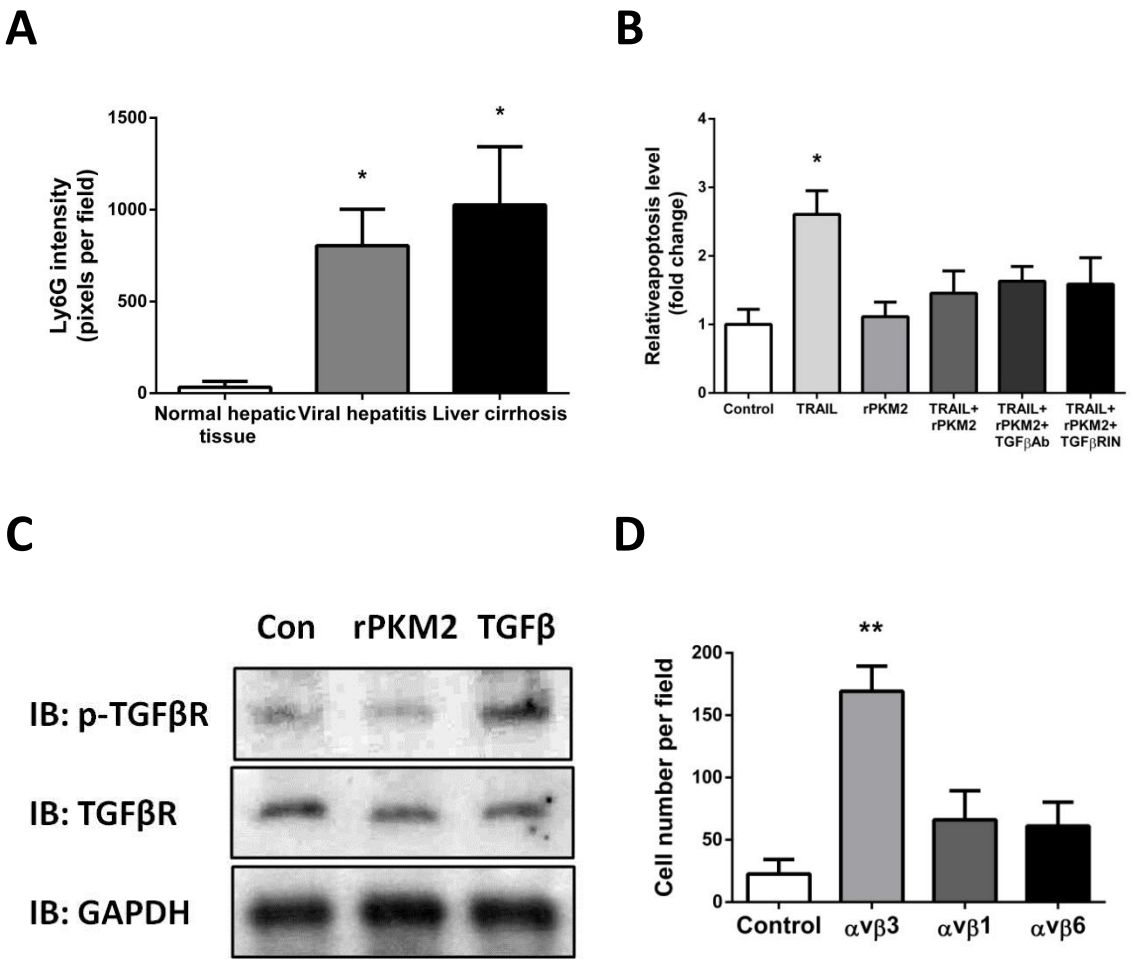

Figure 4.14 PKM2 activated integrin αvβ3 signal is independent of TGFβ signal.

Figure 4.15 Diagram of the whole process.

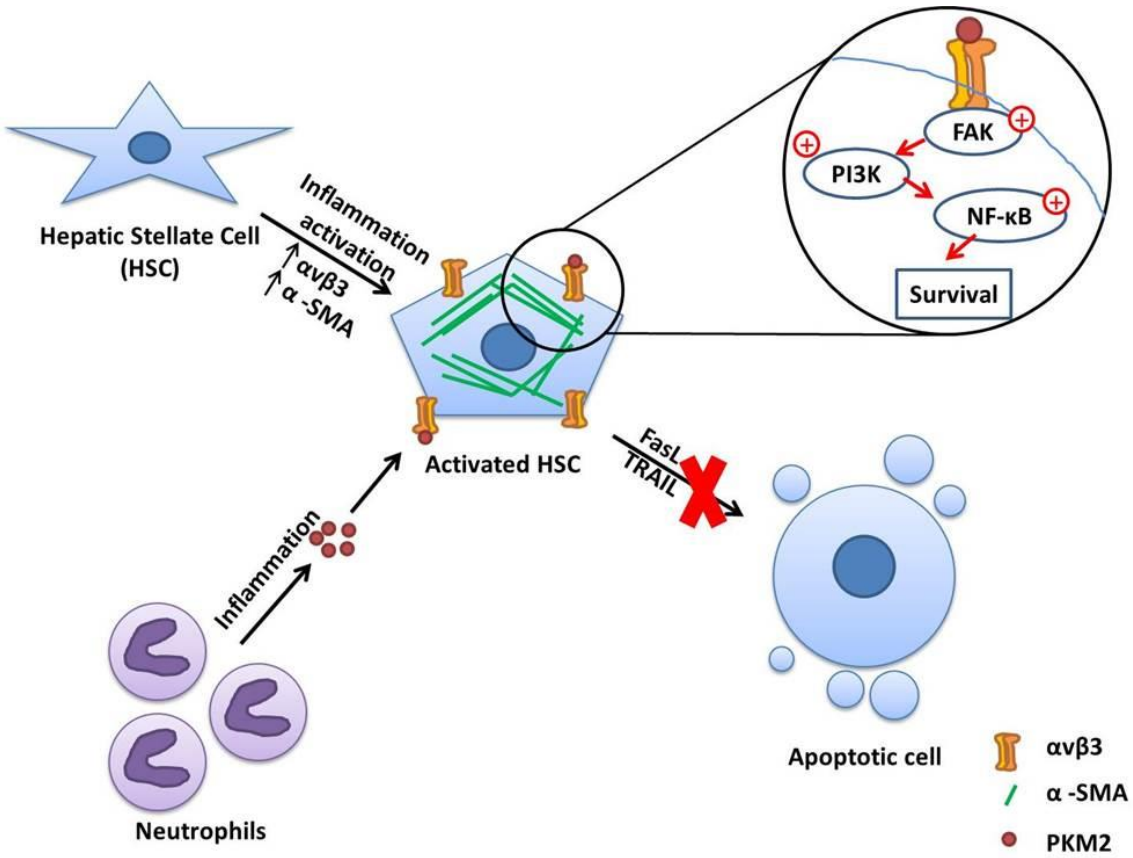

Figure 4.15 Diagram of the whole process.

CHAPTER 5 MATERIALS AND METHODS

5.1 Materials

5.1.1 Chemicals

Acetic Acid	VWR international
Acrylamide	VWR international
Agar	Sigma Aldrich
Agarose	Sigma Aldrich
Ammonium Persulfate (APS)	Sigma Aldrich
Ampicillin	Sigma Aldrich
ATP	Sigma Aldrich
Autoradiography film	Fisher Scientific
Bacto Yeast Extract	BD Biosciences
Bacto Tryptone	BD Biosciences
Bis-Acrylamide (w/v 29:1)	VWR International
β-Mercaptoethanol	Sigma Aldrich
Bromophenol Blue	EMD
Calcium Chloride	Sigma Aldrich
Cell culture media	Cellgro
Coomassie blue	Sigma Aldrich
Crystal Violet	Sigma Aldrich
Dithiothreitol (DTT)	Sigma Aldrich
Dimethyl Sulfoxide (DMSO)	Sigma Aldrich
ECL Western Blot substrate	Thermo Scientific
Ethanol, 200 Proof	VWR International
Ethidium Bromide	Sigma Aldrich
Ethylenediaminetetraacetic Acid (EDTA).	Sigma Aldrich
FAK inhibitor 14	Millipore
Fetal Bovine Serum (FBS)	Invitrogen Life Technologies
Formaldehyde	Sigma Aldrich
Formalin, 10% solution	Sigma Aldrich
Glycerol	VWR International
Glycine	VWR International
Hank's Balanced Salt Solution (HBSS)	Invitrogen Life Technologies
HEPES	Sigma Aldrich
Hydrochloric acid	VWR International
Imidazole	Sigma Aldrich
Isopropyl Alcohol	VWR International
Isopropyl ß-D-1-thiogalactopyranoside(IPTG)	Sigma Aldrich

Kanamycin	Sigma Aldrich
Magnesium Chloride	Sigma Aldrich
Methanol	VWR International
Nail Polish	Fisher Scientific
Ni-NTA agarose	Qiagen Inc.
Penicillin-Streptomycin solution	Cellgro
Phenylmethylsulfonyl Fluoride (PMSF)	Sigma Aldrich
Ponceau solution	Sigma Aldrich
Potassium Chloride	Sigma Aldrich
Prolong gold anti-fade reagent with DAPI	Invitrogen Life Technologies
Protein A agarose	Thermo Scientific
Protein G agarose	Millipore
Protein inhibitor cocktail	Sigma Aldrich
Phosphatase inhibitor cocktail I (Ser/Thr)	Sigma Aldrich
Phosphatase inhibitor cocktail II (Tyr)	Sigma Aldrich
RIPA buffer, 10X	Millipore
Sodium Acetate	Sigma Aldrich
Sodium Chloride	VWR International
Sodium Bicarbonate	Sigma Aldrich
Sodium Dodecyl Sulfate	Sigma Aldrich
Sodium Fluoride	Sigma Aldrich
Sodium Hydroxide	Sigma Aldrich
Sodium Pyruvate solution	Cellgro
N,N,N',N'-TetramethylEthylenediamine (TEMED)	Sigma Aldrich
Thiazolyl Blue Tetrazolium Bromide (MTT)	Sigma Aldrich
Tris base	Fisher Scientific
Triton X-100	Sigma Aldrich
Trypan Blue solution	Sigma Aldrich
0.25% Trypsin-EDTA	Cellgro
Tween-20	Sigma Aldrich
Western Blot Stripping Buffer	Thermo Scientific

5.1.2 Kits

Bio-Rad Protein Assay	Bio-Rad Laboratories
Biocoat Cell Migration System	BD Bioscience
Nuclear Extraction Kit	Active Motif
QIAprep Spin Miniprep Kit	Qiagen Inc.
QIAquick Gel Extraction Kit	Qiagen Inc.

Wizard® plus DNA purification System	Promega

5.1.3 Laboratory Equipments

7500 Fast Real-Time PCR System	Life Technologies
Allegra 6R Refrigerated Benchtop Centrifuge	Beckman Coulter
C25 Incubated Floor Shaker	New Brunswick Scientific
Class II Biosafety Cabinet	Labconco
EC3 BioImaging System	UVP
Film Processor	Kodak
French Presure Cell Press	Aminco
Mastercycler Gradient	Eppendorf
UV-1700 Spectrophotometer	Shimadzu
Victor3 Multilable Plate Reader	Perkin Elmer

5.1.4 Enzymes and Recombinant Proteins

Alkaline phosphatase, Shrimp	Promega
C-Abl protein tyrosine kinase	New England BioLabs
DNase	Promega
MBD3	BioClone
Pfu-DNA polymerase	Promega
Proteinase K	Sigma Aldrich
PDGF-AA	Pepro Tech
PDGF-BB	Pepro Tech
RNase A	Thermo Scientific
Restriction enzymes	Thermo Scientific
T4 Polynucleotide Kinase	Promega
T4-DNA ligase	Thermo Scientific
YOP protein tyrosine phosphatase	New England BioLabs

5.1.5 Antibodies

β-Actin antibody (mouse monoclonal)	Santa Cruz Biotechnology
E-cadherin (mouse, monoclonal)	BD Biosciences
GAPDH antibody (mouse monoclonal)	Thermo Scientific
HA antibody (mouse monoclonal)	Roche Applied Science
HA antibody (rabbit polyclonal)	Lab generated

6x-His antibody (rabbit polyclonal)	Abcam
Histone 2A (rabbit polyclonal)	Cell Signaling Technology

5.1.6 Bacteria strains and mammalian cell lines

BL21-CodonPlus (DE3)-RIL	Stratagene
JM109	Promega
Human Dermal Fibroblasts, adult (HDFA).	Thermo Fisher Scientific
LX-2 Human Hepatic Stellate Cell Line	Millipore
Primary Human Stellate Cells (HSC).	Zen-Bio, Inc.

5.2 Methods

5.2.1 Bacteria Culture

Different types of *E. coli* were cultured in LB (Lysogeny broth) medium with 1% kanamycin at 37˚C and 250 RPM. JM109 was used for plasmid DNA duplication, BL21 (DE3)-pLysS and Tuner were used for recombinant protein expression. For colony selection, agar plates were made with LB medium-kanamycin and 15 g/L agar. For strain storage, the transformed bacteria were mixed with sterile glycerol (30% (v/v)) and stored at -80˚C.

5.2.2 Transformation

To prepare the competent cells, single clone of bacteria strain was inoculated from the plate to a 25 mL LB culture medium and shook at 37 ˚C overnight. The culture medium was then centrifuged at 4 ˚C 5000 rpm for 20 min. The cell pellet was resuspended in sterile $CaCl_2$ and centrifuged again. The cell pellet was resuspended in sterile water and aliquot to save in -80 aliquot.

For transformation, the competent cells were thawed on ice. The plasmids were add into the cells and incubated on ice for 5 min. The mix was then transfer to 42 ˚C water bath to

incubate for 90 seconds, and then on ice for 2 min. 500 μL of LB medium was added into the mix and shaking incubate at 37 ˚C for 1 hour. After incubation, the mix was spread on the plates using spatula.

5.2.3 Protein Purification

Cells were inoculated from one colony (or 10 μL stored cells) and shaking cultured in 5 mL LB with 0.1 % kanamycin at 37 ℃ overnight. Cells were transferred into 1 L LB medium with 0.1 % kanamycin and shaking cultured for 3 to 5 hours at 37 ℃ to reach OD600 of 0.4. Isopropyl β-D-1-thiogalactopyranoside (IPTG) was added to reach 1 mM and incubated at 16 ℃ overnight. Cells were harvested by centrifugation at 4 ℃, 7000 rpm for 15 min. Cell pellets were resuspended in buffer A (50mM Tris, pH 7.5, 0.1M KCl, 25mM MgCl2, 20% glycerol, 2 mM DTT, and PMSF) and then lysed by french press. The lysates were centrifuged at 4 ℃, 14000 rpm for 30 min. The supernatants were collected and filtered for protein purification. For protein purification, PKM2 was fused with his-tag, therefore Ni^{2+} column was used to purify the protein in FPLC. After purification, protein in tubes were collected and dialysis with buffer A overnight at 4 ℃. The purified protein was tested using SDS-PAGE.

5.2.4 Antibody Generation and Purification

The hybridoma with rabbit monoclonal PKM2 antibody production was generated by Epitomics, Inc. Hybridoma was thawed in warm RPMI1640 medium with Epitomics' rabbit hybridoma supplement A, 55 μM β-mercaptoehanol cell culture grade, and 10 % FBS in a 10 cm petri-dish. The medium was changed every day until cells reached 80 % confluency. The cells were trypsinized and cultured in T175 flask, then gradually moved to a 1 L cell culture bottle. To stimulate the antibody production, culture medium was switch from RPMI1640 to serum-free medium (Irvine scientific IS MAB-CD with 1% antibiotic/antimycotic, and 1% Glutamax). The

cells were culture in serum-free medium for 7 to 10 days. To harvest the antibody, the cells suspension was centrifuged at 4 ℃, 3000 rpm for 15 min. The supernatant was collected for antibody purification.

The rabbit monoclonal PKM2 antibody was purified using Protein G Agrose beads at 4 ℃. The beads was packed into a column, and washed with ten column volumes of cold PBS. The supernatant containing antibody was loaded in the column, and then washed with ten volumes of cold PBS. The antibody was eluted with 50 mM glycine pH 2.7 into 1 mL fractions containing the neutralization buffer (1M Tris, pH 8.0, 1.5 M NaCl, 1 mM EDTA).. Bradford protein assay was used to measure the antibody concentration in each fraction. The high concentration fractions were mixed, filtered, and aliquoted.

5.2.5 Cell Proliferation Assay

BrdU assay was used to measure cell proliferation. Cells were seeded into 96 well plate at about 10^5 cells per well. Blank (no cells) and background (no BrdU label) controls were established. BrdU label was diluted 1:2000, and 20 μL of it was added into each well. The cells were incubated with BrdU label for 24 hours in the cell culture incubator. The wells were emptied and refilled with 200 μL Fixative/Denaturing Solution, and then incubated at room temperature for 30 min. The cells were incubated with diluted Anti-BrdU Antibody at room temperature for 1 hour. After washing three times with Wash Buffer, the Peroxidase Goat Anti-Mouse IgG HRP Conjugate was diluted and added into each well to incubate at room temperature for 30 min. The cells were washed again three times with Wash Buffer, and incubated with Substrate Solution in the dark for 15 min followed with Stop Solution. The readings were recorded at wavelength of 450 nm.

5.2.6 Boyden Chamber Assay

The cells were cultured in good condition and prepared for the migration assay. 24-well plate was used and fitted chambers were inserted into each well. 2 mL of culture medium with 10% FBS was added into each bottom well. The cells were resuspended into serum-free culture medium. Each well was added with 2 x 10^4 cells. rPKM2 or other reagents were added into the upper chamber as well. The plate was incubated in the incubator for 16 hours. After incubation, the chambers were washed three times with PBS and stained with crystal violet for 3 min. The wells were then washed and observed under microscope.

5.2.7 SDS-PAGE

The SDAS-PAGE gel was prepared before electrophoresis. The separating gel was first set up at bottom with 6~12% acrylamide, 0.375M Tris-HCl pH 8.8, 0.1% SDS, 0.04% APS, and 0.08% TEMED). 1 mL of water was added on the separating gel to help it to polymerize firmly. While waiting for polymerization of the separating gel, the stacking gel was prepared with 5% acrylamide, 0.125M Tris-HCl pH 6.8, 0.1% SDS, 0.05% APS, and 0.15% TEMED. The stacking gel was poured onto the separating gel and the comb was inserted to generate wells. The lysates were diluted with 5X loading buffer (175 mM Tris-HCl pH 7.0, 5 mM EDTA, 10% SDS, 20% sucrose, 0.01% bromophenol blue, and 28.8 mM β-mercaptoehanol) and boiled for 5 min. The samples and protein ladder were loaded in the wells. The gel was ran at constant voltage 60 V first at the stacking stage, and then increased to 80 V at the separating stage.

5.2.8 Western Blot

The protein samples were separated by SDS-PAGE. Proteins were transferred from gel to a nitrocellulose membrane at constant current of 80 mA for 2 hours. The membrane was blocked in 5% BSA solution (5% BSA in TBST (20mM Tris-HCl pH 7.5, 150 mM NaCl, 0.1% Tween-

20)) at room temperature for 30 min. The membrane was washed with TBST three times, each time 5 min. The primary antibody was diluted in the 5% BSA solution. The membrane was incubated in it on a flat shaker at 4 ˚C overnight, and then washed three times again with TBST. The membrane was incubated with appropriate secondary antibody against the primary with a dilution of 1:2000 at room temperature for 30 min and followed with three times wash with TBST. The signal was detected with chemiluminescence reagents and developed in dark room.

5.2.9 ELISA (enzyme-linked immuno assay)

ELISA was performed using ELISA 96-well plate. PKM2 antibody was first coated on the plate at 4 ˚C overnight. Culture medium or serum were added into the plate and incubated at room temperature for 2 hours. The plate was washed twice with PBST and then incubated with detect antibody at 4 ˚C overnight. The plate was washed three times with PBST and followed with secondary antibody treating at room temperature for 1 hour. TMB substrate solution was added into the plate and incubated for 30 min. The reaction was terminated with adding stop solution. The reading was recorded with spectrophotometer at wavelength 450 nm.

5.2.10 Preparation of Plasmid DNA

Purification of DNA plasmid from bacteria was using QIAprep Spin Miniprep Kit. 2 mL of bacteria medium was inoculated with single colony from an agar plate, and then shaking incubated at 37 ˚C overnight. The cell pellet was generated by centrifuging at 5000 rpm for 5 min and the supernatant was removed. The cell pellet was suspended in 250 μL of suspension buffer supplemented with RNase A, and followed by adding 250 μL alkaline lysis buffer to lyse the cells. After the lysate was adjusted to high-salt binding condition, the protein precipitation was showed up and removed by centrifugation at 13000 rpm for 10 min. The supernatant

containing DNA was applied to the QIAprep column, and washed for several times. The plasmid DNA was eluted by adding 50 μL of elution buffer and centrifugation.

5.2.11 Quantification of DNA Concentration

Concentration of DNA was determined by spectrophotometer at the wavelength of 260 nm. One unit of OD260 equated to 50 μg/mL of double-stranded DNA. The ratio of OD260 to OD280 provided the purity of the DNA sample. If the ratio of OD260 to OD280 was higher than 1.8, the sample was considered as pure DNA.

5.2.12 Preparation of Whole Cell Lysates

After treatments, cells were washed three times with ice-cold PBS. RIPA buffer supplemented with protease inhibitors cocktail was used to lyse the cells. The cells attached on the plate were added with RIPA buffer and scraped off with a rubber scraper or pipette tip. The lysates were transferred into a microtube and vortexed for 10 seconds. The lysates were then rotated at 4 ˚C for 30 min, and centrifuged at 13000 rpm at 4 ˚C for 15 min. The supernatants were stored at -20 ˚C freezer.

5.2.13 Quantification of Protein Concentration

The protein concentration in cell lysates and tissue homogeneous were measured by Bio-Rad protein assay. A standard curve was generated using gradient concentrations of BSA standard. To measure the protein concentration, 10 μL of lysates was mixed with 790 μL water and 200 μL of Bio-Rad dye in a cuvette. The absorption readings were recorded with a spectrophotometer at wavelength 595 nm. Each absorption reading was plotted into the BSA standard curve to calculate the protein concentration.

5.2.14 Immunofluorescence Staining

The frozen section slides were fixed in 95% ethanol and the extra gel was cleared. The samples were circled with PAP pen and blocked with 5% BSA solution at room temperature in humidity box for 30 min. The slides were incubated with primary antibody with 1:500 dilutions in 5% BSA solution at 4 ˚C overnight. The slides were washed with PBST three times each time 5 min and then incubated with secondary antibody conjugated with fluorescence dye at room temperature for 30 min. If another fluorescence dye was needed, the slides were incubated with another primary antibody at room temperature for 2 hours and secondary antibody conjugated with fluorescence dye for 30 min. The slides were washed and mounted with Prolong Gold Antifade Mountant with DAPI. The coverslip was sealed by nail polish. The results of immunofluorescence staining were acquired by using Zeiss LSM 700 Confocal.

5.2.15 Quantification of IF Staining

IF staining was quantified using ImageJ software. The fields were chosen randomly from each group. Micro-vesicular density (MVD) and total positive area were quantified. MVD was measured by counting the positive staining point in each field. Total positive area was measured by selecting the positive staining pattern and calculating the area of each pattern.

5.2.16 Immunohistochemistry (IHC). Staining

IHC staining was performed following the protocol in Dr. Shi-Yong Sun's lab in Emory. Generally, the slides were baked at 60 ˚C for 2 hours, and then hydrated by continuously incubating in the following solution in order (three times xylene, twice 100% ethanol, 90% ethanol, 70% ethanol, 50% ethanol, 30% ethanol, and distilled water). The antigen retrieval was done by incubating in 10 mM Sodium Citrate buffer pH 6.0 and microwaved for 5 min in high and 10 min in low. After the slides were cooled down to room temperature for 39 min, they were

washed with PBS for 5 min. The slides were incubated with Dual Endogenous Enzyme Block at room temperature for 30 min and wash again. The slides were incubated with primary antibody diluted in antibody diluents 1:500 at 4 ˚C overnight. The slides were washed with PBST twice and PBS once. The slides were treated with Labeled polymer-HRP at room temperature for 30 min, followed by the same washes. Substrate chromogen solution was made by mixing 1 mL of DAB+ substrate buffer plus 1 drop of DAB+ chromogen. The slides were added by DAB+ solution and monitored under microscope. The slides were counter stained with hematoxylin QS for 1 min. The slides were dehydrated by reversely incubating from distilled water to xylene. The slides were mounted and sealed with nail polish.

5.2.17 Quantification of IHC Staining

Quantification of IHC staining was done by using FRIDA (FRamework for Image Dataset Analysis) software. All images ready to be analyzed were saved in the same folder. A mask was selected by picking positive signals in different images. After the mask was well defined, the software would calculate the area of expression pattern in other images. The results from different groups were compared.ng the area.

CHAPTER 6 CONCLUSIONS AND DISCUSSIONS

6.1 Extracellular PKM2 released from neutrophils facilitates wound healing by promoting angiogenesis

Wound healing is a slow and complicated process that every step needs to organize well for a proper recover. Since extracellular PKM2 promotes angiogenesis during tumor progression, and angiogenesis is critical for the proliferation stage of wound healing, we study wound repair with a mouse cutaneous wound model by topical application of rPKM2. Our results showed that topical application of rPKM2 facilitates wound closure. Immune staining analysis using CD31 antibody found that topical application of PKM2 stimulates the growth of microvessel during wound healing.

In mouse cutaneous wound model, the wound in rPKM2 treated group started to close rapidly at day 3 compared with the wounds in control groups. However, the wound sizes in all three groups were similar at day 8. What could be the reason of slower closure in the rPKM2 treated group after day 6? Since the wound pictures only showed the outside of mouse skin recovery which is called re-epithelization, the outside appearance does not reflect the whole process of wound repair. To examine what happen inside the wound site, we examined the wound underneath of mouse skin. The rPKM2 treated group showed more established capillary vessel structure and granulation tissues, compared with those in buffer and rPKM1 treated groups. We thought that the topical application of rPKM2 facilitated the wound healing process by promoting the angiogenesis in proliferation stage, which led to faster repair at day 3. Given that the re-epithelization process is paralleled with angiogenesis and granulation tissue formation, other factors slowed down the closure of wound in rPKM2 treated group to insure a well-organized wound repair. It is also possible that the capillary structure in rPKM2 treated

group might be excessive compared with those in normal wound repair. As it is known that the process of wound healing needs to be regulated in an ordered manner. Angiogenesis and formation of granulation tissue should be stopped at a certain time point. It was possible that angiogenesis was extended due to addition of rPKM2 at day 6 in our experiment. To find a better way of applying rPKM2 in the cutaneous wound healing, we should design a strategy to apply rPKM2 at different time points to find the best fit for facilitating wound healing. This strategy may lead to proper growth of granulation tissue.

In addition to the effect on angiogenesis, topical application of rPKM2 was also found to promote growth of granulation tissue underneath the skin wound. Is the growth of granulation tissue directly stimulated by extracellular PKM2 or by the PKM2 induced angiogenesis? At the beginning, angiogenesis is very important for proliferation stage to support granulation tissue growth. Thus, we believed that topical application of rPKM2 promoted angiogenesis, and the newly grown capillary brought more nutrients to support the growth of granulation tissue. However, we measured the thickness of granulation tissue and stained the fibroblast at the wound site. The results suggested that rPKM2 might play a role on dermal fibroblasts during cutaneous wound. I will discuss it in the second section of this chapter.

We discovered that endogenous PKM2 located in extracellular space at the wound site by IHC staining of PKM2. Presence of PKM2 in the extracellular space of wound tissues suggested a possible intrinsic mechanism of secretion of PKM2 during the wound repair process. Due to a close correlation between neutrophils and PKM2 in a numbers of inflammatory diseases, we performed a time course of staining of neutrophils and PKM2 during cutaneous wound healing. Both neutrophils and PKM2 exhibited a similar timing of appearance peaked around day 3. It is known that neutrophils express PKM2. Thus, we isolated neutrophils from mouse bone marrow

and activated by fMLP. PKM2 was detected in the culture medium of activated neutrophils. The release of PKM2 was inhibited by several degranulation inhibitors. To prove that extracellular PKM2 is released from neutrophils in vivo during wound healing, we used beige mouse that carries deficiency of neutrophil migration. Both neutrophils and PKM2 were not presented at the wound site of beige mice. Neutrophils and PKM2 were found at wound site in the normal mice. Therefore, we concluded that extracellular PKM2 was released from activated neutrophils during wound healing.

In the future study, we would like to answer two questions. The first question is how PKM2 is released from activated neutrophils. In cancer cells, reports suggested that PKM2 is secreted from exosome. One proteomics study stated that PKM2 locates at the primary and secondary granules. We found release of PKM2 correlated with the degranulation of neutrophil. Degranulation activator fMLP and damnacanthal stimulated the release of PKM2. We thought that PKM2 might interact with some granule proteins in the primary and secondary granules. Screening of different degranulation inhibitors showed partial effects of all tested inhibitor individually. To test which type of granule releases PKM2, we can co-stain PKM2 with the cargo protein in granules to find the transportation pathway. Electron microscopy is another method to study the transportation of PKM2. The second question is do other types of immune cells release PKM2? PKM2 is reported to be expressed in platelets, neutrophils, macrophages, and lymphocytes. (Hapa et al., 2011) As an example, it is possible that PKM2 is released from macrophages to promote angiogenesis. We stained wound tissue sections with antibody against one of macrophage markers F4/80 at day 2 of wound. No staining of macrophages was observed compared with high level staining of Ly6G and PKM2. To see the correlation at late time points, the samples from later stage of wound should to be stained with F4/80 and PKM2. Isolating

monocytes and activating them is another way to test whether PKM2 is release from macrophages in vitro.

If extracellular PKM2 released from neutrophils facilitates wound healing, then neutralization by PKM2 antibody should affect the wound repair process. We designed another experiment with mouse cutaneous wound model by injecting PKM2 antibody and followed by the similar process in the previous experiment. The healing of wound was slowed down in the PKM2 antibody treated group compared with buffer and IgG controls. The micro-vessels were also limited in the PKM2 antibody treated group.

In brief, our study revealed an unexpected role of extracellular PKM2 in facilitating wound healing by promoting angiogenesis. Release of PKM2 through degranulation of activated neutrophils suggested a new and important link between immune response and proliferation phase. This link provided an explanation of how neutrophil infiltration triggers early angiogenesis during wound healing which indicated a physiological role of neutrophils in addition to the anti-microbial function.

6.2 PKM2 promotes myofibroblast differentiation via integrin αvβ3

During the mouse wound healing experiment, we discovered that the granulation tissue of PKM2 treated group was much thicker than those of control groups. We thought only by promoting angiogenesis was not enough to stimulate the growth of granulation tissue. Extracellular PKM2 released from activated neutrophils may play a role in fibroblast. Dermal fibroblasts expressed high levels of integrin αvβ3. Myofibroblast differentiation is a key feature during granulation tissue formation. Clearly, α-SMA, the myofibroblast marker, was upregulated in the rPKM2 treated group during the wound healing.

We questioned how extracellular PKM2 triggered the upregulation of α-SMA in fibroblasts at the wound site. First, we tested the effect of extracellular PKM2 on HDFa cell proliferation and migration. PKM2 did not exhibited any effect on HDFa proliferation, but rPKM2 treated HDFa had significant increase in migration. Thus, we believed that extracellular PKM2 at wound site activated migration of dermal fibroblasts and recruited more of fibroblasts to the wound site. We subsequently tested the effect of extracellular PKM2 on HDFa differentiation, and compared the effects of TGFβ, the well-known myofibroblast differentiation activator. Surprisingly, rPKM2 independently induced the expression of α-SMA in fibroblasts. PKM2 is as effective as TGFβ in inducing α-SMA expression in fibroblasts. Combination of rPKM2 and TGFβ had an enhanced effect on α-SMA expression. Both rPKM2 and TGFβ treated HDFa demonstrated a typical feature of differentiated myofibroblast with stress fiber bundles and collagen secretion. To further test whether the activation of fibroblast by rPKM2 is independent of TGFβ, TGFβ antibody was added to neutralize residue TGFβ and TGFβ receptor inhibitor was also employed to inhibit the downstream signal pathway. The effect of TGFβ in the presence of antibody and inhibitor was reduced, whereas the effect of rPKM2 was not affected. Therefore, we concluded that extracellular PKM2 independently stimulates HDFa cell migration and differentiation.

Several questions were raised regarding the promotion of HDFa differentiation by extracellular PKM2. Is PKM2 itself enough to activate full differentiation of myofibroblast? Mechanical force and other factors can partially activate myofibroblast differentiation. TGFβ is required for fully activation of myofibroblast differentiation. α-SMA expression, collagen secretion, fibers bundle, and cell contractile ability are used to analyze the degree of differentiation. In our study, rPKM2 independently induced expression of α-SMA and secretion

of collagen. However, rPKM2 induced less α-SMA expression and collagen secretion compared with that of TGFβ treatment. In a confocal microscopic study of co-stain α-SMA with actin, both rPKM2 and TGFβ treatments had increased spreading morphological change, increased α-SMA expression, and α-SMA/actin bundles (yellow). To study the contractile ability of HDFa, we can use collagen gel contraction assay that functionally tests the degree of myofibroblast differentiation.

Our laboratory previously found that extracellular PKM2 interacted with integrin αvβ3 and activated integrin signaling in endothelial cells. Since HDFa also have integrin αvβ3 expression, it is highly possible that integrin αvβ3 is the target of extracellular on HDFa. We performed chemical crosslinking followed by mass spectrometry analysis. We found that integrin αvβ3 interacted with PKM2. Immunoblot of PKM2 pull-down further confirmed that integrin αvβ3 was the target of extracellular PKM2. Attachment assay with plate coated with rPKM2 showed the interaction between PKM2 and integrin αvβ3 was blocked by LM609, an integrin αvβ3 antibody. To test the downstream signaling pathway of PKM2-αvβ3 in myofibroblast differentiation, we used several different inhibitors that inhibit the downstream protein kinases of FAK. PI3K was found to be the major target. Furthermore, rPKM2 induced the activity of PI3K in HDFa. Additional tests following PI3K demonstrated that PAK2 was the downstream pathway in stimulating α-SMA expression.

Is integrin αvβ3 the only target of extracellular PKM2 in HDFa? One group reported that PKM2 interacts with tumor endothelial factor 8 (TEM-8) on tumor endothelial cells. Our laboratory observed that PKM2 interacted with integrin αvβ3 on endothelial cells. PKM2 interacted with TEM-8 weakly. In the mass spectrometry analysis of PKM2 interacting partners, we identified several other proteins, including G3P, Hexokinase-1, ATP synthase, multiple

coagulation factor deficiency protein 2, myosin regulatory light chain 12B, filamin-A, α-actinin, tubulin, and HNRNP, could be PKM2 interacting proteins. These proteins can be separated into several groups, such as glycolytic enzymes, skeleton proteins, and cell transportation proteins. Apparently, none of these identified proteins located on the cell membrane. In our test, integrin αvβ3 was the only cell surface receptor identified in mass spectrometry. If other membrane targets exist, more detailed and specific mass spectrometry method should be applied in the future.

TGFβ activates myofibroblast differentiation through TGFβ receptor and Smad family pathway. Activation of fibroblast differentiation by PKM2-integrin αvβ3 interaction was independent of TGFβ pathway. Do these two signal pathways crosstalk? TGFβ up-regulated the expression of integrin αvβ3 in fibroblasts, endothelial cells, and cancer cells. TGFβ cooperated with integrin to form a feedforward loop to induce integrin expression. In addition, TGFβ activated integrin ligands, including vitronectin, fibronectin, laminin, and collagen. TGFβ was also involved in the activation of integrin "inside-out" signaling. On the other hand, integrin can regulate TGFβ activation. Integrin αvβ3 associates with TGFβ receptor II, and activates the expression of TGFβ receptor I&II in lung fibroblasts. The latent form of TGFβ needs to be cleaved to generate active TGFβ. Integrin αvβ3 acts as a docking site for MMP2 and MMP9, which are the proteases responsible for latent TGFβ activation. In our study, TGFβ and PKM2 shared a similar PI3K pathway of activating myofibroblast differentiation.

If both TGFβ and PKM2 exist in the wound site at early time, it is interesting to ask which one plays the major role in activating myofibroblast differentiation. In wound healing, the major sources of TGFβ are from platelets and macrophage, whereas PKM2 is released from neutrophils. Although the level of extracellular PKM2 at neutrophil infiltration peak can be very

high, the activation of myofibroblast differentiation by TGFβ is still stronger due to its high efficiency. If TGFβ is the major stimulator, then what is the role of extracellular PKM2? The possible work flow could be that TGFβ and mechanical tension partially induces the myofibroblast differentiation at early time of inflammation. High level of extracellular of PKM2 released from neutrophils interacts with integrin αvβ3 on the fibroblast surface which is induced by TGFβ stimulation. This interaction further facilitates the differentiation process. Thus, TGFβ can fully activate myofibroblast differentiation under the help of PKM2 activated integrin αvβ3 pathway.

In summary, our data demonstrated that extracellular PKM2 independently promoted myofibroblast differentiation by activating integrins αvβ3 on cell surface of dermal fibroblasts. In this regard, our discovery may uncover a new target that may help to develop therapeutic strategies in facilitating wound repair. TGFβ is considered as the major stimulator which activates myofibroblast differentiation that provides early collagen deposition and granulation tissue formation. However, several studies have shown that TGFβ activation was not the only one for myofibroblast differentiation. We suggested that release of PKM2 from activated neutrophils at wound site replaced and strengthen the effect of TGFβ for myofibroblast differentiation during wound healing.

6.3 Extracellular PKM2 prevents apoptosis of activated hepatic stellate cells during liver fibrosis

Liver fibrosis is induced by chronic liver damage and inflammation. Neutrophils infiltrate to the damaged area and release large amount of PKM2. To study the function of extracellular PKM2 in liver fibrosis, we established a TAA/alcohol mouse model with rPKM2 after two and a half weeks. The body weight was reduced in the TAA treated fibrotic mice, further decreased

with addition of rPKM2. After TAA+rPKM2 treatment, both weight and size of liver were increased compared with controls. Typical fibrotic feature was seen on the surface of those livers. Serum marker screening showed that fibrosis induction by TAA/alcohol treatment increased albumin, ALT and AST level in the blood. Addition of rPKM2 further increased serum ALT and AST level. Sirius Red staining was used to examine the liver collagen contents. TAA+rPKM2 treatment showed intensive collagen levels and thick collagen cross networks.

HSCs apoptosis is related to liver fibrosis progression. We found that TAA+rPKM2 treatment had increased α-SMA and reduced apoptosis that indicated function of extracellular PKM2 in protecting HSCs from apoptosis. In vitro study showed that rPKM2 relieved the apoptotic stress of HSCs and LX-2 cells from FasL and TRAIL induced apoptosis. rPKM2 interacted with integrin αvβ3 on the cell surface of activated LX-2 cells. Integrin αvβ3 activated FAK, and PI3K to stimulate survival signal of HSC. Neutralization of extracellular PKM2 using a specific antibody against PKM2 in TAA/alcohol liver fibrosis mouse model reduced liver fibrosis progression. The collagen staining of IgGPK group showed less signal and very thin collagen cross networks.

Our study revealed an unexpected role of extracellular PKM2 in facilitating liver fibrosis progression by protecting activated HSCs from apoptosis. Reverse of liver fibrosis is the most important task in the treatment of cirrhosis. HSCs apoptosis is a key to prevent progression of liver fibrosis. Our results showed that antibody against PKM2 that disrupt the PKM2-integrin αvβ3 interaction are very effective in reversing liver fibrosis in TAA/alcohol mouse model, indicating a potential anti-fibrotic strategy and target.

6.4 Physiological and pathological functions of extracellular PKM2

PKM2 is the enzyme acting at last step of glycolysis converting PEP to pyruvate. The default function of PKM2 is same as other pyruvate kinases in glycolysis. However, the pyruvate kinase activity of PKM2 is lower compared with that of other isoenzymes. PKM2 is expressed in highly proliferating cells, suggesting a unique function related to proliferation. Slow glycolysis rate caused by low pyruvate kinase activity of PKM2 results in the accumulation of intermediated materials which in favor of proliferation. In the recent study, function of PKM2 involving in cancer cell proliferation was highlighted in cell nucleus. PKM2 translocates into nucleus and acts as protein kinase to phosphorylate histone H3 and STAT3 to promote proliferation. PKM2 also binds with HIF1 to regulate β-catenin.

PKM2 has two conformations existing in the cells, dimer and tetramer. Tetrameric PKM2 has higher affinity to substrate PEP and better pyruvate kinase activity, whereas dimeric PKM2 shows low pyruvate kinase activity due to weak affinity to PEP. In metabolic pathway, pyruvate kinase catalyzes the last step of glycolysis by converting PEP to pyruvate and generating ATP. This is the key connection between glycolysis and oxidative phosphorylation. In cancer cells, PKM2 dimer with reduced pyruvate kinase activity holds glycolysis at the last step, and facilitates the synthesis of intermediate metabolites for the need of proliferation. This is why cancer cells develop the mechanism of alternative splicing to produce PKM2 over PKM1 in favor of its metabolism (Mazurek, 2011).

In addition to the metabolic shifting role of PKM2 in the Warburg effect, PKM2 possesses an important relationship with HIF-1 and c-Myc which are two critical proteins in metabolism pathway. PKM2 interacts with HIF-1α subunit and promotes activation of HIF-1 targeted genes. PHD3 enhances the interaction between PKM2 and HIF-1α. This indicates a

positive feedback loop of PKM2 promoting HIF-1 transactivation and regulating metabolism in cancer cells (Luo & Semenza, 2011). c-Myc was found to be the key regulator for the shift from PKM1 to PKM2 in cancer cells. c-Myc upregulates the transcription of hnRNPA1 and hnRNPA2 to bind more to exon 9 (PKM1) in order to include exon 10 (PKM2) in the splicing result, thus high PKM2/PKM1 ratio (David et al., 2010).

The study of PKM2 was focused in cytosol as a pyruvate kinase to regulate metabolism or in cell nucleus as a protein kinase to promote proliferation. Extracellular PKM2 was considered as diagnostic marker for diseases without any specific physiological or pathological functions. Serum PKM2 level is used as diagnostic marker in several cancer cases, including colorectal cancer, kidney cancer, gastric cancer, lung cancer, and cervical tumors. Our laboratory discovered that extracellular PKM2 secreted by cancer cells promoted angiogenesis through activation of integrin αvβ3 on endothelial cells. We also found PKM2 located extracellularly at cutaneous wound site and in liver fibrosis. Neutrophil is another source of extracellular PKM2 in addition to cancer cells. PKM2 was detected from blood circulation and stool samples in several immune diseases, but the secretory pathway was not clear. PKM2 secretion is related with exosome in cancer cells. In immune diseases, extracellular PKM2 was thought to be released by dead immune cells. We discovered that PKM2 was released from activated neutrophils via degranulation. Whether PKM2 is located in granules is still need to be examined.

In wound repair, macrophage is the dominant origin of secreting growth factors and cytokines to activate angiogenesis and granulation tissue formation. Macrophages can influence each phase of angiogenesis, including ECM rearrangement, endothelial cell proliferation and migration, and capillary differentiation. TGFβ secreted from macrophage is considered the main activator for myofibroblast differentiation. The classical concept of the connection between

inflammation and proliferation stage is that neutrophils come first for cleaning, then macrophages arrive later to finish cleaning and promote angiogenesis and granulation tissue formation. We found that extracellular PKM2 released from neutrophils facilitated cutaneous wound healing by promoting angiogenesis and fibrogenesis. This provides another aspect in addition to the conception of macrophage activating proliferation stage. Neutrophils are considered the early initiator of angiogenesis and fibrogenesis during wound repair. However, extracellular PKM2 activated endothelial cell and fibroblast through integrin αvβ3, which is only expressed after activation by TGFβ. It is not feasible for extracellular PKM2 from neutrophils to activate angiogenesis and fibrogenesis before TGFβ from macrophages. Another possibility is that small amounts of TGFβ are released from platelets early in wound repair and partially activate endothelial cells and dermal fibroblasts. Large amounts of PKM2 released during neutrophil infiltration enhance the activation and then together with TGFβ from macrophages to further augment angiogenesis and fibrogenesis.

Given the fact that PKM2 is released from neutrophils, a key question is whether the released PKM2 is dimer as released from cancer cells. Our lab previously demonstrated that PKM2 translocates into cell nucleus and acts as a protein kinase to regulate gene transcription. PKM2 dimer functions as a protein kinase, while the tetramer is a pyruvate kinase (Gao et al., 2012). PKM2 is released from cancer cells and promotes angiogenesis. The released PKM2 is in dimeric conformation and shows low pyruvate kinase activity compared with PKM1. The dimer/tetramer ratio of PKM2 is also correlated with protein concentration (L. Li et al., 2014). In cancer cells, the pathway of PKM2 release is still not well understood. Our preliminary data indicated that the release of PKM2 is involved in the secretion of exosome and microvesicle. In part two of this dissertation, we discovered PKM2 is released from neutrophil through

degranulation, which is a similar secretory pathway as in exosome and microvesicle. Several other reports revealed that PKM2 exists in the dimeric conformation upon different modifications and mutations (Mazurek, 2007; Stetak et al., 2007). Therefore, we suspect the released PKM2 from neutrophils is also in dimeric conformation. The cytosolic PKM2 should still be tetramer. After modification such as phosphorylation or binding with other proteins, PKM2 may dissociate from tetramer to dimer and further interact with the vesicle or granule components during release.

In this dissertation, we revealed that PKM2 activated FAK-PI3K-PAK2 pathway through integrin αvβ3 in dermal fibroblasts and leads to myofibroblast differentiation. This signal pathway is independent of TGFβ-Smad pathway. Several factors have been shown to activate myofibroblast differentiation without besides TGFβ, such as IL-6, NGF, Fizz1, angiotensin-II, endothelin-1, and thrombin. However, the effect of TGFβ is not ruled out in those studies. We used TGFβ antibody to neutralize TGFβ residue and TGFβ receptor antibody to inhibit TGFβ signal pathway. rPKM2 still can induce expression of α-SMA in the previous two treatments. This is a novel signal pathway of myofibroblast differentiation in addition to the classic TGFβ one. Extracellular PKM2 can augment the TGFβ effect or even act alone when TGFβ is absence.

On the pathological side, we claimed that extracellular PKM2 released from activated neutrophils protected activated HSCs from apoptosis that results in progression of liver fibrosis. In HSCs, extracellular PKM2 activated PI3K signal pathway to stimulate the survival signal. Currently, no effective treatment of reversing liver fibrosis/cirrhosis has been found. Most studies are focused on the apoptosis of activated HSCs. Our results showed that specific PKM2 antibody that disrupts the PKM2-αvβ3 interaction is very effective in relieve liver fibrosis in TAA/alcohol induced mouse model, indicating a potential anti-fibrosis strategy and target.

Compared to fibrosis in liver, the fibrosis progression is very similar in other tissue such as lung and kidney. In the future study, we should test the function of extracellular PKM2 in other fibrosis models.

6.5 Conclusions and Future Perspectives

In summary, extracellular PKM2 shares the same membrane target integrin αvβ3 on different cell types and leads to different downstream pathways favoring to the function of cells. As the similar proliferating function of nuclear PKM2 in cancer cells, extracellular PKM2 plays a similar role of regeneration (angiogenesis and fibrogenesis) in wound healing. Extracellular PKM2 acts as a cytokine or growth factor to activate endothelial cells and fibroblasts in favors of regeneration. Release of PKM2 from activated neutrophils reveals the connection between neutrophil infiltration and tissue regeneration. Nevertheless, in the pathological condition of tissue regeneration, extracellular PKM2 acts as a double-edged sword. For example, when you have an injury in liver, regeneration of liver undergoes the similar procedure as in the cutaneous wound repair. Extracellular PKM2 functions as a supporter to heal injury. If injury persists, chronic damage of the tissue leads to continuously influx of neutrophils to the injury site. Accumulation of extracellular PKM2 becomes a destroyer by protecting HSCs from apoptosis. Therefore, targeting extracellular PKM2 during liver fibrosis can be a valid method of pushing HSCs to apoptosis, and finally reversing of liver fibrosis.

Currently, the study of PKM2 is divided into three parts. First, the canonical function of PKM2 is to regulate metabolism in highly proliferating cells. Dimeric PKM2 catalyzes the last step of glycolysis with rate limitation. Binding with FBP converts PKM2 to tetramer, and enhances the pyruvate kinase activity of PKM2. The balance between PKM2 dimer and tetramer is dynamically regulated (Dombrauckas et al., 2005). In cancer cells, to favor proliferation, the

balance is more toward to dimeric PKM2 as a result of different modifications, including phosphorylation of tyrosine 105 by tyrosine kinase, acetylation of lysine 305 by glucose stimulation, and oxidation of cysteine 358 by ROS insult (Hitosugi et al., 2009; Lv et al., 2011). The transition from tetramer to dimer PKM2 leads to an increased accumulation of metabolic intermediates which support the proliferation of cancer cells. In order to inhibit cancer cell proliferation and tumor growth, researchers aim on the discovery of PKM2 activator to drive the conversion back to tetrameric PKM2. FBP and serine are the known allosteric activator of PKM2. Succinyl-5-aminoimidazole-4-carboxamide-1-ribose-5'-phosphate (SAICAR) also regulates PKM2 allosterically (Keller et al., 2012). Two small molecules were identified in a screen for PKM2 activator, thieno[3,2-b]pyridazinone (TEEP-46) and N,N'-diarylsulfonamide (DASA-58). These to molecules functions similar to FBP to significantly increase the pyruvate kinase activity of PKM2. They stabilize PKM2 in a tetramer conformation even with key residue mutation such as K305 (Anastasiou et al., 2012).

Second, in addition to the original role of regulating glycolysis in cytosol, PKM2 translocates into the nucleus and functions as a protein kinase to promote cancer cell proliferation. PKM2 can phosphorylate several protein substrates by using PEP or ATP as the phosphate donor. The possible protein substrates include histone H3 on T11, STAT3 on Y705, MLC2 on Y118, Bub3 on Y207, and ERK1 on T202. However, the molecular mechanism of this protein kinase activity is still not clear. The function of nuclear PKM2 is involved with gene expression and cell cycle progression. Nuclear PKM2 interacts with β-catenin and enhances the transactivation activity of β-catenin to assist the phosphorylation of histone H3 by PKM2 (W. Yang et al., 2011). PKM2 interacts with Oct4 and reduces the transcription activity of Oct4 which leads to the differentiation of glioma spheroids (Morfouace et al., 2014). PKM2 is also

involved in cell cycle and cytokinesis. PKM2 regulates G1-S phase transition by phosphorylating Bub3. Aurora B can phosphorylate PKM2 on T45 to stimulate the phosphorylation of MLC2 by PKM2. This phosphorylation together with Rho-associated protein kinase 2 (ROCK2) mediated phosphorylation on S15 are critical in the process of cytokinesis (Jiang et al., 2014).

Third, PKM2 is found in extracellular space. Cancer patients have high level of PKM2 in the blood serum. Serum PKM2 is used as an un-invasive diagnostic marker for cancer diagnosis. Our laboratory discovered that the extracellular PKM2 is released from cancer cells. Extracellular PKM2 interacts with integrin αvβ3 on the cell surface of endothelial cells and promotes adhesion and migration. In this dissertation, we found PKM2 is also released from neutrophils during inflammation. Extracellular PKM2 interacts with integrin αvβ3 on the cell surface of both endothelial cells and fibroblasts. PKM2 activates integrin αvβ3 signaling pathway to stimulate myofibroblast differentiation. Extracellular PKM2 also activates a survival signal through integrin αvβ3 to protect activated HSCs from apoptosis and promotes liver fibrosis. Overall, the original function of PKM2 is still in cytosol. After different modifications or interacting with other factors, PKM2 tetramer converts to dimer, and then translocates into nucleus or releases to the extracellular space.

The function of extracellular PKM2 is not well elucidated. Previously, we only knew that it is correlated with tumor growth. In this dissertation, we observed that neutrophils or other immune cells could be another source of extracellular PKM2. If we consider extracellular PKM2 as a cytokine using integrin αvβ3 as the cell surface receptor, then it is a connection between neutrophil infiltration and angiogenesis/fibrogenesis. It helps us to better understand the function of neutrophils during inflammation. We revealed that extracellular PKM2 promotes myofibroblast differentiation independently of TGFβ. It indicates that neutrophil infiltration

places a positive role in myofibroblast differentiation. Alternative PKM2- integrin αvβ3 pathway can activate fibroblast without the involvement of the classical TGFβ-Smad pathway. Extracellular PKM2 plays another important role during liver fibrosis. Everyone tries to find the way to reverse liver fibrosis and focuses on activated HSCs as the target. We think extracellular PKM2 could be the key modulator in liver fibrosis. Insult induces inflammation and activates different immune cells. The activated immune cells release PKM2 and other cytokines to promote differentiation of HSCs. PKM2, together with other growth factors, stimulates the survival signal of activated HSCs and keeps them at the damaged liver tissue to induce a chronic fibrotic status. We generated a specific antibody against PKM2 and tested it for liver fibrosis. The fibrotic damage was well reduced and liver condition was partially reversed to the healthy condition. The future study of extracellular PKM2 should be focused on its role in fibrogenesis. Animal models with different types of tissue fibrosis should be studied to test the effect PKM2 antibody.

REFERENCES

Akhtar, K., Gupta, V., Koul, A., Alam, N., Bhat, R., & Bamezai, R. N. (2009). Differential behavior of missense mutations in the intersubunit contact domain of the human pyruvate kinase M2 isozyme. *J Biol Chem, 284*(18), 11971-11981. doi:10.1074/jbc.M808761200

Anan, A., Baskin-Bey, E. S., Bronk, S. F., Werneburg, N. W., Shah, V. H., & Gores, G. J. (2006). Proteasome inhibition induces hepatic stellate cell apoptosis. *Hepatology, 43*(2), 335-344. doi:10.1002/hep.21036

Anastasiou, D., Yu, Y., Israelsen, W. J., Jiang, J. K., Boxer, M. B., Hong, B. S., Tempel, W., Dimov, S., Shen, M., Jha, A., Yang, H., Mattaini, K. R., Metallo, C. M., Fiske, B. P., Courtney, K. D., Malstrom, S., Khan, T. M., Kung, C., Skoumbourdis, A. P., Veith, H., Southall, N., Walsh, M. J., Brimacombe, K. R., Leister, W., Lunt, S. Y., Johnson, Z. R., Yen, K. E., Kunii, K., Davidson, S. M., Christofk, H. R., Austin, C. P., Inglese, J., Harris, M. H., Asara, J. M., Stephanopoulos, G., Salituro, F. G., Jin, S., Dang, L., Auld, D. S., Park, H. W., Cantley, L. C., Thomas, C. J., & Vander Heiden, M. G. (2012). Pyruvate kinase M2 activators promote tetramer formation and suppress tumorigenesis. *Nat Chem Biol, 8*(10), 839-847. doi:10.1038/nchembio.1060

Arthur, M. J. (2000). Fibrogenesis II. Metalloproteinases and their inhibitors in liver fibrosis. *Am J Physiol Gastrointest Liver Physiol, 279*(2), G245-249.

Ashizawa, K., Willingham, M. C., Liang, C. M., & Cheng, S. Y. (1991). In vivo regulation of monomer-tetramer conversion of pyruvate kinase subtype M2 by glucose is mediated via fructose 1,6-bisphosphate. *J Biol Chem, 266*(25), 16842-16846.

Bainbridge, P. (2013). Wound healing and the role of fibroblasts. *J Wound Care, 22*(8), 407-408, 410-412. doi:10.12968/jowc.2013.22.8.407

Barrientos, S., Stojadinovic, O., Golinko, M. S., Brem, H., & Tomic-Canic, M. (2008). Growth factors and cytokines in wound healing. *Wound Repair Regen, 16*(5), 585-601. doi:10.1111/j.1524-475X.2008.00410.x

Bataller, R., & Brenner, D. A. (2001). Hepatic stellate cells as a target for the treatment of liver fibrosis. *Semin Liver Dis, 21*(3), 437-451. doi:10.1055/s-2001-17558

Bataller, R., & Brenner, D. A. (2005). Liver fibrosis. *J Clin Invest, 115*(2), 209-218. doi:10.1172/jci24282

Baum, J., & Duffy, H. S. (2011). Fibroblasts and myofibroblasts: what are we talking about? *J Cardiovasc Pharmacol, 57*(4), 376-379. doi:10.1097/FJC.0b013e3182116e39

Benyon, R. C., & Iredale, J. P. (2000). Is liver fibrosis reversible? *Gut, 46*(4), 443-446.

Bergers, G., & Benjamin, L. E. (2003). Tumorigenesis and the angiogenic switch. *Nat Rev Cancer, 3*(6), 401-410. doi:10.1038/nrc1093

Borregaard, N., & Cowland, J. B. (1997). Granules of the human neutrophilic polymorphonuclear leukocyte. *Blood, 89*(10), 3503-3521.

Bowman, H. S., & Procopio, F. (1963). Hereditary non-spherocytic hemolytic anemia of the pyruvate-kinase deficient type. *Ann Intern Med, 58*, 567-591.

Brinkmann, V., Reichard, U., Goosmann, C., Fauler, B., Uhlemann, Y., Weiss, D. S., Weinrauch, Y., & Zychlinsky, A. (2004). Neutrophil extracellular traps kill bacteria. *Science, 303*(5663), 1532-1535. doi:10.1126/science.1092385

Brown, G. L., Nanney, L. B., Griffen, J., Cramer, A. B., Yancey, J. M., Curtsinger, L. J., 3rd, Holtzin, L., Schultz, G. S., Jurkiewicz, M. J., & Lynch, J. B. (1989). Enhancement of wound healing by topical treatment with epidermal growth factor. *N Engl J Med, 321*(2), 76-79. doi:10.1056/nejm198907133210203

Bustamante, E., & Pedersen, P. L. (1977). High aerobic glycolysis of rat hepatoma cells in culture: role of mitochondrial hexokinase. *Proc Natl Acad Sci U S A, 74*(9), 3735-3739.

Chen, C. X., Soto, I., Guo, Y. L., & Liu, Y. (2011). Control of secondary granule release in neutrophils by Ral GTPase. *J Biol Chem, 286*(13), 11724-11733. doi:10.1074/jbc.M110.154203

Chen, M., Zhang, J., & Manley, J. L. (2010). Turning on a fuel switch of cancer: hnRNP proteins regulate alternative splicing of pyruvate kinase mRNA. *Cancer Res, 70*(22), 8977-8980. doi:10.1158/0008-5472.can-10-2513

Chen, T. M., Subeq, Y. M., Lee, R. P., Chiou, T. W., & Hsu, B. G. (2008). Single dose intravenous thioacetamide administration as a model of acute liver damage in rats. *Int J Exp Pathol, 89*(4), 223-231. doi:10.1111/j.1365-2613.2008.00576.x

Christofk, H. R., Vander Heiden, M. G., Harris, M. H., Ramanathan, A., Gerszten, R. E., Wei, R., Fleming, M. D., Schreiber, S. L., & Cantley, L. C. (2008). The M2 splice isoform of pyruvate kinase is important for cancer metabolism and tumour growth. *Nature, 452*(7184), 230-233. doi:10.1038/nature06734

Christofk, H. R., Vander Heiden, M. G., Wu, N., Asara, J. M., & Cantley, L. C. (2008). Pyruvate kinase M2 is a phosphotyrosine-binding protein. *Nature, 452*(7184), 181-186. doi:10.1038/nature06667

David, C. J., Chen, M., Assanah, M., Canoll, P., & Manley, J. L. (2010). HnRNP proteins controlled by c-Myc deregulate pyruvate kinase mRNA splicing in cancer. *Nature, 463*(7279), 364-368. doi:10.1038/nature08697

Ding, Q., Gladson, C. L., Wu, H., Hayasaka, H., & Olman, M. A. (2008). Focal adhesion kinase (FAK)-related non-kinase inhibits myofibroblast differentiation through differential MAPK activation in a FAK-dependent manner. *J Biol Chem, 283*(40), 26839-26849. doi:10.1074/jbc.M803645200

Dombrauckas, J. D., Santarsiero, B. D., & Mesecar, A. D. (2005). Structural basis for tumor pyruvate kinase M2 allosteric regulation and catalysis. *Biochemistry, 44*(27), 9417-9429. doi:10.1021/bi0474923

Eckes, B., Zigrino, P., Kessler, D., Holtkotter, O., Shephard, P., Mauch, C., & Krieg, T. (2000). Fibroblast-matrix interactions in wound healing and fibrosis. *Matrix Biol, 19*(4), 325-332.

Ellis, T. N., & Beaman, B. L. (2004). Interferon-gamma activation of polymorphonuclear neutrophil function. *Immunology, 112*(1), 2-12. doi:10.1111/j.1365-2567.2004.01849.x

Elsharkawy, A. M., Oakley, F., & Mann, D. A. (2005). The role and regulation of hepatic stellate cell apoptosis in reversal of liver fibrosis. *Apoptosis, 10*(5), 927-939. doi:10.1007/s10495-005-1055-4

Engler, C., Chakravarti, S., Doyle, J., Eberhart, C. G., Meng, H., Stark, W. J., Kelliher, C., & Jun, A. S. (2011). Transforming growth factor-beta signaling pathway activation in Keratoconus. *Am J Ophthalmol, 151*(5), 752-759.e752. doi:10.1016/j.ajo.2010.11.008

Exton, J. H., & Park, C. R. (1969). Control of gluconeogenesis in liver. 3. Effects of L-lactate, pyruvate, fructose, glucagon, epinephrine, and adenosine 3',5'-monophosphate on gluconeogenic intermediates in the perfused rat liver. *J Biol Chem, 244*(6), 1424-1433.

Falanga, V. (2004). The chronic wound: impaired healing and solutions in the context of wound bed preparation. *Blood Cells Mol Dis, 32*(1), 88-94.

Ferguson, E. C., & Rathmell, J. C. (2008). New roles for pyruvate kinase M2: working out the Warburg effect. *Trends Biochem Sci, 33*(8), 359-362. doi:10.1016/j.tibs.2008.05.006

Friedman, S. L. (2003). Liver fibrosis -- from bench to bedside. *J Hepatol, 38 Suppl 1*, S38-53.

Gallucci, R. M., Lee, E. G., & Tomasek, J. J. (2006). IL-6 modulates alpha-smooth muscle actin expression in dermal fibroblasts from IL-6-deficient mice. *J Invest Dermatol, 126*(3), 561-568. doi:10.1038/sj.jid.5700109

Gao, X., Wang, H., Yang, J. J., Liu, X., & Liu, Z. R. (2012). Pyruvate kinase M2 regulates gene transcription by acting as a protein kinase. *Mol Cell, 45*(5), 598-609. doi:10.1016/j.molcel.2012.01.001

Gong, Y., & Koh, D. R. (2010). Neutrophils promote inflammatory angiogenesis via release of preformed VEGF in an in vivo corneal model. *Cell Tissue Res, 339*(2), 437-448. doi:10.1007/s00441-009-0908-5

Gonzalez, A. L., El-Bjeirami, W., West, J. L., McIntire, L. V., & Smith, C. W. (2007). Transendothelial migration enhances integrin-dependent human neutrophil chemokinesis. *J Leukoc Biol, 81*(3), 686-695. doi:10.1189/jlb.0906553

Gressner, A. M., Weiskirchen, R., Breitkopf, K., & Dooley, S. (2002). Roles of TGF-beta in hepatic fibrosis. *Front Biosci, 7*, d793-807.

Grinnell, F. (1994). Fibroblasts, myofibroblasts, and wound contraction. *J Cell Biol, 124*(4), 401-404.

Gupta, V., Kalaiarasan, P., Faheem, M., Singh, N., Iqbal, M. A., & Bamezai, R. N. (2010). Dominant negative mutations affect oligomerization of human pyruvate kinase M2 isozyme and promote cellular growth and polyploidy. *J Biol Chem, 285*(22), 16864-16873. doi:10.1074/jbc.M109.065029

Hammond, M. E., Lapointe, G. R., Feucht, P. H., Hilt, S., Gallegos, C. A., Gordon, C. A., Giedlin, M. A., Mullenbach, G., & Tekamp-Olson, P. (1995). IL-8 induces neutrophil chemotaxis predominantly via type I IL-8 receptors. *J Immunol, 155*(3), 1428-1433.

Hapa, A., Erkin, G., Hascelik, G., Pektas, D., & Arslan, U. (2011). Plasma TM2-PK levels in mycosis fungoides patients. *Arch Dermatol Res, 303*(1), 35-40. doi:10.1007/s00403-010-1085-9

Hinz, B. (2007). Formation and function of the myofibroblast during tissue repair. *J Invest Dermatol, 127*(3), 526-537. doi:10.1038/sj.jid.5700613

Hinz, B., Mastrangelo, D., Iselin, C. E., Chaponnier, C., & Gabbiani, G. (2001). Mechanical tension controls granulation tissue contractile activity and myofibroblast differentiation. *Am J Pathol, 159*(3), 1009-1020. doi:10.1016/s0002-9440(10)61776-2

Hirata, M., Akbar, S. M., Horiike, N., & Onji, M. (2001). Noninvasive diagnosis of the degree of hepatic fibrosis using ultrasonography in patients with chronic liver disease due to hepatitis C virus. *Eur J Clin Invest, 31*(6), 528-535.

Hitosugi, T., Kang, S., Vander Heiden, M. G., Chung, T. W., Elf, S., Lythgoe, K., Dong, S., Lonial, S., Wang, X., Chen, G. Z., Xie, J., Gu, T. L., Polakiewicz, R. D., Roesel, J. L., Boggon, T. J., Khuri, F. R., Gilliland, D. G., Cantley, L. C., Kaufman, J., & Chen, J. (2009). Tyrosine phosphorylation inhibits PKM2 to promote the Warburg effect and tumor growth. *Sci Signal, 2*(97), ra73. doi:10.1126/scisignal.2000431

Hoshino, A., Hirst, J. A., & Fujii, H. (2007). Regulation of cell proliferation by interleukin-3-induced nuclear translocation of pyruvate kinase. *J Biol Chem, 282*(24), 17706-17711. doi:10.1074/jbc.M700094200

Iwamoto, H., Sakai, H., Tada, S., Nakamuta, M., & Nawata, H. (1999). Induction of apoptosis in rat hepatic stellate cells by disruption of integrin-mediated cell adhesion. *J Lab Clin Med, 134*(1), 83-89.

Jeffery, J., Lewis, S. J., & Ayling, R. M. (2009). Fecal dimeric M2-pyruvate kinase (tumor M2-PK) in the differential diagnosis of functional and organic bowel disorders. *Inflamm Bowel Dis, 15*(11), 1630-1634. doi:10.1002/ibd.20946

Jiang, Y., Wang, Y., Wang, T., Hawke, D. H., Zheng, Y., Li, X., Zhou, Q., Majumder, S., Bi, E., Liu, D. X., Huang, S., & Lu, Z. (2014). PKM2 phosphorylates MLC2 and regulates cytokinesis of tumour cells. *Nat Commun, 5*, 5566. doi:10.1038/ncomms6566

Johnson, M. W., Maestranzi, S., Duffy, A. M., Dewar, D. H., Ciclitira, P. J., Sherwood, R. A., & Nicholls, J. R. (2009). Faecal M2-pyruvate kinase: a novel, noninvasive marker of ileal pouch inflammation. *Eur J Gastroenterol Hepatol, 21*(5), 544-550. doi:10.1097/MEG.0b013e3283040cb3

Keller, K. E., Tan, I. S., & Lee, Y. S. (2012). SAICAR stimulates pyruvate kinase isoform M2 and promotes cancer cell survival in glucose-limited conditions. *Science, 338*(6110), 1069-1072. doi:10.1126/science.1224409

Kim, M. H., Liu, W., Borjesson, D. L., Curry, F. R., Miller, L. S., Cheung, A. L., Liu, F. T., Isseroff, R. R., & Simon, S. I. (2008). Dynamics of neutrophil infiltration during cutaneous wound healing and infection using fluorescence imaging. *J Invest Dermatol, 128*(7), 1812-1820. doi:10.1038/sj.jid.5701223

Kolaczkowska, E., & Kubes, P. (2013). Neutrophil recruitment and function in health and inflammation. *Nat Rev Immunol, 13*(3), 159-175. doi:10.1038/nri3399

Kopylov, U., Rosenfeld, G., Bressler, B., & Seidman, E. (2014). Clinical utility of fecal biomarkers for the diagnosis and management of inflammatory bowel disease. *Inflamm Bowel Dis, 20*(4), 742-756. doi:10.1097/01.mib.0000442681.85545.31

Lacy, P. (2006). Mechanisms of degranulation in neutrophils. *Allergy Asthma Clin Immunol, 2*(3), 98-108. doi:10.1186/1710-1492-2-3-98

Le Mellay, V., Houben, R., Troppmair, J., Hagemann, C., Mazurek, S., Frey, U., Beigel, J., Weber, C., Benz, R., Eigenbrodt, E., & Rapp, U. R. (2002). Regulation of glycolysis by Raf protein serine/threonine kinases. *Adv Enzyme Regul, 42*, 317-332.

Lee, J., Kim, H. K., Han, Y. M., & Kim, J. (2008). Pyruvate kinase isozyme type M2 (PKM2) interacts and cooperates with Oct-4 in regulating transcription. *Int J Biochem Cell Biol, 40*(5), 1043-1054. doi:10.1016/j.biocel.2007.11.009

Leibovich, S. J., Polverini, P. J., Shepard, H. M., Wiseman, D. M., Shively, V., & Nuseir, N. (1987). Macrophage-induced angiogenesis is mediated by tumour necrosis factor-alpha. *Nature, 329*(6140), 630-632. doi:10.1038/329630a0

Leibovich, S. J., & Wiseman, D. M. (1988). Macrophages, wound repair and angiogenesis. *Prog Clin Biol Res, 266*, 131-145.

Li, J., Zhang, Y. P., & Kirsner, R. S. (2003). Angiogenesis in wound repair: angiogenic growth factors and the extracellular matrix. *Microsc Res Tech, 60*(1), 107-114. doi:10.1002/jemt.10249

Li, L., Zhang, Y., Qiao, J., Yang, J. J., & Liu, Z. R. (2014). Pyruvate kinase M2 in blood circulation facilitates tumor growth by promoting angiogenesis. *J Biol Chem, 289*(37), 25812-25821. doi:10.1074/jbc.M114.576934

Lominadze, G., Powell, D. W., Luerman, G. C., Link, A. J., Ward, R. A., & McLeish, K. R. (2005). Proteomic analysis of human neutrophil granules. *Mol Cell Proteomics, 4*(10), 1503-1521. doi:10.1074/mcp.M500143-MCP200

Luedde, T., & Schwabe, R. F. (2011). NF-kappaB in the liver--linking injury, fibrosis and hepatocellular carcinoma. *Nat Rev Gastroenterol Hepatol, 8*(2), 108-118. doi:10.1038/nrgastro.2010.213

Luo, W., & Semenza, G. L. (2011). Pyruvate kinase M2 regulates glucose metabolism by functioning as a coactivator for hypoxia-inducible factor 1 in cancer cells. *Oncotarget, 2*(7), 551-556. doi:10.18632/oncotarget.299

Lv, L., Li, D., Zhao, D., Lin, R., Chu, Y., Zhang, H., Zha, Z., Liu, Y., Li, Z., Xu, Y., Wang, G., Huang, Y., Xiong, Y., Guan, K. L., & Lei, Q. Y. (2011). Acetylation targets the M2 isoform of pyruvate kinase for degradation through chaperone-mediated autophagy and promotes tumor growth. *Mol Cell, 42*(6), 719-730. doi:10.1016/j.molcel.2011.04.025

Majno, G. (1998). Chronic inflammation: links with angiogenesis and wound healing. *Am J Pathol, 153*(4), 1035-1039. doi:10.1016/s0002-9440(10)65648-9

Marra, F. (1999). Hepatic stellate cells and the regulation of liver inflammation. *J Hepatol, 31*(6), 1120-1130.

Masur, S. K., Dewal, H. S., Dinh, T. T., Erenburg, I., & Petridou, S. (1996). Myofibroblasts differentiate from fibroblasts when plated at low density. *Proc Natl Acad Sci U S A, 93*(9), 4219-4223.

Mazurek, S. (2007). Pyruvate kinase type M2: a key regulator within the tumour metabolome and a tool for metabolic profiling of tumours. *Ernst Schering Found Symp Proc*(4), 99-124.

Mazurek, S. (2011). Pyruvate kinase type M2: a key regulator of the metabolic budget system in tumor cells. *Int J Biochem Cell Biol, 43*(7), 969-980. doi:10.1016/j.biocel.2010.02.005

Mazurek, S., Boschek, C. B., Hugo, F., & Eigenbrodt, E. (2005). Pyruvate kinase type M2 and its role in tumor growth and spreading. *Semin Cancer Biol, 15*(4), 300-308. doi:10.1016/j.semcancer.2005.04.009

Mazurek, S., Drexler, H. C., Troppmair, J., Eigenbrodt, E., & Rapp, U. R. (2007). Regulation of pyruvate kinase type M2 by A-Raf: a possible glycolytic stop or go mechanism. *Anticancer Res, 27*(6b), 3963-3971.

Midgley, A. C., Rogers, M., Hallett, M. B., Clayton, A., Bowen, T., Phillips, A. O., & Steadman, R. (2013). Transforming growth factor-beta1 (TGF-beta1)-stimulated fibroblast to myofibroblast differentiation is mediated by hyaluronan (HA)-facilitated epidermal growth factor receptor (EGFR) and CD44 co-localization in lipid rafts. *J Biol Chem, 288*(21), 14824-14838. doi:10.1074/jbc.M113.451336

Morfouace, M., Lalier, L., Oliver, L., Cheray, M., Pecqueur, C., Cartron, P. F., & Vallette, F. M. (2014). Control of glioma cell death and differentiation by PKM2-Oct4 interaction. *Cell Death Dis, 5*, e1036. doi:10.1038/cddis.2013.561

Naito, M., Hasegawa, G., Ebe, Y., & Yamamoto, T. (2004). Differentiation and function of Kupffer cells. *Med Electron Microsc, 37*(1), 16-28. doi:10.1007/s00795-003-0228-x

Newton, P. M., Watson, J. A., Wolowacz, R. G., & Wood, E. J. (2004). Macrophages restrain contraction of an in vitro wound healing model. *Inflammation, 28*(4), 207-214.

Noguchi, T., Inoue, H., & Tanaka, T. (1986). The M1- and M2-type isozymes of rat pyruvate kinase are produced from the same gene by alternative RNA splicing. *J Biol Chem, 261*(29), 13807-13812.

Nozawa, H., Chiu, C., & Hanahan, D. (2006). Infiltrating neutrophils mediate the initial angiogenic switch in a mouse model of multistage carcinogenesis. *Proc Natl Acad Sci U S A, 103*(33), 12493-12498. doi:10.1073/pnas.0601807103

Ortega, S., Ittmann, M., Tsang, S. H., Ehrlich, M., & Basilico, C. (1998). Neuronal defects and delayed wound healing in mice lacking fibroblast growth factor 2. *Proc Natl Acad Sci U S A, 95*(10), 5672-5677.

Pastar, I., Stojadinovic, O., Yin, N. C., Ramirez, H., Nusbaum, A. G., Sawaya, A., Patel, S. B., Khalid, L., Isseroff, R. R., & Tomic-Canic, M. (2014). Epithelialization in Wound Healing: A Comprehensive Review. *Adv Wound Care (New Rochelle), 3*(7), 445-464. doi:10.1089/wound.2013.0473

Paulus, Y. M., Kuo, C. H., Morohoshi, K., Nugent, A., Zheng, L. L., Nomoto, H., Blumenkranz, M. S., Palanker, D., & Ono, S. J. (2015). Serum inflammatory markers after rupture retinal laser injury in mice. *Ophthalmic Surg Lasers Imaging Retina, 46*(3), 362-368. doi:10.3928/23258160-20150323-11

Peng, X. C., Gong, F. M., Zhao, Y. W., Zhou, L. X., Xie, Y. W., Liao, H. L., Lin, H. J., Li, Z. Y., Tang, M. H., & Tong, A. P. (2011). Comparative proteomic approach identifies PKM2 and cofilin-1 as potential diagnostic, prognostic and therapeutic targets for pulmonary adenocarcinoma. *PLoS One, 6*(11), e27309. doi:10.1371/journal.pone.0027309

Pierce, G. F., Mustoe, T. A., Altrock, B. W., Deuel, T. F., & Thomason, A. (1991). Role of platelet-derived growth factor in wound healing. *J Cell Biochem, 45*(4), 319-326. doi:10.1002/jcb.240450403

Popescu, N. C., & Cheng, S. Y. (1990). Chromosomal localization of the gene for a human cytosolic thyroid hormone binding protein homologous to the subunit of pyruvate kinase, subtype M2. *Somat Cell Mol Genet, 16*(6), 593-598.

Popper, H., & Uenfriend, S. (1970). Hepatic fibrosis. Correlation of biochemical and morphologic investigations. *Am J Med, 49*, 707-721.

Powers, C. J., McLeskey, S. W., & Wellstein, A. (2000). Fibroblast growth factors, their receptors and signaling. *Endocr Relat Cancer, 7*(3), 165-197.

Qu, Z., Lou, D., & Pan, Y. (2007). The role of IkappaBalpha in TNF-alpha-induced apoptosis in hepatic stellate cell line HSC-T6. *J Huazhong Univ Sci Technolog Med Sci, 27*(4), 407-410. doi:10.1007/s11596-007-0414-5

Risau, W. (1997). Mechanisms of angiogenesis. *Nature, 386*(6626), 671-674. doi:10.1038/386671a0

Robey, R. B., & Hay, N. (2006). Mitochondrial hexokinases, novel mediators of the antiapoptotic effects of growth factors and Akt. *Oncogene, 25*(34), 4683-4696. doi:10.1038/sj.onc.1209595

Sato, M., Suzuki, S., & Senoo, H. (2003). Hepatic stellate cells: unique characteristics in cell biology and phenotype. *Cell Struct Funct, 28*(2), 105-112.

Schulz, J., Sparmann, G., & Hofmann, E. (1975). Alanine-mediated reversible inactivation of tumour pyruvate kinase caused by a tetramer-dimer transition. *FEBS Lett, 50*(3), 346-350.

Segal, A. W. (2005). How neutrophils kill microbes. *Annu Rev Immunol, 23*, 197-223. doi:10.1146/annurev.immunol.23.021704.115653

Singer, A. J., & Clark, R. A. (1999). Cutaneous wound healing. *N Engl J Med, 341*(10), 738-746. doi:10.1056/nejm199909023411006

Smith, J. A. (1994). Neutrophils, host defense, and inflammation: a double-edged sword. *J Leukoc Biol, 56*(6), 672-686.

Stetak, A., Veress, R., Ovadi, J., Csermely, P., Keri, G., & Ullrich, A. (2007). Nuclear translocation of the tumor marker pyruvate kinase M2 induces programmed cell death. *Cancer Res, 67*(4), 1602-1608. doi:10.1158/0008-5472.can-06-2870

Takahra, T., Smart, D. E., Oakley, F., & Mann, D. A. (2004). Induction of myofibroblast MMP-9 transcription in three-dimensional collagen I gel cultures: regulation by NF-kappaB, AP-1 and Sp1. *Int J Biochem Cell Biol, 36*(2), 353-363.

Tang, A., & Gilchrest, B. A. (1996). Regulation of keratinocyte growth factor gene expression in human skin fibroblasts. *J Dermatol Sci, 11*(1), 41-50.

Teller, P., & White, T. K. (2009). The physiology of wound healing: injury through maturation. *Surg Clin North Am, 89*(3), 599-610. doi:10.1016/j.suc.2009.03.006

Thampanitchawong, P., & Piratvisuth, T. (1999). Liver biopsy:complications and risk factors. *World J Gastroenterol, 5*(4), 301-304.

Thannickal, V. J., Lee, D. Y., White, E. S., Cui, Z., Larios, J. M., Chacon, R., Horowitz, J. C., Day, R. M., & Thomas, P. E. (2003). Myofibroblast differentiation by transforming growth factor-beta1 is dependent on cell adhesion and integrin signaling via focal adhesion kinase. *J Biol Chem, 278*(14), 12384-12389. doi:10.1074/jbc.M208544200

Tonnesen, M. G., Feng, X., & Clark, R. A. (2000). Angiogenesis in wound healing. *J Investig Dermatol Symp Proc, 5*(1), 40-46. doi:10.1046/j.1087-0024.2000.00014.x

Trim, N., Morgan, S., Evans, M., Issa, R., Fine, D., Afford, S., Wilkins, B., & Iredale, J. (2000). Hepatic stellate cells express the low affinity nerve growth factor receptor p75 and undergo apoptosis in response to nerve growth factor stimulation. *Am J Pathol, 156*(4), 1235-1243. doi:10.1016/s0002-9440(10)64994-2

Valentine, W. N., Tanaka, K. R., & Miwa, S. (1961). A specific erythrocyte glycolytic enzyme defect (pyruvate kinase) in three subjects with congenital non-spherocytic hemolytic anemia. *Trans Assoc Am Physicians, 74*, 100-110.

Versteeg, H. H., Heemskerk, J. W., Levi, M., & Reitsma, P. H. (2013). New fundamentals in hemostasis. *Physiol Rev, 93*(1), 327-358. doi:10.1152/physrev.00016.2011

Wang, H. J., Hsieh, Y. J., Cheng, W. C., Lin, C. P., Lin, Y. S., Yang, S. F., Chen, C. C., Izumiya, Y., Yu, J. S., Kung, H. J., & Wang, W. C. (2014). JMJD5 regulates PKM2 nuclear translocation and reprograms HIF-1alpha-mediated glucose metabolism. *Proc Natl Acad Sci U S A, 111*(1), 279-284. doi:10.1073/pnas.1311249111

Wegener, G., & Krause, U. (2002). Different modes of activating phosphofructokinase, a key regulatory enzyme of glycolysis, in working vertebrate muscle. *Biochem Soc Trans, 30*(2), 264-270. doi:10.1042/

Weis, S. M., & Cheresh, D. A. (2011). Tumor angiogenesis: molecular pathways and therapeutic targets. *Nat Med, 17*(11), 1359-1370. doi:10.1038/nm.2537

Wilkes, M. C., Mitchell, H., Penheiter, S. G., Dore, J. J., Suzuki, K., Edens, M., Sharma, D. K., Pagano, R. E., & Leof, E. B. (2005). Transforming growth factor-beta activation of phosphatidylinositol 3-kinase is independent of Smad2 and Smad3 and regulates fibroblast responses via p21-activated kinase-2. *Cancer Res, 65*(22), 10431-10440. doi:10.1158/0008-5472.can-05-1522

Wilkes, M. C., Murphy, S. J., Garamszegi, N., & Leof, E. B. (2003). Cell-type-specific activation of PAK2 by transforming growth factor beta independent of Smad2 and Smad3. *Mol Cell Biol, 23*(23), 8878-8889.

Witko-Sarsat, V., Rieu, P., Descamps-Latscha, B., Lesavre, P., & Halbwachs-Mecarelli, L. (2000). Neutrophils: molecules, functions and pathophysiological aspects. *Lab Invest, 80*(5), 617-653.

Yang, E. Y., & Moses, H. L. (1990). Transforming growth factor beta 1-induced changes in cell migration, proliferation, and angiogenesis in the chicken chorioallantoic membrane. *J Cell Biol, 111*(2), 731-741.

Yang, P., Li, Z., Fu, R., Wu, H., & Li, Z. (2014). Pyruvate kinase M2 facilitates colon cancer cell migration via the modulation of STAT3 signalling. *Cell Signal, 26*(9), 1853-1862. doi:10.1016/j.cellsig.2014.03.020

Yang, W., & Lu, Z. (2013). Nuclear PKM2 regulates the Warburg effect. *Cell Cycle, 12*(19), 3154-3158. doi:10.4161/cc.26182

Yang, W., Xia, Y., Cao, Y., Zheng, Y., Bu, W., Zhang, L., You, M. J., Koh, M. Y., Cote, G., Aldape, K., Li, Y., Verma, I. M., Chiao, P. J., & Lu, Z. (2012). EGFR-induced and PKCepsilon monoubiquitylation-dependent NF-kappaB activation upregulates PKM2 expression and promotes tumorigenesis. *Mol Cell, 48*(5), 771-784. doi:10.1016/j.molcel.2012.09.028

Yang, W., Xia, Y., Hawke, D., Li, X., Liang, J., Xing, D., Aldape, K., Hunter, T., Alfred Yung, W. K., & Lu, Z. (2012). PKM2 phosphorylates histone H3 and promotes gene transcription and tumorigenesis. *Cell, 150*(4), 685-696. doi:10.1016/j.cell.2012.07.018

Yang, W., Xia, Y., Ji, H., Zheng, Y., Liang, J., Huang, W., Gao, X., Aldape, K., & Lu, Z. (2011). Nuclear PKM2 regulates beta-catenin transactivation upon EGFR activation. *Nature, 480*(7375), 118-122. doi:10.1038/nature10598

Yang, W., Zheng, Y., Xia, Y., Ji, H., Chen, X., Guo, F., Lyssiotis, C. A., Aldape, K., Cantley, L. C., & Lu, Z. (2012). ERK1/2-dependent phosphorylation and nuclear translocation of PKM2 promotes the Warburg effect. *Nat Cell Biol, 14*(12), 1295-1304. doi:10.1038/ncb2629

Yu, Z., Zhao, X., Huang, L., Zhang, T., Yang, F., Xie, L., Song, S., Miao, P., Zhao, L., Sun, X., Liu, J., & Huang, G. (2013). Proviral insertion in murine lymphomas 2 (PIM2) oncogene phosphorylates pyruvate kinase M2 (PKM2) and promotes glycolysis in cancer cells. *J Biol Chem, 288*(49), 35406-35416. doi:10.1074/jbc.M113.508226

Zhang, X. L., Topley, N., Ito, T., & Phillips, A. (2005). Interleukin-6 regulation of transforming growth factor (TGF)-beta receptor compartmentalization and turnover enhances TGF-beta1 signaling. *J Biol Chem, 280*(13), 12239-12245. doi:10.1074/jbc.M413284200

Zhang, Z., Liu, Q., Che, Y., Yuan, X., Dai, L., Zeng, B., Jiao, G., Zhang, Y., Wu, X., Yu, Y., Zhang, Y., & Yang, R. (2010). Antigen presentation by dendritic cells in tumors is disrupted by altered metabolism that involves pyruvate kinase M2 and its interaction with SOCS3. *Cancer Res, 70*(1), 89-98. doi:10.1158/0008-5472.can-09-2970

Zhao, J., Chen, L., Shu, B., Tang, J., Zhang, L., Xie, J., Qi, S., & Xu, Y. (2014). Granulocyte/macrophage colony-stimulating factor influences angiogenesis by regulating the coordinated expression of VEGF and the Ang/Tie system. *PLoS One, 9*(3), e92691. doi:10.1371/journal.pone.0092691

Zhou, X., Murphy, F. R., Gehdu, N., Zhang, J., Iredale, J. P., & Benyon, R. C. (2004). Engagement of alphavbeta3 integrin regulates proliferation and apoptosis of hepatic stellate cells. *J Biol Chem, 279*(23), 23996-24006. doi:10.1074/jbc.M311668200

Zhu, J., Bi, Z., Yang, T., Wang, W., Li, Z., Huang, W., Wang, L., Zhang, S., Zhou, Y., Fan, N., Bai, Y., Song, W., Wang, C., Wang, H., & Bi, Y. (2014). Regulation of PKM2 and Nrf2-ARE pathway during benzoquinone induced oxidative stress in yolk sac hematopoietic stem cells. *PLoS One, 9*(12), e113733. doi:10.1371/journal.pone.0113733

SUPPLEMENTARY RESULTS

PKM2 translocates into cell nucleus and phosphorylates histone H4

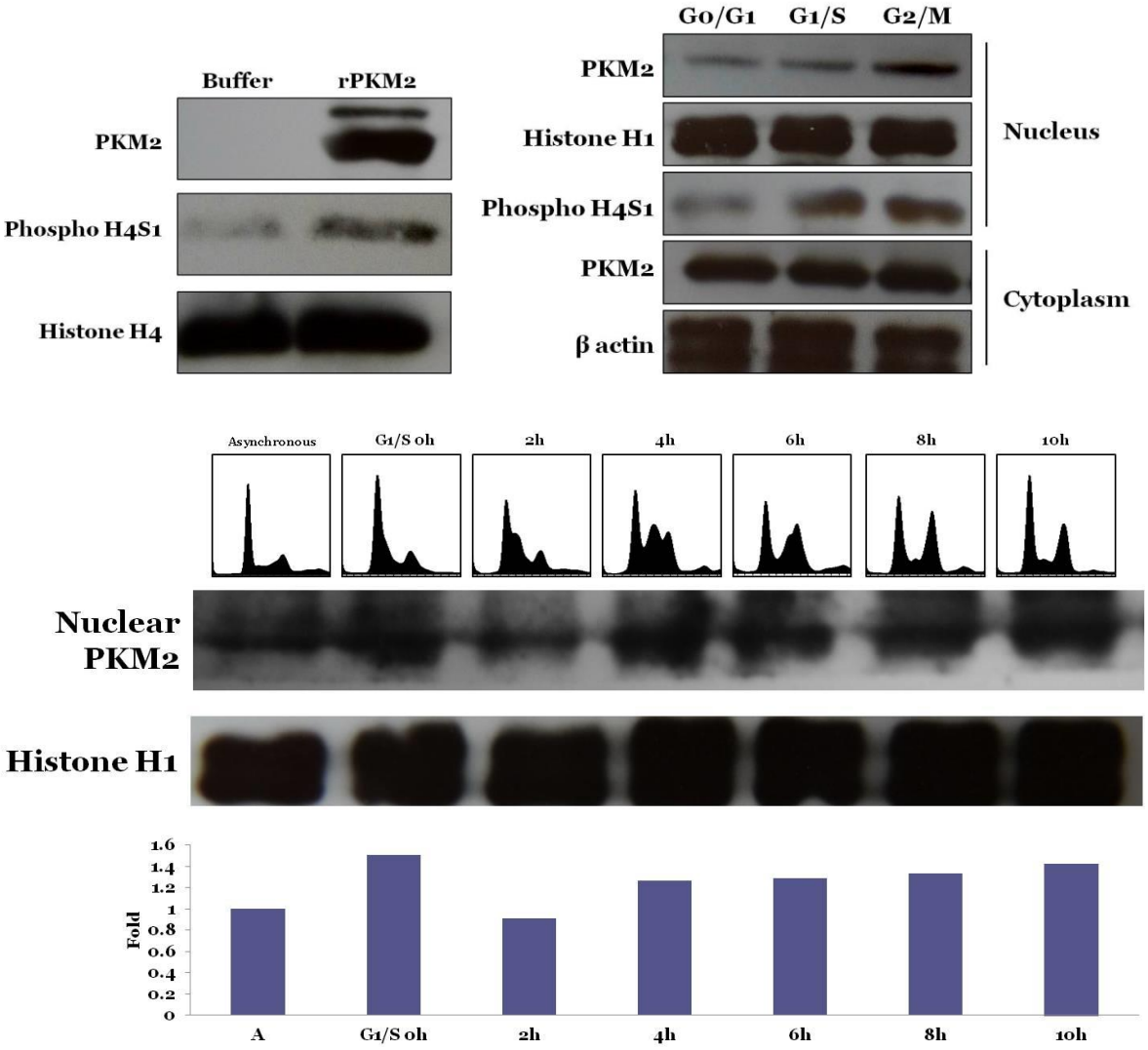

Recombinant PKM2 used PEP as substrate to phosphorylate histone H4 at Serine 1 in vitro. PKM2 translocated into cell nucleus at S and G2 phases which was correlated with histone H4S1 phosphorylation.